Techniques for performance improvement of Radio-over-fiber WLAN

Document status and date:
Published: 06/09/2017

Document Version:
Publisher's PDF, also known as Version of Record (includes final page, issue and volume numbers)

Please check the document version of this publication:

• A submitted manuscript is the version of the article upon submission and before peer-review. There can be important differences between the submitted version and the official published version of record. People interested in the research are advised to contact the author for the final version of the publication, or visit the DOI to the publisher's website.
• The final author version and the galley proof are versions of the publication after peer review.
• The final published version features the final layout of the paper including the volume, issue and page numbers.
Link to publication

Techniques for Performance Improvement of Radio-over-Fiber WLAN

Diptanil DebBarma

Techniques for Performance Improvement of Radio-over-Fiber WLAN

PROEFSCHRIFT

ter verkrijging van de graad van doctor aan de
Technische Universiteit Eindhoven, op gezag van de
rector magnificus, prof.dr.ir F.P.T. Baaijens, voor een
commissie aangewezen door het College voor
Promoties in het openbaar te verdedigen
op woensdag 6 september 2017 om 16.00 uur

door

Diptanil DebBarma

geboren te Agartala, India.

Dit proefschrift is goedgekeurd door de promotoren en de samenstelling van de promotiecommissie is als volgt:

Voorzitter: prof.dr.ir. A.B. Smolders
Promotor: prof.dr.ir. S.M. Heemstra de Groot
Co-promotor: prof.dr.ir. I.G.M.M Niemegeers (TU Delft)
Leden: prof.dr.ir. I. Moerman (Universiteit Gent)
                 prof.dr.ir. C.H. Slump (Universiteit Twente)
                 prof.ir. A.M.J. Koonen
                 dr.ir. A. Lo (Bell Labs & CTO Nokia)
                 dr.ir. E. Tangdiongga

Het onderzoek of ontwerp dat in dit proefschrift wordt beschreven is uitgevoerd in overeenstemming met de TU/e Gedragscode Wetenschapsbeoefening.

Summary

Techniques for Performance Improvement of Radio-over-Fiber WLAN

The expected traffic surge in indoor networks due to hyper-connectivity of user devices calls for immediate attention. WiFi serves the lion's share of the indoor data traffic. But the inherent architecture of WiFi is not suited for such massive data traffic growth by itself. The main problems are threefold. Firstly, the indoor network should be able to cope with the temporal and spatial variations in user traffic while providing the demanded services with the required quality. Secondly, the energy efficiency of the network should be much better ($100+$ times, as envisioned in the $5G$ roadmap) than the present WiFi to reduce the total cost of operation. Finally, the network capacity has to scale up by three orders of magnitude (Peak user data rate ≥ 10 Gbps and minimum guaranteed user data rate ≥ 100 Mbps). A Radio-over-Fiber (RoF) based hybrid Fiber-Wireless (Fi-Wi) indoor architecture could meet these requirements. Fi-Wi encompasses the benefits achievable from both distributed antenna systems and centralized resource management.

In this dissertation, we study and quantify the benefits of the Fi-Wi architecture for leveraging the network adaptability for resource management, energy efficiency and improving physical layer performance. We propose new techniques like a dynamic assignment for re-allocation of network elements to improve user throughput and delay and resource on demand techniques for energy efficiency. We also propose a Power-Managed-Load-Balanced strategy that achieves dynamic traffic-load balancing while reducing the total energy spent by the network. Moreover, different physical layer aspects and techniques are also addressed. We propose an uplink MU-MIMO scheme that utilizes both the optical and spatial degrees of freedom to achieve a significantly higher user capacity. We also propose a precoding and scheduling MU-MIMO scheme that improves downlink throughput while assuring QoS support for the users in the network.

Contents

1

Introduction

1.1 Introduction

There has been a major evolution in mobile communication from just providing simple analog voice connectivity through telephones to ultra-smart hand-held mobile devices (MDs) supporting hundreds of thousands of different applications, which are connecting billions of users worldwide. It is projected that, by 2020, there will be 25 billion [1] connected devices globally, supporting a multitude of wireless connections. These devices are capable of supporting many emerging services like Voice over Internet Protocol (VoIP), ultra high-definition video streaming, social networking, augmented reality, cloud computing, and machine-to-machine communication to name a few. The aforementioned services have different service requirements, e.g., the continuous growth of video resolution demands extremely high data rates of the order of 1 Gbps [2]; cloud computing, online gaming and augmented reality require large amounts of data exchange with extremely low latency of the order of milliseconds. The fifth generation (5G) of mobile networks are developed and projected to be deployed by 2020 [1, 3] to meet the new service requirements. The different engineering requirements for 5G can be broadly classified into three categories [4, 5]:

- **Data Rate:** 5G envisions a $1000\times$ increase in aggregate data rate or area capacity from fourth generation (4G). The edge rate or 5% rate requirement ranges from 100 Mbps to 1 Gbps (for ultra high-definition video streaming), thus requiring a 100 fold improvement over present 4G systems edge rates.

- **Latency:** Applications such as augmented reality, cloud-based "tactile Internet", online gaming, etc., require a very low roundtrip latency of the

order of 1 ms.

- **Energy:** As the projected data rate per link is expected to grow by a factor of 100, the amount of energy consumption in Joules per bit should also be scaled down by the same factor of 100. This will ensure reasonable power scaling.

Thus the aforementioned requirements, owing to the growth in the number of devices and the connectivity services they require, are placing an enormous pressure on the network. According to a study from CISCO [6], at least 80 % of the data traffic originates indoor. Moreover, the mobile market is estimated to approximately double in revenue (to roughly 8.5 billion dollars) by 2019 [7]. Thus managing the indoor network efficiently is of utmost importance. The challenges that are faced by the indoor networks can be classified into three broad categories. Firstly, the indoor network capacity has to scale up to cope with the increasing traffic demands. Secondly, the indoor network must be able to configure and adapt itself, to deliver the required services and to meet the MD's demands, without bothering the users with network technicalities. And finally, the indoor network should be energy efficient, to reduce the total cost of operation, and should be able to operate with ultra-low transmission power to minimize human exposure to electromagnetic radiation. Researchers believe that the challenges offered can be met by (a) densification of the network [4, 8], (b) increasing spectral efficiency via advanced multiple input multiple output (MIMO) techniques [8--10] and (c) increasing bandwidth by taking a leap towards mm-wave communication [11]. In this dissertation, we however restrict our efforts to the first two categories.

Today's indoor networks are generally rolled out as a single large wireless network with complete site coverage. This network architectural design does not satisfy the challenges mentioned above. Densification of the network, by creating smaller wireless network clusters, has been first demonstrated for mobile technologies as an effective measure for increasing the outdoor network capacity [12, 13]. This is not just true for deployment of outdoor mobile technologies but also holds for indoor networks and is in-line with the heterogeneous networking (HetNet) architecture of 5G [14]. Diminishing cell sizes and creating femto-cells offers many benefits like (a) re-use of spectral resources, (b) lowering the number of competing MDs per cell, (c) reduced transmission distances and (d) reduced electromagnetic radiation. However, a centrally managed indoor architecture partitioning the overall coverage area into smaller cells needs to be dynamic in nature. It should adapt the topology based on the space and time-varying user demands. Adoption of advanced physical layer solutions like massive

multi-user multiple input multiple output (MIMO) systems also play a big part in meeting the aforementioned challenges [8]. Apart from forming smaller clusters of femto-cells and adoption of advanced physical layer technologies, an efficient indoor network architecture design should also incorporate the following important features:

- It should provide seamless inter-working between different radio standards.

- It should allow for lower network energy consumption and operate at lower transmit power levels.

- It should be future proof, i.e., it should be able to incorporate new technologies as they appear on the market.

- It should be scalable, with respect to number of MDs and users served.

An indoor hybrid Fiber-Wireless (Fi-Wi) network architecture based on Radio-over-Fiber (RoF), as proposed in [15, 16], is a good basis for providing these features. This dissertation is based on the research work carried out under the framework of the Management and control of Energy-efficient Ad-hoc Networks and Services (MEANS) project [17]. The project has been funded by the Dutch Ministry of Economic Affairs [18] in the IOP Generieke Communicatie Program [19]. In this dissertation, we study techniques for attaining solutions towards the aforementioned challenges using RoF-based hybrid Fi-Wi architecture.

1.2 Research challenges

The indoor fiber links are typically short range (of the order of a few hundred meters) and are assumed not to add large propagation delays, which could adversely affect the MAC protocols of the radio standards [20]. However, the architecture[1] does present some significant challenges.

The following six research challenges were identified in the MEANS project [17].

- Dynamic radio resource assignment via topology and configuration management.

- Energy efficient indoor communication.

- Improvement of network capacity.

---
[1]A detailed description of the Fi-Wi architecture is provided in Chapter 2.

- Multiple wireless standard networking.

- Support of mobility and session management.

- Security management.

There is a lot of literature dealing with the aforementioned issues. For example, in [21, 22], the authors deal with the issues of seamless mobility, session management and multiple wireless standard networking in hybrid Fi-Wi networks. In [21] the extended cell technique was proposed for seamless handovers of devices between adjacent femto-cells. This was based on grouping several adjacent femto-cells into one cell, where the same signals were transmitted from the transmit antennas over the same frequency channels. In [22] solutions were provided to the problem of multiple wireless standard networking, via vertical handover, between wireless local area network (WLAN) and 60 GHz communication radio technologies. [22] used Decision Theory and Markov Decision Processes to study the problem of vertical handover between the aforementioned technologies, taking into account the quality of experience perceived by the MDs. In [23], models for indoor energy-efficiency of Wireless Fidelity (WiFi) network based on RoF distributed antenna system (DAS) have been studied and shown to perform better in terms of coverage and energy efficiency as compared to the traditional WiFi deployment. In [24] security management issues like mutual authentication and data confidentiality of Fi-Wi networks were tackled, and the list goes on.

This dissertation, however, deals with the first three aforementioned research challenges, which influence the different engineering requirements of the 5G network. We discuss each of them in the following sections.

1.2.1 Dynamic radio resource management

The RoF-based Fi-Wi architecture, used in the MEANS project, consists of access points (APs) colocated at the central residential gateway (namely, the Home Communication Controller (HCC)), with the transmit antennas (namely, the Cell Access Nodes (CANs)) located in the building. The connectivity decisions, between the CANs and the APs, are managed by a central entity at the HCC, namely the Radio Network Manager (RNM) (see Fig. 1.1). The main purpose of choosing a hybrid Fi-Wi architecture is to satisfy the demands of the indoor MDs, with a satisfactory quality of service (QoS), through user-centric network resource sharing. For example, an extra cell can be added (or removed) to handle a surge in the traffic demand caused by an increase in the number of MDs and the services they demand. The transmit power levels, at the transmit antennas, are also controllable
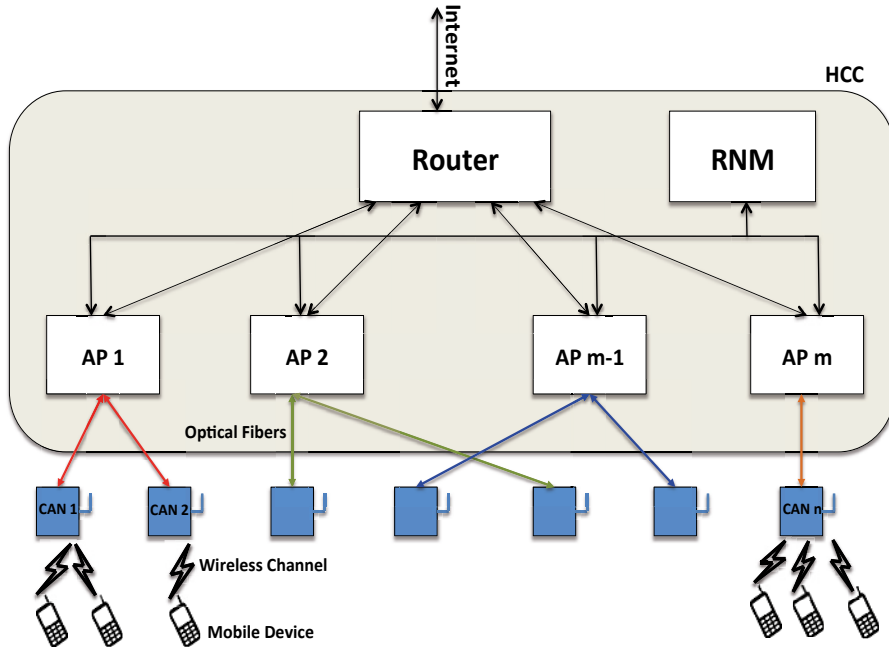
HCC : Home Communication Controller; CAN : Cell Access Node; AP : Access Point; RNM : Radio Network Manager.

Figure 1.1: *Flexible AP-CAN-Mobile device assignment in RoF-based Fi-Wi architecture*

to dynamically adjust the size and capacity of the served radio cells. However, the individual transmitting power level across each antenna needs to be monitored and managed carefully to adapt the cell size. Too high transmit power levels can cause unwanted mutual interference between cells thus diminishing the capacity offered. Similarly, too low transmit power levels can hamper the transmission performance and can cause outage among users and devices. Thus by applying dynamic radio resource assignment techniques at the HCC, the topology, the network capacity, the QoS and the fairness across the MDs and network services can be improved. This is of utmost importance because the user traffic demands across each cell and the QoS requirements are changing over time. The fluctuations can be attributed to the mobility of users and devices, users demanding different services, ongoing service sessions with time varying QoS needs or even devices being powered on or switched off.

The architecture thus allows better load balancing and congestion control for the overall network. Moreover, vertical handovers of the user traffic among the

supported wireless standards are also possible, allowing for better utilization of the network resources among its varied user categories. Thus in a hybrid Fi-Wi architecture there are a lot of network parameters that could be adjusted dynamically for better management of the network. The challenge is to utilize these parameters and formulate efficient radio resource management techniques to guarantee QoS across heterogeneous MD traffic categories. In this dissertation, we, therefore, formulate efficient load balancing algorithms that can reduce the overall congestion of the centralized enterprise WLAN network.

1.2.2 Energy efficient indoor communication

Energy consumption of the information and communications technology (ICT) has become a big challenge for sustainable development. The ICT industry contributed about 3% to the global annual electricity bill in 2010, and the amount is increasing by 15 to 20 % each year [25]. With the rapid deployment of enterprise WLANs, $4G$ networks, as well as the $5G$ vision of a totally connected world by 2020 [3], the situation is getting worse. The indoor network operation efficiency and energy efficiency need further enhancements by taking into account the time varying traffic load and interference management.

The dynamic radio resource management for a hybrid Fi-Wi architecture, to attain QoS across MDs and network services, discussed above, is done by utilizing the flexibility in connections between the APs and the CANs. But this also has a major impact in reducing the aggregate energy consumption of the whole indoor network. In an indoor network, there are two major causes for energy consumption. Firstly, as the number of MDs is increasing, the network adds more redundancy, by installing more APs to provide overlapping coverage, considering the worst case scenario in traffic demands. Thus almost all of the APs are kept switched on all the time. But those worst-case traffic demand situations occur rarely and even vary over space, i.e., they might occur more frequently in specific areas than others. Secondly, the transmit power levels across the APs are kept high as they serve a larger area indoor. But as the number of MDs varies over time and space such high power transmission may not be justifiable, e.g., when there are fewer MDs in the network and all of them are very close to the APs. Thus the first aforementioned issue leads to high energy wastage due to the continuous operation of all network elements like APs and central network manager managing the WLAN, if any. It reduces both energy and spectral efficiency and causes unnecessary mutual interference between radio channels if the radio planning is not performed properly. This creates congestion and eventually brings down the network capacity. The second issue discussed above also leads

to low energy efficiency and can cause mutual interference between neighboring cells. Furthermore, it is not clear yet whether the electromagnetic radiation also impacts the long-term health of the users [26].

The hybrid Fi-Wi network architecture (see Fig. 1.1) can considerably reduce the total energy wastage in the network. As optical fiber is used for a major part of the link between the APs and mobile devices (MD), the amount of power used for transmitting information is much less than that of a copper medium. Moreover as the transmitting antennas (CANs) are kept as close as possible to the MDs the transmission power is reduced considerably. Furthermore, due to the centralized management of the indoor network, the hybrid Fi-Wi architecture can utilize the knowledge about the varying MD traffic demand. This creates the opportunity to reduce the energy wastage due to the redundancy of the coverage, via dynamic on and off switching of the network elements (CANs and APs), thus reducing the mutual interference between cells and lowering the electromagnetic radiation levels.

This dissertation will analyze the problem of energy consumption in centralized enterprise WLANs and demonstrate the energy efficiency of the hybrid Fi-Wi network.

1.2.3   Improving network performance

Finally, the hybrid Fi-Wi indoor network should improve the overall network performance. Deployment of femto-cells along with flexible and transparent optical interconnection between APs and CANs provides a basis for significantly improving network performance in terms of capacity and coverage.

Advanced physical layer techniques can help to increase the capacity of such a Fi-Wi network. A key technology for increasing the network capacity is the use of MIMO antenna techniques [27]. Many wireless standards (e.g., WiFi, Long Term Evolution (LTE), LTE-Advanced) have incorporated MIMO. MIMO involves a variety of techniques aiming at different objectives for different scenarios. In general, they can be broadly divided into two categories namely single-user MIMO (SU-MIMO) and multi-user MIMO (MU-MIMO). In the Fi-Wi architecture, since we have a large number of CANs, we can make use of them to perform both SU-MIMO and MU-MIMO. A large number of devices (wired or wireless) co-existing in the network allows us to make use of MU-MIMO techniques to enhance per MD throughput as well as the overall network capacity and also the reliability experienced by the MDs. While a variety of MIMO techniques can be utilized in the downlink because of the availability of a large number of CANs, our options are limited in the uplink because of the limited processing and antenna slots across

MDs. Consequently as networks designer we have to push all the MIMO implementation issues to the HCC to bring the MIMO virtues at the MDs. Thus in particular MU-MIMO techniques can be interesting. MU-MIMO exploits the multiuser diversity in allocating a group of MDs into the same time-frequency resource [28]. It thus achieves higher transmission capacity while requiring simpler MDs. In the general setting, we assume that the MDs are transmitting to the APs (colocated at the HCC) utilizing one or more antennas. There is generally no coordination assumed among the MDs. Hence the main challenge lies in scheduling the MDs in the downlink. As the MDs are generally dispersed over the femto-cell areas and are not predictable in their behavior, scheduling the group of MDs to attain maximum network capacity while guaranteeing individual MD performance is challenging. The different techniques used in MU-MIMO are beam-forming, space-division multiplexing and transmit diversity.

In this dissertation, we analyze and propose MU-MIMO techniques for uplink and downlink. While in the uplink we propose an optical and spatially multiplexed MU-MIMO scheme that can significantly improve the total network capacity, in the downlink we propose MU-MIMO precoding and scheduling schemes, based on the metric of successive leakage to noise ratio, that guarantees QoS as demanded by the MDs.

1.3   Methodology & techniques

In the previous section, we mentioned the research challenges that we tackle in this dissertation. The hybrid Fi-Wi architecture is unique as it provides several new opportunities to address the issues. This section lists possible interesting optimization solutions that can be implemented by utilizing the degrees of freedom provided by such RoF-based hybrid Fi-Wi architecture. Fig. 1.2 provides an overview of the design principles and optimization framework of the hybrid Fi-Wi architecture. The objective inputs are categorized in the architecture by listing them under the resources available. The Fi-Wi network design and performance is optimized using the offered degrees of freedom as optimization variables. The offered degrees of freedom are,

- **Power:** The transmit power across each CANs is a controllable parameter. The network can vary the transmit power to control the cell sizes covered by the CANs, thus reducing interference or controlling the number of users and devices supported by each CAN.
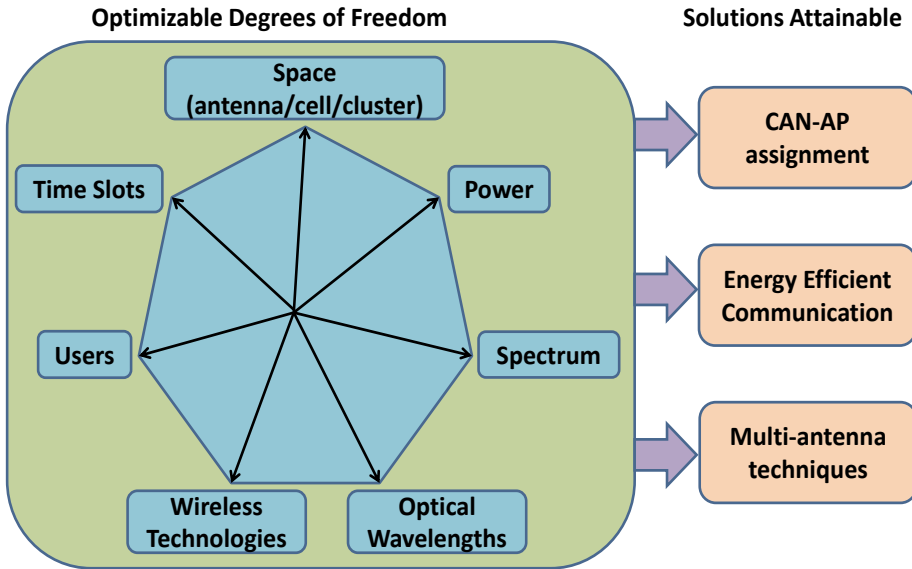
Figure 1.2: *Overview of the degrees of freedom along with the optimization solutions attainable*

- **Spectrum:** The network can control the bandwidth offered across each indoor femto-cell. Based on the knowledge of the location of the user traffic generation, the network can decide to offer more spectrum to locations where the user traffic demand is high.

- **Users:** Managing the users, or the MDs, can yield important degrees of freedom. Based on the knowledge of the user traffic profile and the services they demand, the network can group classes of MDs intelligently to reduce congestion in the network. The network can even use the diversity provided by the varied user traffic demand and can perform MU-MIMO techniques or provide cooperative communication support.

- **Wireless technologies:** Support for a plurality of wireless standards allows the network to divide the user traffic based on the QoS demands. It helps to relieve congestion in the network, thus reducing the latency in both the uplink and downlink.

- **Optical wavelengths:** As the radio signals from the HCC to the CANs and vice-versa are transported by multiplexing them onto optical carriers, the optical wavelengths allow the network to provide service differentiation

across users.

- **Time-scheduling:** Time-slots are an important dimension. Advanced physical layer techniques like MU-MIMO, cooperative communication, and Massive MIMO require scheduling of MDs over both time and frequency slots. Thus controlling the MAC time-slot scheduling can maximize the aggregate capacity by proper scheduling of MDs.

- **Space:** Finally another important degree of freedom is space. Here space refers to the antennas across CANs or the femto-cells they provide coverage to or even a cluster of femto-cell grouped together as a single cell. In designing a robust network, which can dynamically manage the topology of the network (for radio resource management or energy efficient communication) or provide advanced physical layer support, the network has to manage the cell areas properly.

Each degree of freedom represents parameters that can be controlled by the network to obtain solutions that can address the challenges we pointed out before. The various solutions that are discussed in this dissertation make use of the available degrees of freedom and can be classified into three main categories namely, CAN-AP assignment, energy efficient communication and multi-antenna techniques. Each of the solutions is discussed below,

- **CAN-AP assignment:** The prioritized degrees of freedom would be space, time-slot, spectrum and wireless technologies. The deployment of a Fi-Wi architecture, which utilizes the DAS approach, provides multiple flexibilities. The APs colocated at the HCC can connect with any CAN using different optical wavelengths. Thus if we consider a single wireless technology (e.g., IEEE 802.11x, where x=a, b, g, n, ac, etc.), multiple CANs can connect to a single WiFi AP or multiple WiFi APs can connect to a single CAN (see Fig. 1.1). This flexibility allows to re-configure the traffic pattern in the network, which in turn allows to fully utilize the network capacity. The indoor network can avoid congestion by changing the connectivity between the APs and the CANs. Thus RoF-based DAS assignment allows for the change of the cell areas served by the APs dynamically over different time-slots. This allows better bandwidth utilization and also helps to reduce inter-cell interference.

- **Energy efficient communication:** As mentioned before one of the major concerns of indoor networks is to reduce the overall energy consumption.

The different degrees of freedom in a Fi-Wi network that can be used for energy-efficient communication are power, grouping of users or MDs, time-slots, space, and spectrum.

- **Multi-antenna techniques:** Multi-antenna techniques are proposed with the intention of improving the overall uplink and downlink capacities. The degrees of freedom used in these criteria are power, space, time-slot and spectrum. As discussed before, one of the most important challenges is to improve the network capacity of the Fi-Wi network. We thus explore multi-antenna techniques, like MU-MIMO, to attain higher overall network capacity.

1.4 Scope & organization of the dissertation

This dissertation focuses on the three aforementioned goals of the project namely (a) Dynamic radio resource assignment, (b) Energy efficient indoor communication and (c) Improving network performance. We provide techniques for better managing indoor Fi-Wi networks which increase the total network capacity (both in uplink and downlink) while guarantying QoS demands and achieving fairness among MDs. We study the widely used indoor small cell technology of WiFi over a hybrid Fi-Wi architecture and provide techniques for dynamically managed indoor WLAN networks.

This dissertation is divided into two main parts: (a) dynamic radio resource management and energy efficient communication and (b) physical (PHY) layer techniques, as shown in Fig. 1.3. Chapter 3, 4, 5, and 6 form the core part of the research.

In Chapter 3 we utilize the dynamic temporal and spatial variations in MD traffic and provide centralized load balancing techniques by shifting the connections between APs (colocated at the HCC) and CANs. Static connections between CANs and APs will lead to poor MD performance in terms of throughput and delay achievable for the requested traffic. Flexible RoF connectivity between CANs and APs ensures that we can dynamically change the association between those network elements (CANs and APs) to improve MD throughput and transmission delay resulting in much-improved network performance.

Chapter 4 provides techniques for energy-efficient communication in Fi-Wi WLAN. In today's world, centralized enterprise WLAN support redundant layers of APs with overlapping cell areas to provide sufficient capacity to all MDs, supporting the required QoS for critical demand situations, and also to protect the network against failures. It has been pointed out in many studies (e.g., [29])
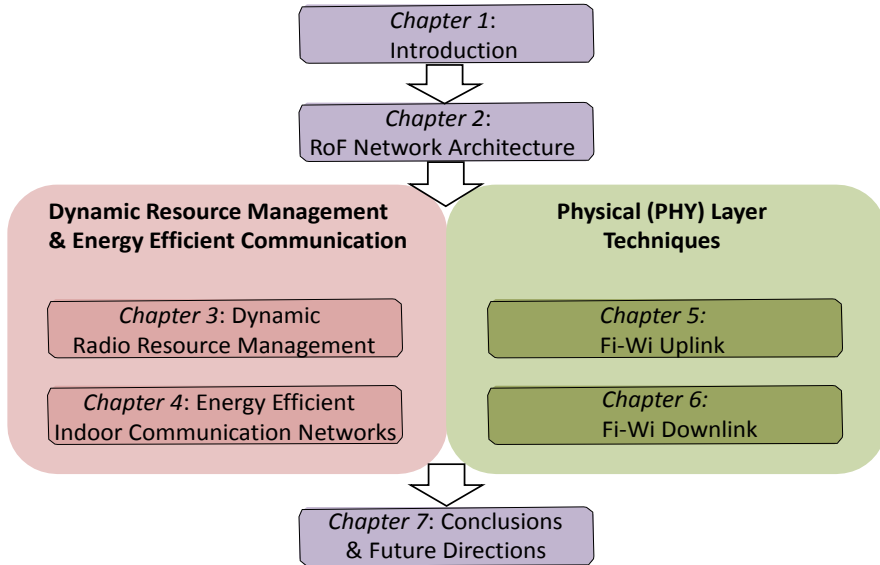
Figure 1.3: *Organization of the dissertation*

that the AP usage varies drastically over a day, week, month and also throughout the year. Such peak MD traffic demands occurs on a shorter time scale causing most of the APs in such enterprise scenario to be in idle mode frequently. Thus hundreds of thousands of APs worldwide are responsible for enormous energy wastage. The numbers of idle APs are bound to increase as enterprises add more redundancy in their networks. This is a major issue, which has received meager attention and is bound to become a problem. The energy consumed in the network is due to the operation of the network elements. In this chapter, we study techniques to switch network elements on or off based on the quantified MD demand. We advocate resource on demand (RoD) techniques for energy efficient communication of centralized enterprise WLAN using the RoF-based hybrid Fi-Wi architecture. Finally, we also combine the techniques proposed for the energy efficient communication along with the dynamic radio resource assignment techniques to provide network solutions that are able to achieve optimal network performance while minimizing the total energy of the network. The throughput and delay are analyzed for heterogeneous traffic categories of MDs.

In Chapters 5 and 6, different physical layer techniques are discussed, that can achieve higher network capacity. In Chapter 5, we discuss the Fi-Wi uplink transmission of WiFi signals. The use of Fi-Wi channels provides the indoor net-

work with two degrees of freedom. First, multiple optical wavelengths are available to transport the radio signals to different CANs. Next, the radio channels at each CAN can be spatially reused. Utilizing both degrees of freedom, we discuss a multi-user detection technique (namely Successive Interference Cancellation (SIC)) and propose an opto-spatial multiplexed multi-user Multiple Input Multiple Output (MU-MIMO) uplink scheme which increases the ergodic network capacity achievable. It also helps in resolving the inherent problem of hidden nodes caused due to the carrier sense multiple access/collision avoidance (CSMA/CA) MAC contention mechanism of WiFi.

Chapter 6 focuses on the Fi-Wi downlink. In this chapter. we propose a downlink MU-MIMO MD scheduling scheme that tries to maximize the overall downlink network capacity by taking into account the different MD's demands of throughput and their respective channel gains. The algorithm also tries to ensure the different QoS demanded by the MDs. We evaluate the proposed scheme under both perfect and imperfect channel state information at the transmitter (CSIT).

Finally, in Chapter 7, we conclude by highlighting our main findings and present directions for future research in this area.

2

RoF Network Architecture

Fiber-to-the-home is increasingly becoming common for supporting high data rate applications in indoor environments [30, 31]. The penetration of the optical fibers from the boundary of the indoor living spaces to individual rooms or hallways provides a future-proof infrastructure installation [32, 33]. Wireless coverage, on the other hand, offers the indoor users the much-needed flexibility and mobility. Thus the Fi-Wi infrastructure is a future-proof solution for broadband access in indoor environments [34, 35]. Fi-Wi hybrid indoor networks have been proposed with the motivation of supporting single wireless technologies such as IEEE 802.11x, where x=a, b, g, n, ac, etc., or for different wireless technologies, e.g., combining small cell and cellular technologies. The main idea is to provide the required network resources, such as spectrum, power, etc., to indoor MDs [36, 37]. This requires dynamic management of these resources. A centralized hybrid Fi-Wi architecture can provide this functionality in a convenient way as we will show in this dissertation.

The hybrid Fi-Wi architecture, as described by the MEANS project [17], consists of fiber links emanating from a central controller, the Home Communication Controller (HCC), to multiple locations, e.g., rooms, terminated by one or more cell access nodes (CAN) (see Fig. 2.1). The CANs connected to the HCC form a distributed antenna system (DAS). DAS is energy efficient and can reduce the hardware cost of installation over a longer period of time [36]. Using RoF technology, the radio signals generated at the HCC are distributed to the CANs, to provide radio coverage inside their cell areas. Thus instead of using a single large wireless network, the Fi-Wi architecture partitions the indoor network into smaller wireless femto-cell clusters with a centralized management. Via a control channel, the radio network manager, in the HCC, adjusts the transmission and reception
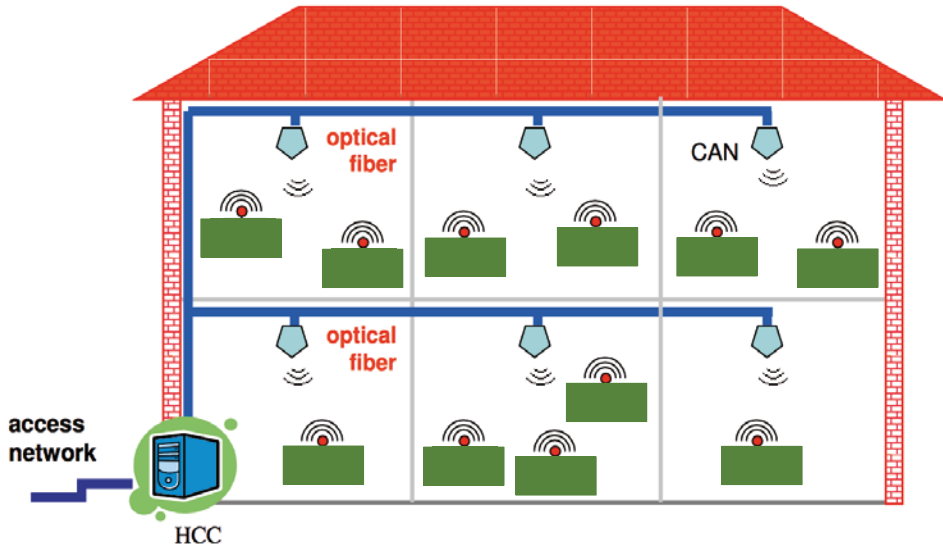
HCC : Home Communication Controller; CAN : Cell Access Node.

Figure 2.1: *Indoor hybrid Fiber-Wireless (Fi-Wi) architecture [17]*

parameters of the CAN to dynamically adapt the transmission power and the network topology, to match the traffic demands. The architecture is thus envisioned to enable the HCC and multiple CANs to provide indoor connectivity for a wide range of devices at data rates approaching the order of Gbps. Furthermore, since an RoF-based hybrid Fi-Wi architecture provides support to a wide range of radio protocols including Wireless Fidelity (WiFi), Long Term Evolution (LTE), Universal Mobile Telecommunications System (UMTS), etc., the entire wireless transmission capacity can be increased.

In this dissertation, however, we study the research challenges (as mentioned in Chapter 1) for hybrid Fi-Wi networks considering the most widely adopted small cell wireless technology, namely WiFi. Most indoor environments today are opting for a centralized deployment of WiFi APs, which follows the control and provisioning of wireless access points (CAPWAP) standard [38], for managing the WiFi radio resources. CAPWAP utilizes a split MAC architecture, where the IEEE 802.11 functions are implemented across multiple entities instead of a single entity. The APs in CAPWAP are referred to as light-weight APs (LWAP) (Fig. 2.2), providing a simplified attachment point for WLAN MDs. They perform functionalities such as (a) real-time 802.11 MAC functions (beacon generation, probe re-
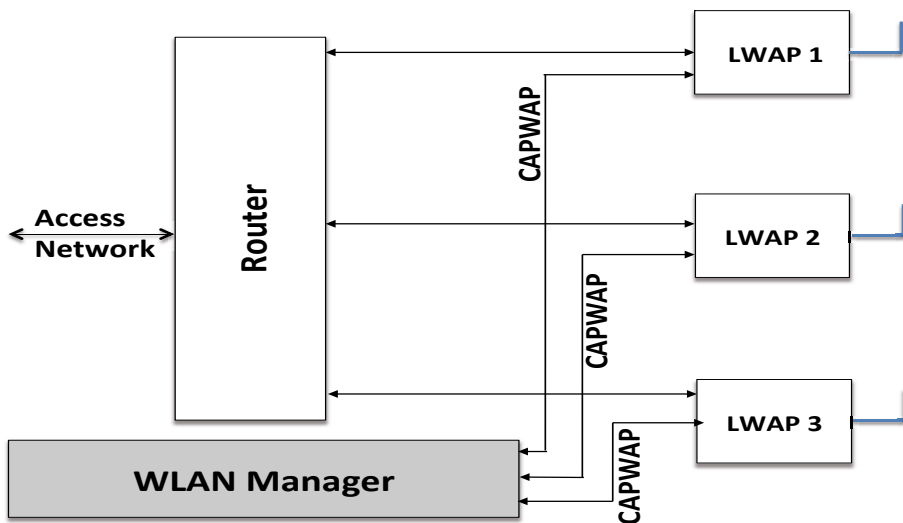
CAPWAP : Control and Provisioning of Wireless Access Point; LWAP : Light-Weight Access Point

Figure 2.2: *Traditional CE-WLAN*

sponses, power management, packet buffering, MAC layer data encryption and decryption, etc.), (b) radio frequency spectral analysis (c) fragmentation and re-assembly, etc. They are connected to a central controller, the WLAN Manager. The WLAN Manager performs functionalities such as (a) security management, (b) configuration management, (c) non real-time 802.11 MAC functions (Association, Disassociation, Reassociation, 802.1X EAP Authentication, Encryption, etc.), etc. It connects to multiple LWAPs via an interconnection medium. This can be a direct connection, layer 2 switched or layer 3 routed network. The Router is used for routing the messages from the access network to several LWAPs and vice-versa. This centralized enterprise WLAN (CE-WLAN) architecture[1] allows for centralized radio resource distribution between the LWAPs that are connected to the WLAN Manager. However, the traditional CE-WLAN architecture still does not allow the network to satisfactorily make use of the dynamic variation in MD traffic load across space. We will show that an RoF-based CE-WLAN has better performance.

In the following sections, we describe in detail the basic building blocks of the Fi-Wi architecture. The generalized description of the building blocks is discussed with respect to the implementation of the RoF CE-WLAN.

---

[1]From henceforth we will refer to this architecture as the traditional CE-WLAN deployment

2.1 Home Communication Controller
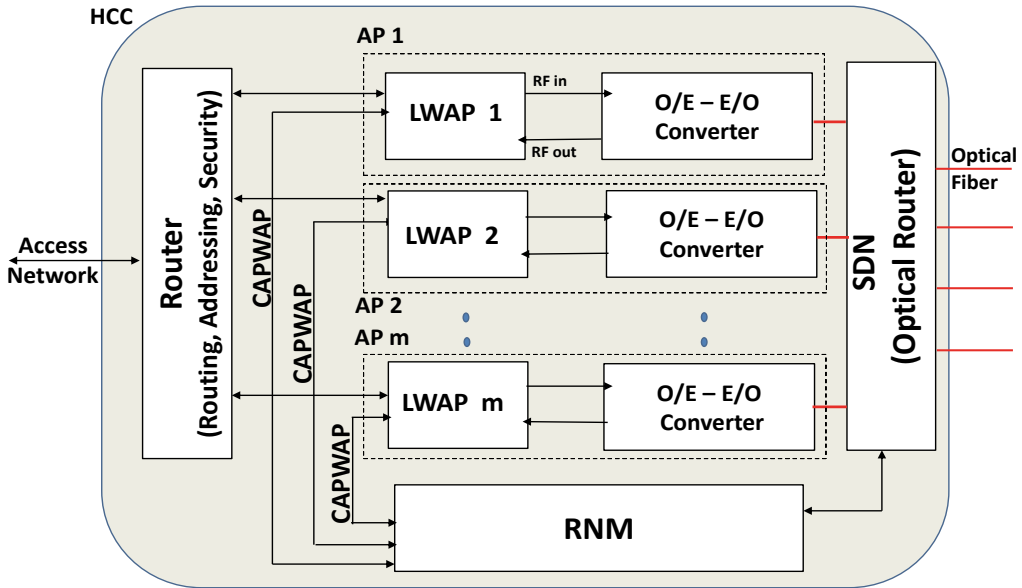
HCC

AP 1

LWAP 1

RF in

RF out

O/E – E/O Converter

LWAP 2

O/E – E/O Converter

AP 2

AP m

LWAP m

O/E – E/O Converter

Router (Routing, Addressing, Security)

CAPWAP

CAPWAP

CAPWAP

Access Network

SDN (Optical Router)

Optical Fiber

RNM

HCC : Home Communication Controller; AP : Access Point; RNM : Radio Network Manager; SDN : Signal Distribution Network; O/E − E/O Converter : Optical/ Electrical and Electrical/Optical Converter; LWAP: Light-Weight AP; CAPWAP: Control and Provisioning of Wireless APs.

Figure 2.3: *Home Communication Controller (HCC) for Centralized Enterprise WLAN*

The Home Communication Controller (HCC) is a home gateway that offers managed services indoors. Its design conforms to the vision of the Home Gateway Initiative (HGI) [39]. The HCC can be thought off as an evolution of the prevailing residential gateways such as the Digital Subscriber Line (xDSL) technology modem or the cable set-top box. It establishes an optically transparent connection between several APs[2] colocated at the HCC and CANs, that are placed indoors, using RoF technology, thus providing optical routing of radio signals between APs and CANs. The HCC performs medium access control (MAC), switching, optical/electrical and electrical/optical conversion, electrical routing and protocol conversion for MDs that communicate using different radio standards. Apart from optical routing as stated above, the HCC may first process the radio signals,

---

[2]Note that in a hybrid Fi-Wi architecture the AP modules, represented in Fig. 2.3, are a combination of LWAP module and an O/E - E/O converter.

for other purposes, by performing optoelectronic conversion first. One of the most important functionalities of the HCC is that it can host management and control intelligence for the whole network including tracking of MDs and robots, and cognitive functions to learn and anticipate the communication needs of the users of the network. An overlay of functional clusters of devices over the physical infrastructure is possible because of the routing functionality of the HCC. This evokes dynamic topology and configuration management services for efficient use of radio resources.

Thus, in a nutshell, the HCC establishes connections between the access network (e.g., DSL network, cable network, satellite network, and fiber network) and the indoor network which allows the users to get access to the public networks and its services. The HCC launches applications for the users and the MDs in the indoor coverage area and it performs intelligent routing, addressing, filtering and security functions for signals that have to be sent to and received from remote applications in the public domain. The HCC is also envisioned to host storage and processing functionalities for devices (e.g., local data server, a multimedia server or a server for local applications).

The architecture of the HCC (see Fig. 2.3) also includes extra components for the management and operation of the system. The management and control functionality at the HCC is performed by a dedicated unit, the radio network manager, which also allows for easy software updates and diagnostic checks to be administered by the operator. Also, a very important component, namely the signal distribution network, allows the optical wavelengths to be multiplexed in the downlink to different CANs or to be de-multiplexed from the CANs to the APs colocated at the HCC in the uplink. The detailed functionalities of the radio network manager and the signal distribution network are discussed below.

2.1.1 Radio Network Manager

The Radio Network Manager (RNM) is an integral part of the HCC. The RNM manages the overall network and has a similar role as that of the wireless network manager described by IETF in the CAPWAP architecture [40] of CE-WLAN. It typically performs the Layer 2 functionality of authentication, encryption and access control. The RNM is assumed to have overall knowledge about the traffic distribution across the CANs (and in-turn across the APs). It decides to which AP a CAN is connected and to which AP a MD is connected, in case a MD finds itself in the coverage area of two CANs.

2.1.2 Signal Distribution Network

The Signal Distribution Network (SDN) routes the optical signals (generated after the optical/electrical conversion across each LWAP, see Fig. 2.3) to the CANs. In the uplink, the SDN is used to demultiplex the optical signals coming from different CANs and feed them to the APs inside the HCC. This routing allows for the high flexibility that is achievable in such hybrid Fi-Wi architecture. The SDN can allow connections of one AP to multiple CANs or multiple CANs to a single AP. Thus the dynamic mapping of CANs to APs is done by the SDN under control of the RNM. A typical example of the SDN is the Micro-Electro-Mechanical Systems (MEMS) switch described in [41], which provides optical cross-connectivity between the number of input and output fibers. This allows for simultaneous connections between the multiple inputs (optical signals from the APs) to output fibers connected to the CANs, or vice-versa. This matrix switch can be found in any $M \times N$ size (up to 16×16) using MEMS mirror technology.

2.2 Cell Access Node
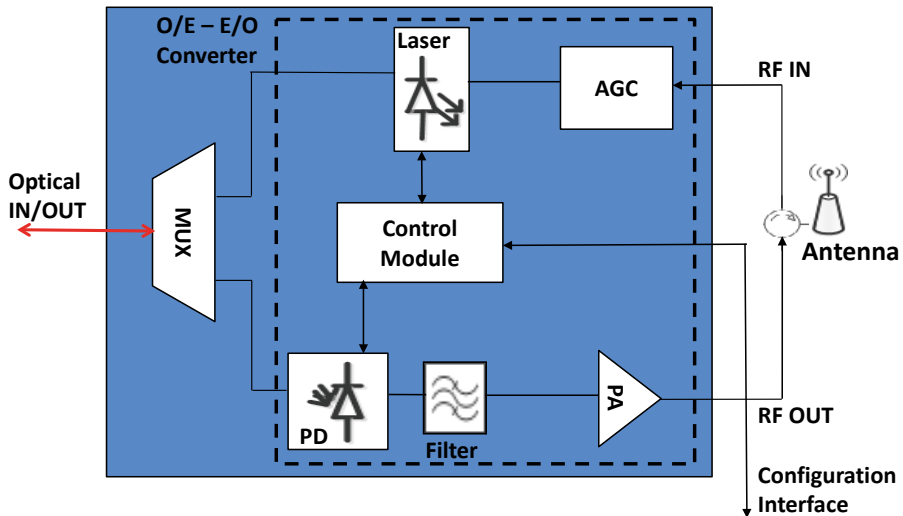
MUX : Multiplexer; AGC: Automatic Gain Controller; PA : Power Amplifier; PD : Photodiode.

Figure 2.4: *Generalized architecture of a Cell Access Node (CAN)*

The Cell Access Nodes (CANs) are antenna units deployed for coverage of in-

door femto-cells. The CANs are connected to the HCC using low-cost fiber links and are fed with RoF microwave signals generated at the HCC. The RF signals are transparently transported from the HCC to the CANs and vice-versa. CANs are thus considered as antenna devices which operate at the physical layer. They are bi-directional network devices that form the interface between the optical and the radio domains and are capable of receiving and transmitting radio signals over a wide range of frequencies.

The generalized architecture of the CAN (as shown in Fig. 2.4) consists of an O/E - E/O converter unit (with additional components for control and management) and a transmit/receive antenna. The O/E - E/O converter converts the optical signal input in the downlink to radio signal (using photo-diode, filter, and power amplifier). Similarly, in the uplink, the O/E - E/O converter converts the radio signal to the optical wavelength (using an automatic gain controller and laser). CANs are placed in close vicinity of the MDs and thus help in reducing the transmit power level of the radio signals. This in turn reduces the interference with the neighboring cells, which helps in increasing the overall network capacity.

It is envisioned that CANs have minimal functionality, as most of the processing operations are performed at the HCC. The connectivity of the CAN can be changed dynamically with the APs colocated at the HCC due to the use of transparent RoF technology supported by the optical backbone. Moreover, multiple antennas across an individual CAN or multiple CANs can be used to provide advanced MIMO support for different wireless technologies. CANs thus form an integral part of the Fi-Wi network architecture and are powered via an external source or possibly via the connecting fiber using Power-over-Fiber technology [42]. The full flexibility in the selection of radio and optical channels across each CAN opens the possibility to use different wavelengths for different services. Thus it is also possible to separate networks for security or other purposes. In addition to the data channels at the CANs, there are control channels to allow communication between the control modules at the CANs and the radio network manager at the HCC (see Fig. 2.4). The control module can control the antenna amplifier gain and selects the wavelength and sub-carrier used by the up and downlink data channels. A detailed description of a prototype implementation of the CAN can be found in [41].

The hybrid Fi-Wi architecture can be thought to form a tree with the HCC at the root, and with the CANs at the leaves. The fundamental physical layer support is the RoF technology. The RoF technology needs to be transparent to any radio standards that are carried on the fiber links. At the HCC, the modulation of various wireless services can be done by either an external modulator or a

direct modulator. The wireless data can be multiplexed using sub-carrier multi-plexing (SCM) when the frequencies overlap in the RF domain. It is also possible to up-convert signals to the mm-wave band by employing the optical frequency multiplication (OFM) method as proposed in [15, 16] for their transportation over fiber. However, one important thing to note is that OFM requires frequency shift-ing or down-conversion, which can be performed at the CANs. Thus an RoF-based hybrid Fi-Wi architecture is able to increase cell capacity by supporting multiple radio standards.

3

Dynamic Radio Resource Management

Introduction

The unlicensed industrial, scientific and medical (ISM) spectrum band, of 2.4 GHz, is getting highly congested due to the enormous growth of WiFi devices, other technologies (e.g., ZigBee, Bluetooth and wireless A/V) and interfering devices (e.g., microwave ovens) in the same band [43]. Moreover, recent studies characterizing traffic loads in public area wireless networks have shown that: (a) mobile device (MD) traffic loads are time-varying and location dependent, (b) MD load is often unevenly distributed across APs, and (c) at any given time the traffic load of the network is not well correlated with the number of MDs associated with those APs [44]. This results in lower achievable data rates by the WiFi MDs. It also causes unbalanced network resource utilization owing to the dynamic variation in MD load across time and space. These issues can be addressed by a proper radio resource management.

As mentioned in Chapter 2, most indoor environments today are adopting a centralized deployment of WiFi APs, which follows the control and provisioning of the CAPWAP standard [38]. The traditional centralized enterprise WLAN (CE-WLAN) architecture (see Fig. 2.2, in Chapter 2) allows for centralized radio resource distribution between the lightweight APs (LWAPs) that are connected to the WLAN manager. However, the architecture does not allow to make use of the dynamic variation in MD traffic load across space.

The hybrid Fi-Wi architecture is pursued as the way forward for our evolving indoor future data communication needs [34, 35, 45, 46] because of the several advantages described in Chapter 2.

This chapter addresses how the hybrid Fi-Wi architecture performs dynamic

radio resource management to balance the load between APs[1] and hence improves the performance. Let us illustrate this by means of the following example.
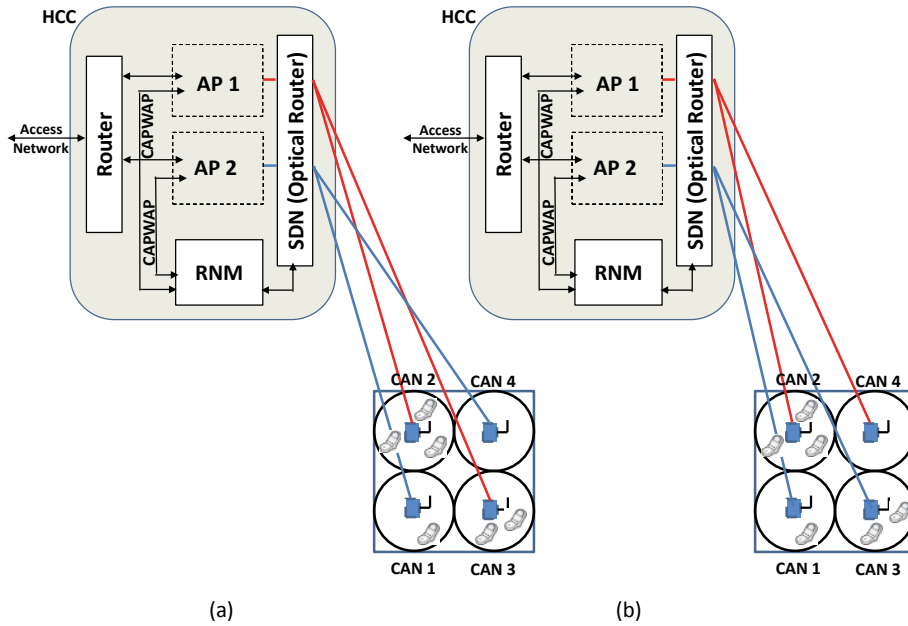
HCC : Home Communication Controller; CAN : Cell Access Node; AP : Access Point; RNM : Radio Network Manager; SDN : Signal Distribution Network; CAPWAP : Control and Provisioning of Wireless APs.

Figure 3.1: *Fi-Wi dynamic resource management (a) Initial CAN-AP association (b) Load balanced CAN-AP association*

Example 3.1.1. In Fig. 3.1(a) we can observe that AP 2 serves CAN 1 and CAN 4 and AP 1 serves CAN 2 and CAN 3. The load level across AP 1 is very high as there are a large number of MDs served by CAN 2 and CAN 3, whereas AP 2 is underutilized, as there is only one MD served by CAN 1 and no MD is served by CAN 4. The Fi-Wi architecture allows us the flexibility of changing connections of APs with CANs. Thus balancing the load level across APs by switching CAN 3 to AP 2 and providing CAN 4's connectivity through AP 1 can improve network performance. Thus offering a more balanced load distribution across APs as seen in Fig. 3.1(b).

---

[1]Note that in a hybrid Fi-Wi architecture the AP module represented in Fig. 2.3 (Chapter 2) is a combination of LWAP module and an optical to electrical/electrical to optical converter.

In the Fi-Wi architecture, the dynamic connectivity between APs and CANs allows for a flexible distribution of the load between APs. This chapter, therefore, addresses the issue of WLAN load balancing for such RoF CE-WLAN via dynamic assignment of CANs to APs.

The remainder of the chapter is organized as follows. Section 3.2 reviews existing literature about load balancing techniques in WLAN. Section 3.3 provides an overview of our research contributions. Section 3.4 provides a description of our system model. In Section 3.5 we utilize the total uplink delay to formulate the load balancing problem. In Section 3.6 we utilize the total downlink delay for formulating the load balancing problem. In Section 3.7 we then propose a heuristic algorithm, the dynamic assignment (DA) algorithm, for load balancing. We study the impact of the algorithm on the uplink and downlink delay, in Section 3.8. The conclusions from the chapter are presented in Section 3.9. Moreover, in Appendix A, utilizing the definitions from coalition game theory, we also prove that the proposed DA algorithm will always give us the optimal assignment between CANs and APs which reduces the total delay (uplink or downlink) of the network.

3.2   Literature survey

An extensive amount of literature is available about the association of MDs with APs. The most commonly used methodology is based on the received signal strength indicator (RSSI). It has been shown that RSSI can be a poor indicator of the AP's performance [47] as it does not provide any information about the number of MDs already associated with an AP.

The least-load association algorithm is implemented across various WLAN equipment [48]. This only takes into account the AP load, as a decision factor and associates the new MD with the least loaded AP. In [49, 50] a distributed association policy is proposed, where MDs associate with the AP that provides the best congestion relief taking into account the data rate and the number of MDs already associated with the AP. In [51] a MD-driven AP association is proposed for load balancing that achieves greater fairness and throughput. A centralized association policy for multi-rate WLANs was proposed in [52] based on the exchange of cell status information between the APs.

Different metrics were used to perform load balancing across APs. In [53] the available bandwidth across APs was used to associate MDs to APs. In [54] the association of MDs to APs was done to balance the download throughput in densely populated multi-cell WLANs. In [55, 56] the airtime cost (representing

the uplink delay) was used as an association metric for MDs to APs. Similarly, different mathematical tools were used to study the problem. In [48, 49, 53, 54], different optimization techniques were used to model the problem. In [57] AP selection is modeled using non-cooperative game theory between MDs and network service providers. In [58] modeling of the multi-homing problem in multiple simultaneous AP selection across MDs is performed using population game, which is a branch of game theory that models strategic games.

But none of the solutions mentioned above have the possibility to dynamically adapt the cell areas (served by CANs) to reduce the congestion level in overloaded cells. Thus, the spatial variation of MD traffic was never effectively addressed. Moreover, most of the heuristic algorithms proposed in the above-mentioned literature could prove that their algorithm would achieve the most efficient Nash equilibrium solution.

A lot of literature exists that investigates the feasibility of WiFi simulcast transmissions from an individual AP to multiple distributed antennas (CANs in our case) over an RoF system [59--61]. But none of those papers proposes any algorithm to dynamically assign the connections between APs and the distributed antennas.

3.3 Problem definition and contribution

Variable MD traffic across APs can lead to a large disparity in the delay observed by the MDs connected to different APs. An RoF CE-WLAN network has the potential to reduce latency experienced by the MDs. Latency has a number of components: propagation delay, queueing delay, and processing delay experienced by the packet sent over a network. In this chapter, we investigate how and to what extent dynamic capacity reconfiguration among APs can improve network performance by changing the connections between CANs and APs.

The MAC and PHY layer at the WiFi APs and the MDs take care of queuing, channel access, and the packet transmission to their respective destinations. In an RoF-based CE-WLAN network, the queueing delay dominates the processing and propagation delay, at high loads, due to the inherent femto-cell network architecture[2]. Queueing delay, at the AP or the MDs, thus reflects the level of congestion in the network. Looking at Fig. 3.2, we can visualize the MAC queues at both AP (downlink queue) and the MDs (uplink queues). WiFi employs a con-

---

[2]This is because, in femto-cell network architecture, the individual cell areas are typically in the order of meters, 10 m or less [62]. Thus processing and propagation delay, including optical fiber propagation delay, is of the order of μs's. While, queueing delay, at high loads, is usually in the order of of ms's, due to the contention based access nature of WiFi.

tention based MAC, so all the MDs and even the AP compete against each other to gain access to the wireless channel to send their packets. A head-of-the-line queued packet intended for a MD (in the downlink) or AP (in the uplink) has to wait its turn until the MD or AP gains access to the channel and transmits it. Moreover, the packet can undergo collisions, e.g., hidden node collisions which could cause the source (MD or AP) to retransmit the same packet until the retry limit for the packet is reached and then the packet is dropped. All this contributes to the delay (both uplink and downlink). Thus, as the packet transmission from the uplink or downlink queue is interleaved, improved network congestion is reflected by a reduction in either uplink or downlink delay. The same explanation holds if we employ different MD traffic categories and QoS support as is specified in the IEEE 802.11e standard [63].
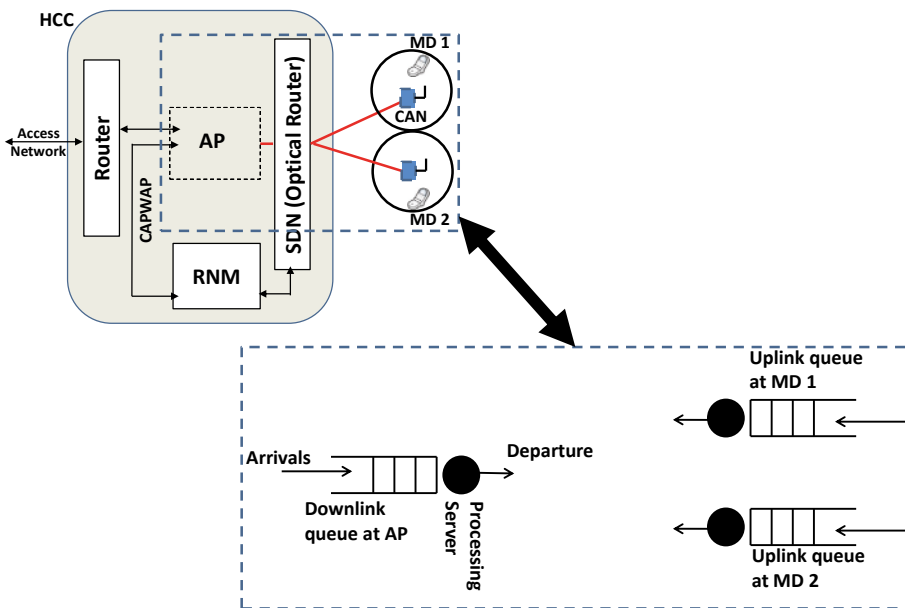
HCC : Home Communication Controller; AP : Access Point; RNM : Radio Network Manager;
SDN : Signal Distribution Network; CAPWAP: Control and Provisioning of Wireless APs.

Figure 3.2: *MAC uplink and downlink queueing model*

Uplink delay

We define uplink delay as the delay experienced by the MD to successfully transmit a packet to the AP. Thus we calculate uplink delay starting from the time that a MD has a packet to send to an AP, located at the HCC, until the time the

packet is successfully received at the AP.

However, the aforementioned metric of uplink delay is difficult to measure. Since the uplink traffic is sent by the MDs to an AP, there is no general way to measure it without modifying the MAC protocol, or utilizing active probes in the wireless cells [64]. Since both approaches are not feasible, indirect approaches are also discussed in [65], but it requires tracking of flows from every MD to the AP which is a costly operation. In [55, 56] the uplink delay is approximated using a much simpler parameter, *airtime cost*, for solving the association problem of MDs to an AP.

Airtime cost

Airtime cost was proposed in [66] as a routing metric for wireless mesh networks in the IEEE $802.11s$ standard. Airtime cost is defined as the amount of channel resources consumed when transmitting a packet over a particular link. It reflects the average per packet delay experienced by a MD to successfully transmit a packet to the AP.

It has been corroborated in [56] as being equivalent to the average uplink transmission delay under saturated conditions, where all the MDs have packets to send. But they do not take into account the effect of hidden node terminals. Hidden nodes cause collisions and thus contribute to the delay. Especially in RoF-based CE-WLANs, where multiple CANs can connect to the same AP, the hidden node effect may be significant. If we look at Fig. 3.1 (a), we observe that AP 1 is connected to CAN 2 and CAN 3. Thus for any MD in CAN 3, all other MDs in CAN 2 are hidden as they are not in the sensing range of each other. So, in this chapter, we model the uplink delay using airtime cost, which also takes into account the hidden node effect.

Airtime cost to approximate the uplink delay is only a good approximation under the saturated condition when MDs always have packets to send [56]. A much simpler calculable parameter, devoid of such approximations, is the downlink delay.

Downlink delay

The downlink delay is defined as the delay experienced by the AP to transmit a packet to a MD successfully. The downlink delay for transmission comprises the queueing delay experienced by the MD packet at the AP, located at the HCC, along with the downlink transmission time from the AP to the MD.

It can be accurately measured at the AP and two approaches can be used,

- The first approach [67] is to associate a time-stamp to individual packets

that arrive at the downlink queue and use this value to measure the delay of each individual packet.

- The second approach [68] monitors the queue length at the AP at fixed intervals and then it approximates the average delay in the interval.

The downlink delay does not depend on the MD, but on the type of MD traffic category (i.e., Access Category) as the dominant component of the delay is queuing delay at the AP, which does not rely on specific flow or packet size. This simplifies delay monitoring. Moreover, downlink delay can be justified as the most crucial parameter because in most traffic scenarios the AP is the first to become saturated. This is because the downlink traffic is usually significantly higher than the uplink traffic, or even when the two are comparable then also it is sent from one source only, namely the AP.

Our main contribution is that we propose a CAN-AP association algorithm that dynamically changes the connectivity between CANs and APs to improve the network performance by distributing the load evenly across APs.

3.4 System model

Let us again consider Fig. 1.1 in Chapter 1. The set $M = \{1, 2, ..., m\}$ of WiFi APs hosted in the HCC is used to provide connections to the set of CANs $N = \{1, 2, ..., n\}$, where $n > m$. In this chapter, we assume that multiple CANs can connect to a single AP[3]. Wavelength Division Multiplexing (WDM) is used as the signal distribution technology, where the optical wavelengths carrying the radio signals generated by the APs are multiplexed to different CANs in the downlink. The management functionality of deciding which CANs to connect to which AP is performed by the RNM. The RNM as mentioned in Chapter 2 serves as the centralized controlling entity, which is assumed to have an overview of the whole network connectivity and traffic load information[4]. The set of MDs covered by the network is represented by $I = \{1, 2....i\}$ and we denote the set of MDs associated with CAN n by I_n. We make the following assumptions:

---

[3]The case where multiple APs can connect to the same CAN is neglected because it is similar to the case where multiple APs connect to different individual CANs where all those CANs are placed very close to each other and they provide coverage to the same cell area.

[4]The RNM is assumed to maintain information about each AP in a state table. Some information is static, e.g., the AP name and IP hardware address. Additionally, some information is dynamically varying like associated MD set to each AP and the AP load, which can be updated at the RNM by sending periodic requests to the APs.

- **The neighboring CANs do not have overlapping cell areas.** Thus each CAN provides coverage to a unique cell area. This assumption separates the problem of load balancing from the problem of frequency planning. We are aware that this assumption is not realistic, as in real life the WiFi cell areas are always overlapped, but this assumption allows us to judge the performance of the load balancing algorithm better. This assumption can impact the continuity of MD's service when moving from one cell area to another, served by different APs. This is because of the start-up latency, owing to authentication and association to the new AP, which is a mandatory cost.

- **The distribution of MDs inside the cell areas is assumed to be random.**

- **The fiber channel is ideal.** This is a valid assumption owing to the fact that the fiber length in average homes would not exceed a few hundred meters and thus fiber dispersion would not be significant.

- **The added extra propagation delay of the signals due to the fiber lengths is negligible.** Extra propagation delay may have a negative impact on the performance of the MAC if it exceeds certain timeouts of the WiFi MAC protocol and the network performance could become worse. The extra propagation delay might require adjustment of MAC parameters, e.g., acknowledgment time-out [69].

3.5 Uplink delay

As mentioned previously, the uplink delay is modeled using airtime cost.

The airtime cost for RoF-based CE-WLAN can be expressed under the following conditions: (a) every MD is saturated, i.e., it always has a packet ready for transmission; (b) the collisions due to hidden nodes are also considered.

Thus for a MD i connected to AP b using CAN a, the airtime cost can be expressed as:

$$\Delta^{b\{a\}}(i) \;\; = \;\; \frac{(O_{ca} + O_p + \frac{B_t}{R_a^b(i)})}{1 - e_{pt}} + \left[\frac{(O_{ca} + O_p + \frac{B_t}{R_a^b(i)})}{1 - e_{pt}} \right]\eta \quad (3.1)$$

The first term in (3.1) represents the channel resources consumed due to the transmission of the packet from MD i assuming saturated conditions across all MDs [56]. The second term represents the extra channel resources consumed due to the hidden nodes [70].

O_{ca} and O_p represent the channel access overhead and protocol overhead respectively. B_t represents the number of bits in a test packet. The values specified in IEEE $802.11b$ for $O_{ca} + O_p$ and B_t are 1.25 ms and 8224 bits. $R_a^b(i)$ embodies the transmission rate between AP b and MD i under CAN a. e_{pt} is used to represent the packet error rate for the test packet.

Packet error rate is the probability that, when a packet of standard size B_t is transmitted at data rate $R_a^b(i)$, the packet is corrupted due to a transmission error. This can be ignored if the transmission error rate at the MD is low.

Finally, η represents the packet collision ratio due to hidden nodes. It is defined as follows.

The **packet collision ratio** is the percentage of time hidden nodes will consume if they get the chance to transmit and can be given as [70]:

$$\eta = 1 - \prod_{j \in \{C^b - \{a\}\}} (1 - TX_j) \tag{3.2}$$

where C^b represents the set of CANs which are operating under the same AP b. TX_j represents the packet transmission time ratio for hidden MD j and is given as [70]:

$$TX_j = \frac{\frac{B_t + \psi}{R_a^b(j)}}{T_t} \tag{3.3}$$

where ψ represents the MAC control packet size and is taken to be 28 bytes. T_t represents the total time interval of the whole test data frame including short interframe space (SIFS), distributed interframe space (DIFS), Acknowledgment (ACK), test data packet and header transmission.

Remark that we can estimate the packet collision ratio by using information about the list of MDs that are hidden from each other and the rate at which all the hidden MDs are connected to the AP [5].

---

[5]Here we assume that the AP connected to multiple CANs can make a list of the MDs connected through different CANs and the packet transmission time ratio for those MDs connected to the AP. We can assume to list the different set of MDs connected through different CANs by using the control modules (see Fig. 2.4 in Chapter 2) at the CANs and the MD authentication information at the APs. Each MD, when it associates with an AP, shares the MAC ID of the device with the AP, which in turn updates the RNM status list of connection between MD and AP. At the same time the MD associates to an AP using a CAN, which sends a control signal to the RNM signaling that it is active. Thus information available at the RNM allows listing MDs connected to an AP through different CANs.

The airtime cost across AP b serving CANs associated with it can be given as:

$$\Delta^b = \sum_{a \in C^b} \sum_{i=1}^{A_a^b} \Delta^{b\{a\}}(i) \tag{3.4}$$

where A_a^b represents the number of MDs associated with CAN a, which is connected to AP b.

3.5.1 Optimization with respect to uplink delay

The main problem now is to decide how to change the association of the CANs with different APs over time.

Problem statement: Given a set of APs $M = \{1, 2, ...m\}$ and CANs $N = \{1, 2, ...n\}$ (where $n > m$) and an initial mapping of APs to CANs, devise a strategy to assign CANs to APs such that the **total uplink delay** is minimized.

We use the total uplink delay to represent the network congestion level because of the following.

We know that the performance bottleneck for Internet traffic is the wireless last hop between the AP and the MD [71]. The WiFi access model does not provide any guarantee about the delay of the transmissions as compared to cellular technologies [72]. Some effort to guarantee QoS is made if IEEE 802.11e is employed. But even then the typical uplink delays for single hop transmission for a single MD communicating with an access point is more than 100 ms, which deteriorates heavily when more MDs use the network. We thus choose the total uplink delay, approximated by total airtime cost, across all the APs as a parameter to be minimized.

Let us suppose CAN j is connected to AP k and it achieves an airtime cost of b_{jk} from all the MDs connected to AP k, using CAN j. An AP can serve a CAN only when both are associated with each other. When CAN j is associated with AP k, the airtime cost of CAN j is:

$$\Delta^{k\{j\}} = b_{jk} \tag{3.5}$$

The airtime cost across AP k for all the CANs associated to it is:

$$\Delta^k = \sum_{\forall j \in C^k} \Delta^{k\{j\}} \tag{3.6}$$

Thus the problem of reducing the *total uplink delay*, approximated by using total airtime cost, can be formulated as the following optimization problem:

$$\text{Minimize} \sum_{k=1}^{m} \Delta^k \tag{3.7}$$

subject to

$$\Delta^{k_{\{j\}}} = b_{jk} \tag{3.8}$$

$$\Delta^k = \sum_{\forall j \in \mathcal{C}^k} \Delta^{k_{\{j\}}} \tag{3.9}$$

$$b_{jk} \geq 0, \quad j \in \mathsf{N}, k \in \mathsf{M} \tag{3.10}$$

3.6 Downlink delay

In Section 3.6.1 we discuss the average queueing time experienced by the MDs and in Section 3.6.2 the downlink transmission time experienced by the MDs.

3.6.1 Average downlink queueing time

We calculate the average queue waiting time for three categories of MDs traffic: video streaming (VS), best effort (BE) and constant bit rate (CBR). We assume separate downlink queues corresponding to each of the MDs ($i \in I$) at the HCC. Let us represent the number of packet arrivals to the queue for MD i as $F_i(t)$. The mean arrival rate to MD i can thus be given by $\nu_i = E\left[F_i(t)\right]$. The mean arrival rate vector is given by $\boldsymbol{\nu} = \{\nu_1, \nu_2, \ldots, \nu_i\}$ and the queue length vectors are represented as $\mathbf{q(t)} = \{q_1(t), q_2(t), \ldots q_i(t)\}$. Using discrete-time queuing law the evolution of the queues [73] can be given as:

$$q_i(t+1) = max\{q_i(t) - R_{mi}^{nD}(t)T_s, 0\} + F_i(t) \tag{3.11}$$

where T_s and R_{mi}^{nD} represent the duration of a slot time and the rate achieved by MD i when connected to AP m using CAN n respectively. By Little's theorem [74], the waiting time of MD i in slot t is:

$$D_i(t) = \frac{\overline{q_i}(t)}{\nu_i} \tag{3.12}$$

where $\overline{q_i}(t)$ represents the average queue length. The queueing models for the three MD types can be found in [75] and their average waiting time is calculated in [76].

- CBR traffic for MDs: These are modeled by a D/G/1 queuing system. The average waiting time is:

$$D_{i_{CBR}} = \frac{\nu_{i_{CBR}} \sigma^2_{\overline{T}_{i_{CBR}}}}{2(1 - \nu_{i_{CBR}} \overline{T}_i)}, \quad \forall i \in I \tag{3.13}$$

where $\nu_{i_{CBR}}$, $\sigma^2_{\overline{T_{i_{CBR}}}}$, $\overline{T_i}$ are the mean arrival rate, the variance of the service time and mean service time respectively and $\overline{T_i} = E\{\frac{1}{R^{nD}_{mi}(t))}\}$.

- VS traffic for MDs: Similarly, these are modeled by a G/G/1 queueing system, using a Gamma Distribution with shape parameter s, that affect the shape of the Gamma distribution. The average queueing time is:

$$D_{i_{VS}} = \frac{\nu_{i_{VS}}(\sigma^2_{\overline{T}_{i_{VS}}} + \frac{s}{\nu_{i_{VS}}})}{2(1 - \nu_{i_{VS}}\overline{T_i})}, \quad \forall i \in I \tag{3.14}$$

- BE traffic for MDs: These are modeled using an M/G/1 queueing system. The average queueing time is:

$$D_{i_{BE}} = \frac{\nu_{i_{BE}}(\sigma^2_{\overline{T}_{i_{BE}}} + \sigma^2_t)}{2(1 - \nu_{i_{BE}}\overline{T_i})}, \quad \forall i \in I \tag{3.15}$$

where σ^2_t is the variance of the inter-arrival time.

3.6.2 Downlink transmission time

For finding the downlink transmission time for a MD, we need to evaluate the downlink throughput that is achievable by the MD from the HCC. More specifically, from the AP. The achievable throughput in the downlink between AP m and MD i when connected through CAN n can be given as:

$$b^{nD}_{mi} = p^D_{mi}\frac{P_m R^{nD}_{mi}}{T_m} \tag{3.16}$$

p^D_{mi} represents the probability of successful transmission between AP m and MD i and $\frac{P_m R^{nD}_{mi}}{T_m}$ represents the normalized data rate for payload transmission from AP m, where P_m represents the transmission time of the payload. R^{nD}_{mi} represents the physical data rate. T_m represents the transmission time of the whole data frame including header and payload and can be given as:

$$T_m = H_m + T_{SIFS} + T_{DIFS} + T_{ACK} \tag{3.17}$$

where T_{SIFS}, T_{DIFS} represent the time consumed by the SIFS and the DIFS. T_{ACK} represents the transmission time due to acknowledgment and H_m represents the actual transmission time consumed by the header packets and the data packet.

Let us calculate p_{mi}^D. There is only one situation in the CSMA/CA based downlink transmission from the AP which accounts for all the collisions and can be given as the probability that other MDs in the CANs which are accessing the same AP m start transmitting in the same time slot as that of the AP. The probability that a MD attempts to transmit in an arbitrary slot can be given as $\vartheta = \frac{1}{CW_{avg}}$, where CW_{avg} represents the average contention window length. In the EDCF mode, VS, BE and CBR traffic have different contention window lengths [77], to provide service differentiation. Table 3.1 gives the values.

Table 3.1: Contention window table based on MD traffic category

MD traffic type	CW_{min}	CW_{max}
BE	15	1023
VS	7	15
Voice(CBR)	3	7

Therefore, the collision probability of AP m's transmission to MD i can be given as [78]:

$$p_{mi}^{collision} = 1 - \sum_{j \in \{BE,VS,CBR\}} (1 - \vartheta_j)^{\sum_{n \in N_m} \sum_{j \in \{BE,VS,CBR\}} i_{n_j}} \qquad (3.18)$$

where $i_{n_j} \; \forall j \in \{BE, VS, CBR\}$ represents the number of MDs with BE, VS, and CBR traffic across CAN n and $i_n = \sum_{j \in \{BE,VS,CBR\}} i_{n_j}$. N_m represents the set of CANs that can connect to AP m. ϑ_j represents the probability that a MD belonging to MD category j attempts to transmit a packet. Therefore, the probability of successful transmission from AP m to MD i can be given as $p_{mi}^D = (1 - p_{mi}^{collision})$. Thus the downlink transmission time of a packet from AP m to MD i is:

$$W_{mi}^{nD} = \frac{L_i}{b_{mi}^{nD}} \qquad (3.19)$$

where b_{mi}^{nD} represents the achievable throughput in the downlink between AP m and MD i connected through CAN n and L_i represents the average packet length for MD i.

The downlink delay for MD i connected to AP m using CAN n can thus be written as the summation of the average queueing time and the downlink transmission time as follows:

$$V_{mi}^{nD} = D_i + W_{mi}^{nD} \qquad (3.20)$$

where V_{mi}^{nD} is the downlink delay. It takes care of the heterogeneous MD categories with different traffic statistics and also of the changing MD density across space, i.e., cell areas and time. The downlink delay across AP m can be given as:

$$V_m^D = \sum_{n \in N_m} \sum_{i \in I_n} V_{mi}^{nD} \tag{3.21}$$

Our goal is to find an allocation policy that allocates CANs to APs to reduce the *total downlink delay* of the network, i.e., $\sum_{\forall m \in M} \sum_{n \in N_m} \sum_{i \in I_n} V_{mi}^{nD}$.

3.6.3 Optimization with respect to downlink delay

Similar to Section 3.5.1, the problem is to decide how to change the association of the CANs with different APs over time.

Problem statement: Given a set of APs $M = \{1, 2, ...m\}$ and CANs $N = \{1, 2, ...n\}$ (where $n > m$) and an initial mapping of APs to CANs, devise a strategy to assign CANs to APs such that the **total downlink delay** is minimized. Formally:

$$\text{Minimize} \sum_{\forall m \in M} \sum_{n \in N_m} \sum_{i \in I_n} V_{mi}^{nD}$$

$$= \sum_{\forall m \in M} \sum_{n \in N_m} \sum_{i \in I_n} (D_i + \frac{L_i}{b_{mi}^{nD}})$$

subject to

$$b_{mi}^{nD} \le p_{mi}^D \frac{P_m R_{mi}^n}{T_m}, \ \forall i \in I, n \in N, m \in M. \tag{3.22}$$

$$p_{mi}^D \le \sum_{j \in \{BE, VS, CBR\}} (1 - \vartheta_j)^{\sum_{n \in N_m} \sum_{j \in \{BE, VS, CBR\}} i_{n_j}} \ \begin{matrix} \forall i \in I, \\ n \in N_m, \\ m \in M \end{matrix} \tag{3.23}$$

$$D_i = \begin{cases} \frac{\nu_{i_{CBR}} \sigma_{\overline{T_{i_{CBR}}}}^2}{2(1 - \nu_{i_{CBR}} \overline{T_i})} & \text{CBR MDs} \\ \frac{\nu_{i_{VS}} (\sigma_{\overline{T_{i_{VS}}}}^2 + \frac{s}{\nu_{i_{VS}}})}{2(1 - \nu_{i_{VS}} \overline{T_i})} & \text{VS MDs} \quad \forall i \in I. \\ \frac{\nu_{i_{BE}} (\sigma_{\overline{T_{i_{BE}}}}^2 + \sigma_t^2)}{2(1 - \nu_{i_{BE}} \overline{T_i})} & \text{BE MDs} \end{cases} \tag{3.24}$$

Constraint (3.22) represents the downlink throughput for MD i connected to AP m using CAN n. Constraint (3.23) represents the probability of successful transmission in the downlink. Constraint (3.24) refers to the average queueing time for MD i's packet, which can belong to any category (VS, BE or CBR).

In the following section, we devise a dynamic assignment algorithm that re-assigns CANs to APs such that the total delay (either total uplink delay or total downlink delay) is minimized.

3.7 Dynamic CAN-AP assignment

The optimization problems, discussed in sections 3.5.1 and 3.6.3, are NP-complete in nature as has been pointed out in the literature [79]. So we propose a heuristic algorithm (Algorithm 1) for dynamic re-assignment of CANs to APs to minimize the total delay (either total uplink or total downlink). Since the connections of APs to CANs are coordinated in a centralized fashion, at the RNM, the APs cooperate among themselves to reduce the total delay. Each CAN will change its connection with a different AP when the total delay and the individual CAN delay can be reduced, which in turn results in a non-increasing total delay. As the algorithm either considers uplink or downlink delay as the congestion metric, we can choose any of them to describe the proposed algorithm. Let us consider the uplink delay.

Crossover operation: For any CAN i connected to AP x, the CAN will crossover to AP z if the following conditions are met.

$$\Delta^x + \Delta^z > \Delta^{x-\{i\}} + \Delta^{z\cup\{i\}} \tag{3.25}$$
$$\Delta^x > \Delta^{z\cup\{i\}} \tag{3.26}$$

Algorithm 1 Dynamic assignment (DA) algorithm

1 Initialize: Set M, N as the set of APs and CANs.
2 Assess load level: Find set, $M_c = max_{m\in M}\ \Delta^m$, of APs with maximum uplink delay.
3 Crossover payoff: Compute $(t, X) = max_{X\in M-M_c}\{\Delta^Z - \Delta^{X\cup\{t\}}\}\forall\{t\} \in Z$, where Z is an AP in M_c with lowest ID.
4 Swap: check if $\{\Delta^Z - \Delta^{X\cup\{t\}}\} > 0$
check if there exists (j, Y) that satisfies swap condition, then swap CAN t to AP Y and CAN j to AP X.
5 Crossover: Else crossover CAN t to X
6 Repeat Steps **3** till **5**, until no more APs in M_c has CAN to perform crossover operation.

CANs connected to the most congested AP x may crossover to a less congested AP z to reduce its uplink delay (see Fig. 3.3 (a)). AP x may thus become

less congested than AP z, but since the whole network uplink delay is reduced, these CANs will never crossover back to AP x. An AP-CAN assignment could be achieved this way, but not necessarily an efficient one.

An **efficient assignment** here implies the best possible outcome from the perspective of a decrease in total uplink delay of the network. This cannot be guaranteed just by following the crossover operation.

Below we first propose a dynamic assignment (DA) algorithm that can control the order of CANs association, using the global information available, so as to guarantee the convergence to an *efficient assignment*, that attains minimal total uplink delay for the network. We assume that each CAN and AP is assigned a unique address and each CAN is assigned to an AP initially.

The DA algorithm proceeds in rounds as follows. In each round, we first find the set of APs M_c with the maximum overall uplink delay, i.e., $\Delta_{max} = \underbrace{max}_{x \in M} \Delta^x$.

Since these sets of APs are the most congested ones, the objective is to find some CANs associated with them that satisfy the crossover condition and crossover these CANs to other less congested APs. By doing so, the congestion level of APs is reduced. Only one CAN is permitted to make a crossover in each time. Firstly, the APs in M_c are sorted in an increasing order according to their addresses, and the AP x with the lowest ID is selected. Then we can compute the crossover payoff for all CANs associated with AP x as follows:

$$\breve{\Delta}^{\{i\}} = max_{z \in M - M_c}\{\Delta^x - \Delta^{z \cup \{i\}}\} \quad \forall \{i\} \in x \qquad (3.27)$$

The crossover payoff is the maximum difference of airtime costs for CAN i to crossover from AP x to any other AP $z \notin M_c$. If $\breve{\Delta}^{\{i\}} \leq 0, \forall\{i\} \in x$, then it means that there is no benefit for any CAN associated with x to crossover to other APs. Otherwise, we can choose the CAN i with the maximum $\breve{\Delta}^{\{i\}}$ to crossover to its corresponding AP. We select the CAN with the lowest address to break a tie between CANs which achieve the same maximum difference $\breve{\Delta}^{\{i\}}$. In this procedure, after a CAN crossover from AP x to other AP not in M_c, the airtime cost of x is reduced, while the airtime costs of other APs in M_c remain the same. By repeating the same process for other APs in M_c, the maximum airtime cost of the whole network will strictly decrease at most in $|M_c|$ moves. The above procedure will be repeated until all APs are properly assigned at the end of this round. At the end of each round, all APs are fixed, but if there are still CANs satisfying the crossover condition in (3.25), (3.26) all APs will be labeled as free again and the above procedure is repeated until none of the CANs satisfies the crossover condition. Note that in each round of this procedure, the maximum uplink delay of the

network is strictly decreased, as given by equation (3.25). However, the assignment achieved with the above procedure is not necessarily an efficient one. If we look at Fig. 3.3(a), AP x is taken as the most congested AP, so we can crossover CAN i from AP x to z since it satisfies the crossover condition in (3.25), (3.26).

Swap operation: A better option for CAN i is to crossover to AP y and CAN j to crossover to AP z as shown in Fig. 3.3(b), which can lead to a lower congestion level across both APs. But this requires CAN j to make a crossover before CAN i, which is not allowed in the above procedure. To address this problem, we introduce a swap operation as shown in Fig. 3.3(b). This allows two CANs i and j to swap their APs if the following conditions are satisfied:

$$\Delta^x + \Delta^y + \Delta^z >> \Delta^{x-\{i\}} + \Delta^{y-\{j\}\cup\{i\}} + \Delta^{z\cup\{j\}} \tag{3.28}$$

$$\Delta^x > \Delta^y + \Delta^{y\{i\}} - \Delta^{y\{j\}}, \ \ \Delta^x > \Delta^z + \Delta^{z\{j\}} \tag{3.29}$$

$$\Delta^y > \Delta^z + \Delta^{z\{j\}} \tag{3.30}$$

$$\Delta^{y\cup\{j\}} + \Delta^{z\cup\{i\}} > \Delta^{y\cup\{i\}} + \Delta^{z\cup\{j\}} \tag{3.31}$$

where (3.28), (3.29) is the condition guaranteeing that the highest uplink delay is decreased strictly; (3.30) ensures that CAN j's interest is satisfied; (3.31) ensures that the swap operation will even further reduce the total uplink delay of the network than only making a crossover of CAN i from x to z.

By using the conditions given above we can perform a dynamic CAN-AP assignment under the availability of the perfect uplink delay, approximated using airtime cost, and global coordination across APs. Thus the algorithm gives a partition of APs and a set of their served CANs. Our main goal now is to prove that this partition is stable and attains the minimum total delay (total uplink or total
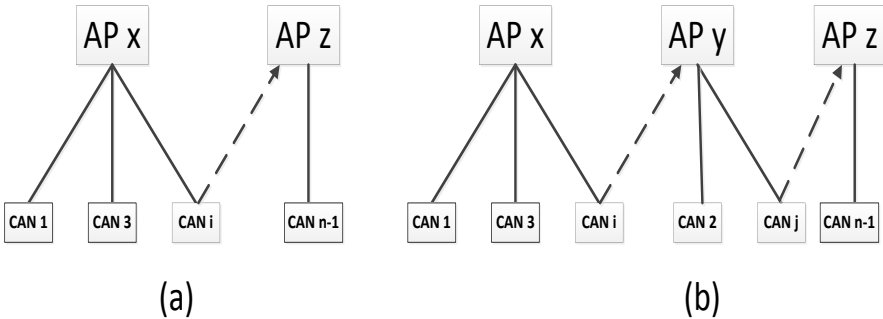

Figure 3.3: *(a) Crossover operation (b) Swap operation*

downlink) for the network. This, in turn, implies that the final partition of APs and the CANs they serve does not fluctuate to form any other partition.

Theorem 3.7.1. *The Dynamic assignment (DA) algorithm produces a stable partition, which achieves minimal total delay for the network.*

We use coalition game theory to prove this in Appendix A.

3.8   Results and discussion

Our analysis compares the performance of the proposed dynamic assignment (DA) against the static assignment (SA), that mimics the traditional WLAN deployment. We present our results from the following perspectives:

- The total airtime cost, i.e., total uplink delay, versus the (a) sorted AP numbers (described later), and (b) the number of MDs for both uniform and non-uniform MD distribution. This shows, how the airtime cost is distributed among different APs, which represents the utilization of the APs for different schemes, and the performance of the schemes when the number of MDs served in the network is increased respectively. Uniform and non-uniform MD distribution cases were studied as they represent scenarios where each AP has a similar amount of traffic to serve, and also the case where the traffic is dense in some areas and sparse in others, resulting in higher variations in AP usage.

- The total downlink delay versus the sorted AP numbers for a different number of MDs. This analysis validates how the same DA algorithm also results in better utilization of the APs as compared to the SA scheme.

For our simulations, we consider an indoor open office space network of size 20 m$\times 20$ m. There are 16 CANs (see Fig. 3.4), which are located at the center of each square grid cell area and are represented by red circles. 8 APs colocated at the HCC are used to provide connection to these 16 CANs[6]. A random deployment of MDs is studied for the network. They are depicted by blue dots in Fig. 3.4. The Fi-Wi network is studied under two different assignments of CANs to APs.

- **Static assignment (SA)**: Here the CANs are assigned a priori to the APs (see Fig. 3.4), and their connections are not changed for the whole simulation

---

[6]Note that each of the CANs is distributed in a square grid cell area of size 5 m$\times 5$ m. This is a typical femto-cell size, which usually ranges in the order of meters, 10 m or less [62].
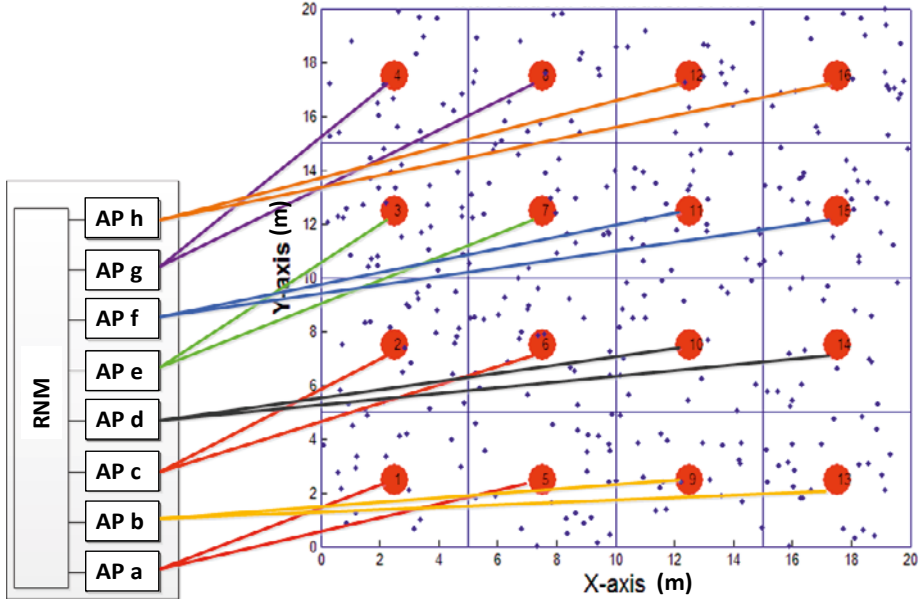
Figure 3.4: *Simulation scenario*

duration. This mimics the traditional deployment.[7] In our SA scheme we have the case which has been described before. In our SA simulation scenario each AP is connected to 2 non-overlapping CANs that are placed next to each other. This is a reasonable simulation scenario as distributing the MDs uniformly over the network topology will ensure that each MD has the same probability of lying in the coverage area of any AP. Moreover, as there is no overlap in the cell areas of the CANs connected to the same AP, the case where CANs connected to the same AP are not neighbors is just the same case as the one we simulated.

- **Dynamic assignment (DA)**: The second scheme is referred to as the DA scheme as described in Section 3.7. DA dynamically reassigns CANs to APs to reduce the network congestion.

---

[7]Note that there is a difference between our SA scheme and the traditional WiFi deployment. In a traditional WiFi AP deployment, the AP is not connected to many distributed antennas at separate indoor locations (CANs in our case), thereby removing the inherent hidden node problem as in the SA case. This is bound to increase delays observed in the uplink and the downlink.

For the association of MDs to APs, we assume RSSI-based association for both cases. We perform Monte Carlo simulations in MATLAB to obtain the numerical results. In our figures, we plot the average values of the total airtime cost (uplink delay) and the downlink delay, obtained over all the simulation runs or iterations. We select the initial location of the MDs randomly for each iteration.

Mobility model: For simulating the movement of MDs in the network, we use the random waypoint mobility model [80]. The mobility model is important in our simulations to model the movement of the MDs in the network. In this mobility model, the MD moves randomly where the destination and speed are all chosen randomly and independently of other MDs. The implementation of this mobility model in our simulations is as follows:

- At the beginning of an iteration, each MD randomly selects a location from the network topology as the destination.

- The MD then travels towards the destination with constant velocity chosen uniformly from $[0 - 1.5]$ m/s, where 1.5 m/s is the maximum allowable walking speed for the MD.

- At the destination, the MD stops for a duration called the pause time. In our simulation, we chose the pause time interval to be uniformly distributed between 0 s and 20 s.

- After this pause time, it again chooses another destination and repeats the process. This procedure is followed for all the MDs independently. The total simulated time in every iteration is kept at 200 s.

However, there are a few remarks about the random waypoint mobility model chosen, which are as follows:

- The random waypoint mobility model was chosen in our evaluation because its a simple model that is easy to implement and analyze our findings and has been used in many previous studies. But this model may be insufficient to capture some realistic scenarios, e.g., random waypoint mobility models are mostly source-destination type of mobility models. They do not take activity and obstructions into account to determine the destination and route choice of MDs. Thus real trace sets of indoor mobility could be a better option for simulating the dynamic resource allocation problem and should be used for further investigations in the future.

- Also, an important point is that it has been observed that random waypoint mobility models result in non-uniform spatial distribution even if the initial

MD distribution is taken to be a uniform distribution. This is called the "border effect" [81]. Thus for our results generated for uniform MD distribution case, we implemented a temporal variant of the random waypoint mobility model described in [82]. Here, uniformity was achieved by changing the speed of MDs as a function of location and the density function of trajectories in the simulated region. For the non-uniform distribution of MDs, the random waypoint model is used as it is.

3.8.1 Uplink delay

Table 3.2: Simulation parameters (Uplink delay)

Parameters	Values
Indoor environment (dimensions)	Open space ($20 \, \text{m} \times 20 \, \text{m}$)
Number of CANs	16
Number of APs	8
Number of MDs	[50-200]
MD location distribution	Uniform, Gaussian ($10 \, \text{m}$, $2.5 \, \text{m}$)
Transmit power at CAN	10 dBM
Channel access overhead+protocol overhead ($O_{ca} + O_p$)	$1.25 \, \text{ms}$
Bits in test packet (B_t)	8224 bits

The parameters[8] for the simulations described in this section are given in Table 3.2. Before we discuss the simulation results, we need to define a parameter, sorted AP number, used for comparing the simulations.

Sorted AP number: The sorted AP number represents the ranking of a particular AP after the APs are sorted in descending order of their individual airtime cost, e.g., AP 1 represents the value for the AP with the highest airtime cost. This is performed in every iteration. We chose to plot the total airtime cost against sorted AP number, because at every iteration of the simulation different APs have different airtime cost values and thus sorting the APs in every iteration makes the trend in total airtime cost more clear.

---

[8]Note that the number of MDs in the simulation scenario can be high (e.g., 200 MDs). This is reasonable as nowadays we can see the trend of hyper-connectivity, especially with the advent of the Internet of Things.

Figure 3.5: *Total airtime cost vs. sorted AP number with SA and uniform MD distribution for different number of MDs*

Figure 3.6: *Total airtime cost vs. number of MDs with SA and uniform MD distribution for different sorted AP number*

Uniform MD distribution

In Fig. 3.5 we plot the total airtime cost against the sorted AP number for a uniform MD distribution and different numbers of MDs. We can observe that the

difference between the airtime cost across sorted AP 1 and sorted AP 8 increases as the number of MDs increases. This is due to the fact that as the number of MDs increases the packet collision ratio increases which result in a higher airtime cost difference.

In Fig. 3.6 the airtime cost is plotted against the number of MDs for different sorted APs and we can observe an increasing trend. Sorted AP 8 has the largest gradient of increase and the ratio of difference in airtime cost for sorted AP 1 and sorted AP 8 for 200 MDs is the smallest as compared to 50 MDs. This can be accounted for by the fact that, as the number of MDs increases the probability of finding an equal number of MDs in each square grid increases.
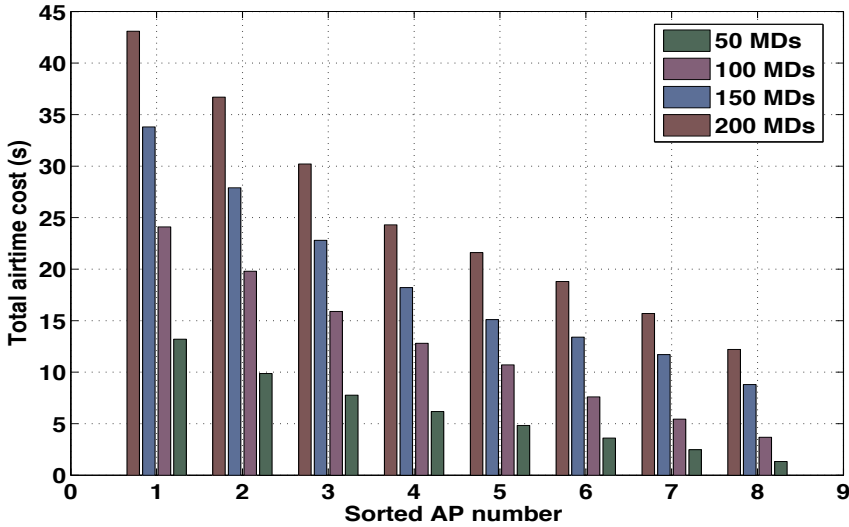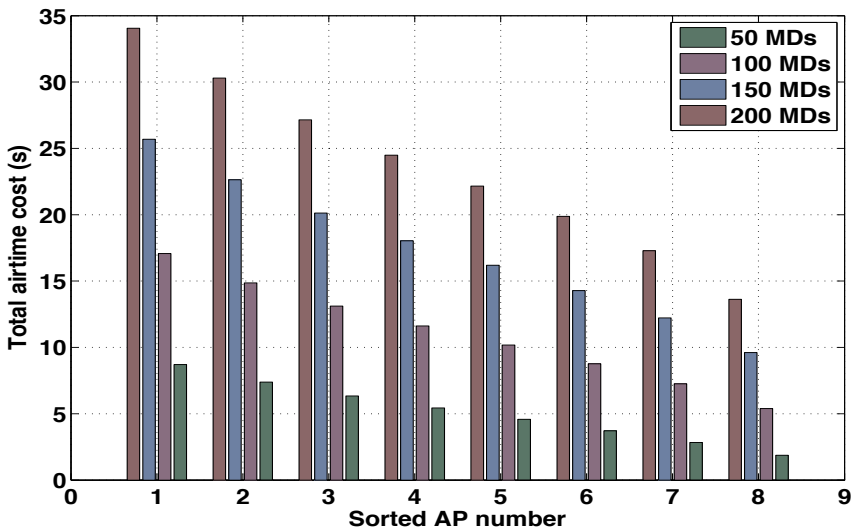

Figure 3.7: *Total airtime cost vs. sorted AP number with DA and uniform MD distribution for different number of MDs*

Now Fig. 3.7 and Fig. 3.8 portrays how the DA scheme performs for a uniform distribution of MDs. Fig. 3.7 compares the airtime cost as a function of the sorted AP number. We can observe that the maximum airtime cost across sorted AP 1 for DA scheme is smaller than the SA scheme for any number of MDs. Also, the aggregate airtime cost across all the sorted APs for any number of MDs is smaller for the DA scheme as compared with the SA scheme.

Fig. 3.8 compares the airtime cost as a function of a number of MDs for different sorted APs. The ratio of difference for airtime cost across sorted AP 1 to sorted AP 8 is decreasing over any number of MDs. This is because the network tends to balance out the airtime cost across all its APs, using the DA scheme.
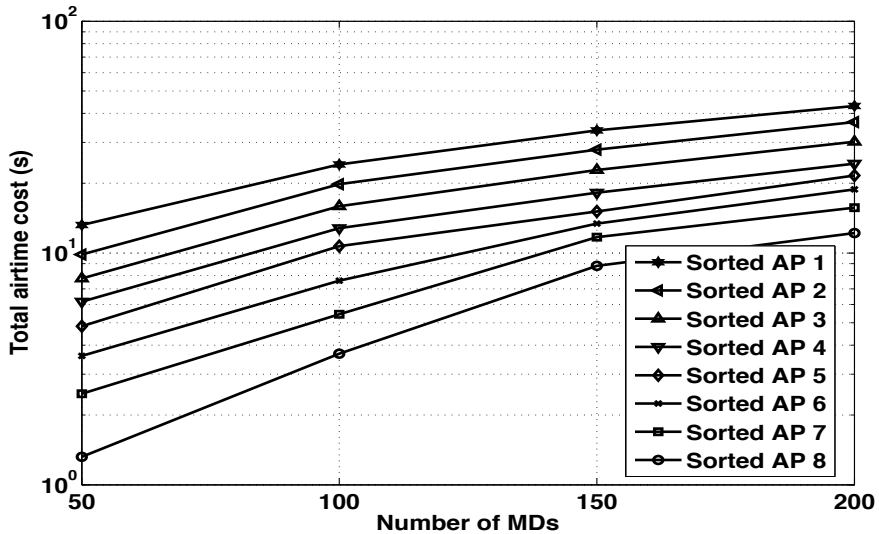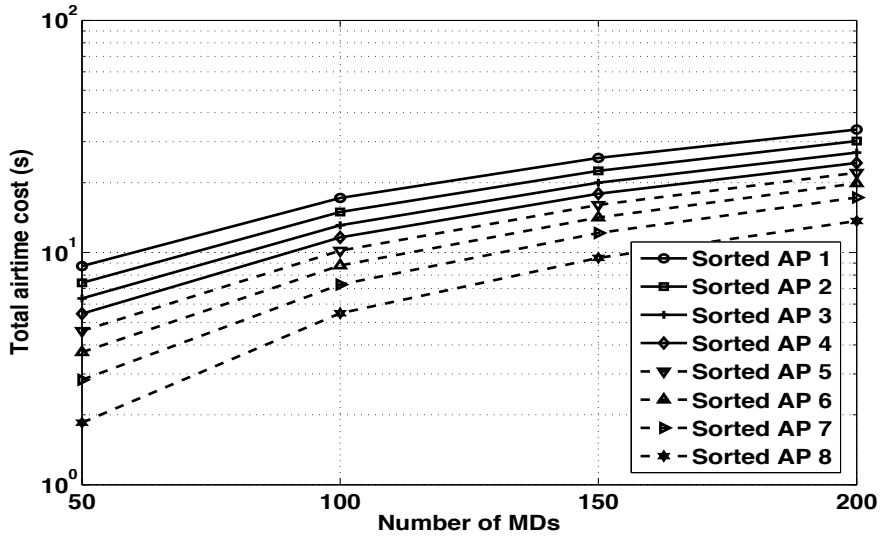
Figure 3.8: *Total airtime cost vs. number of MDs with DA and uniform MD distribution for different sorted AP number*
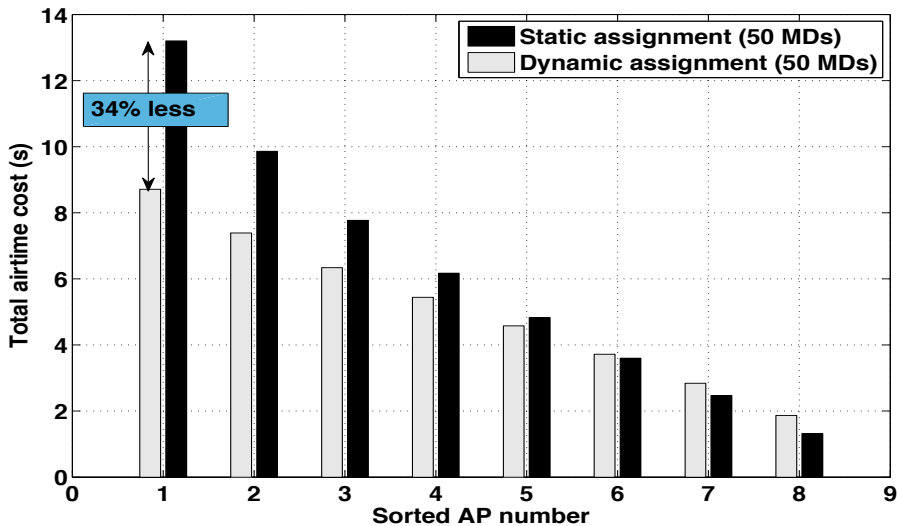
Figure 3.9: *Comparison of total airtime cost for DA and SA schemes under uniform distribution of 50 MDs*

Fig. 3.9 clearly illustrates that dynamic assignment of CANs to APs helps in significantly reducing the total network congestion. The DA scheme achieves 34%

lesser airtime cost across sorted AP 1, as compared to the SA scheme, for 50 MDs. Even the total airtime cost across all the APs, under the DA scheme, achieves 17% lesser value as compared to the SA scheme.
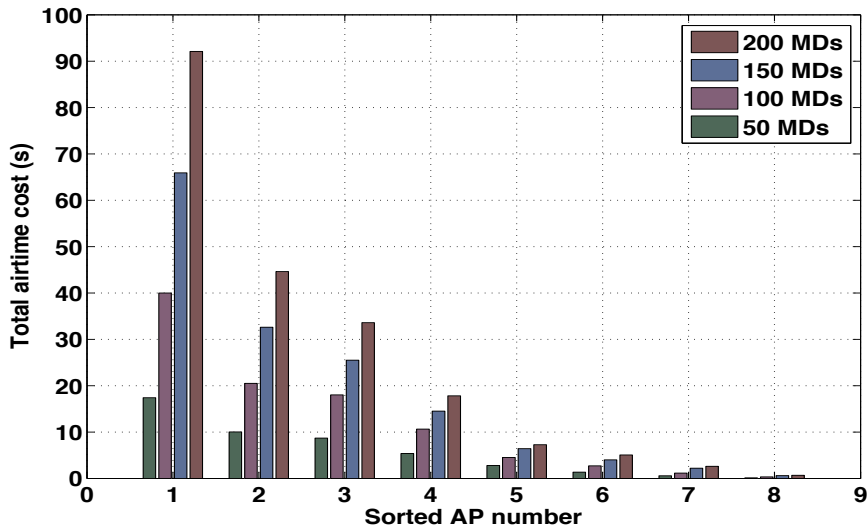
Figure 3.10: *Total airtime cost vs. sorted AP number with SA and non-uniform MD distribution for a different number of MDs*

Non-uniform MD distribution

Let us now try to evaluate how for a non-uniform distribution of MDs the SA scheme performs in terms of total airtime cost. We consider a Gaussian distribution of the x and y positions of the MDs with a mean of 10 m and a variance of 2.5 m. The non-uniform distribution of MDs is a more realistic scenario because MDs are likely to be more concentrated in some locations and tend to be sparse in some other locations.

Fig. 3.10 plots the total airtime cost as a function of the sorted AP number, whereas Fig. 3.11 plots it against the number of MDs. From Fig. 3.10 we can see that there is a very large difference in airtime cost between sorted AP 1 and sorted AP 8, for any number of MDs. In fact, we can see from the figure that the airtime costs across sorted AP $5-8$ are very small. This is due to the non-uniform distribution of MDs, where the probability of finding MDs at the corners of the network topology is very small and thus those corner CANs connect to their respective APs with very small airtime cost. In Fig. 3.11 the ratio of the difference
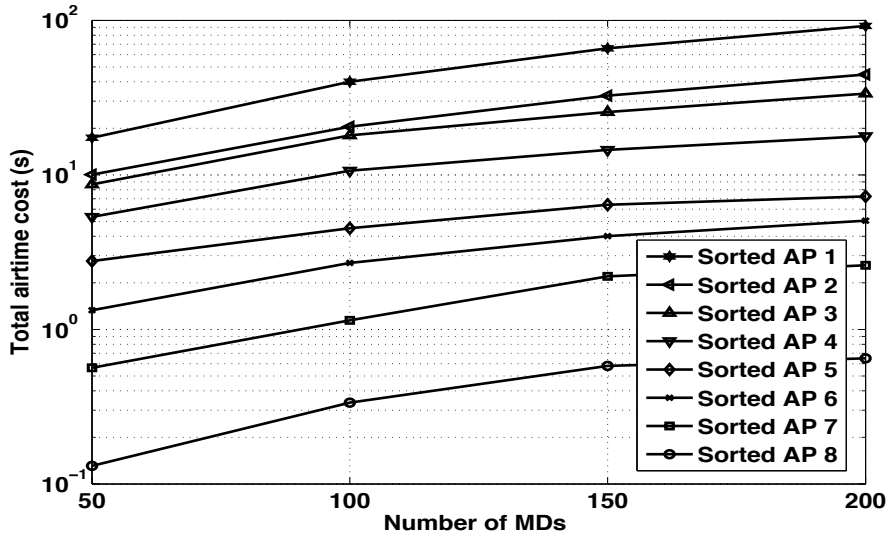
Figure 3.11: *Total airtime cost vs. number of MDs with SA and non-uniform MD distribution for a different sorted AP number*

in airtime cost for sorted AP 1 and AP 8 is almost the same for 50 MDs as is for 200 MDs.
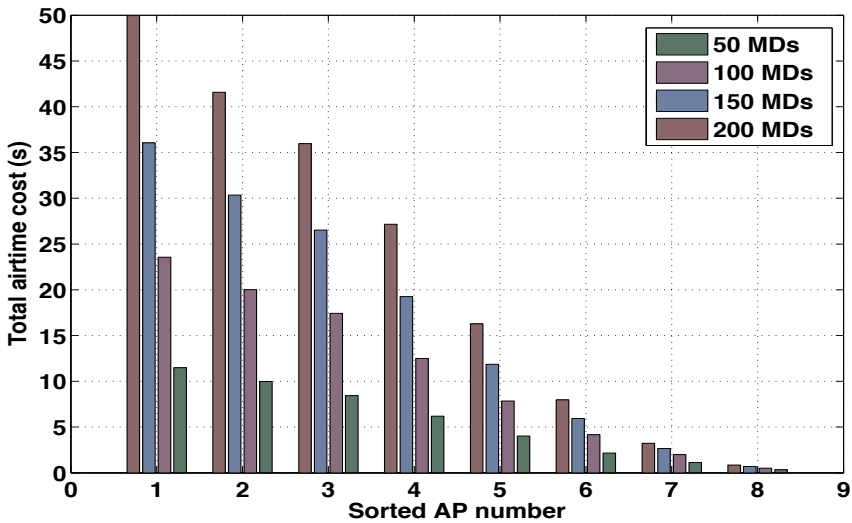
Figure 3.12: *Total airtime cost vs. sorted AP number with DA and non-uniform MD distribution for a different number of MDs*
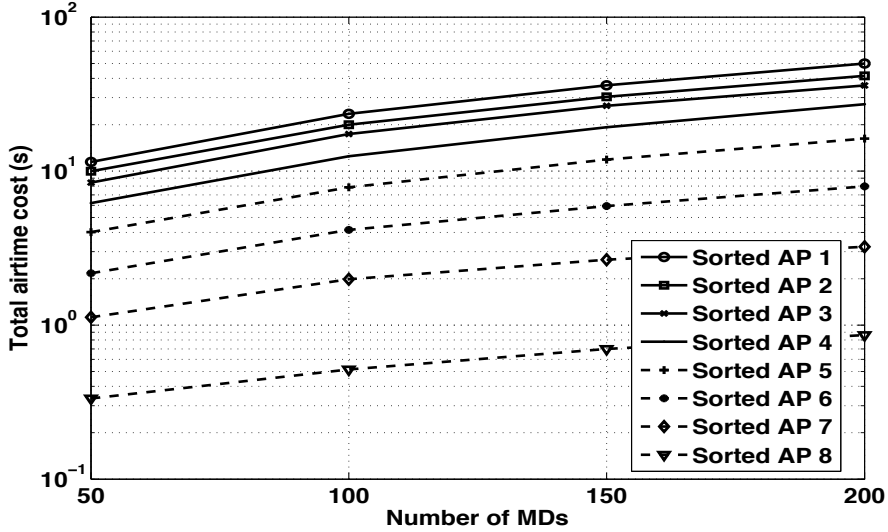
Figure 3.13: *Total airtime cost vs. number of MDs with DA and non-uniform MD distribution for a different sorted AP number*

Similarly, if we look at Fig. 3.12 and Fig. 3.13 it projects how the DA scheme performs under the non-uniform distribution of MDs. Looking at Fig. 3.12, we can visualize that the maximum airtime across sorted AP 1 is reduced for any number of MDs and it is shared by other APs.

Fig. 3.14 clearly illustrates how the DA scheme performs in comparison to the SA scheme, for a non-uniform distribution of 200 MDs. The maximum airtime cost is reduced by 45.7% across sorted AP 1. Sorted AP $3-8$ were underutilized for the SA scheme. Whereas, using the DA scheme the APs are more utilized, thus distributing the airtime cost across the APs as much as possible.

3.8.2 Downlink delay

Next, we study the performance of the DA algorithm, w.r.t. the SA scheme for the downlink delay. The simulation setup is the same as described above. The parameters for the simulations described in this section are given in Table 3.3. Here we consider heterogeneous MD traffic categories namely BE, CBR and VS. The arrival rates for CBR, VS and BE MDs are randomly distributed between $75-125$ kbps, $200-256$ kbps and within a range of $150-180$ kbps respectively [76]. The value of T_{SIFS}, T_{DIFS}, T_{ACK} and the header transmission time are kept according to IEEE 802.11b standard as $10, 50, 248, 192$ μs [83]. The simulations
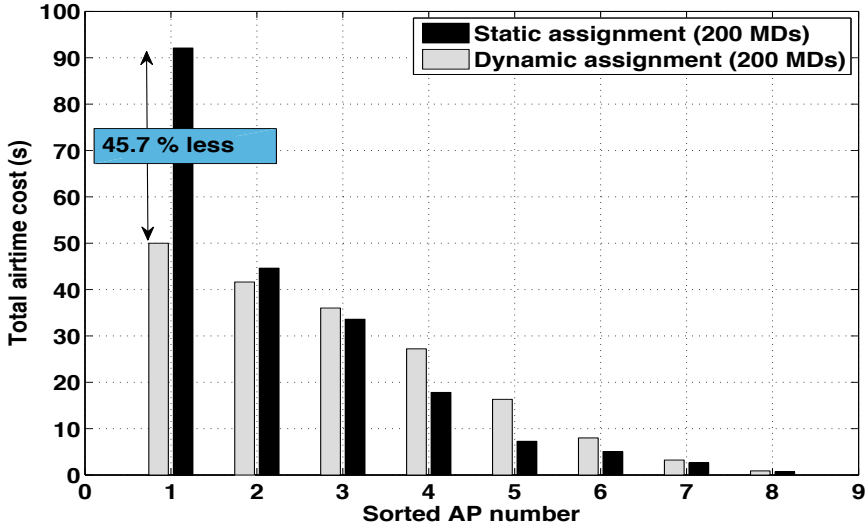
Figure 3.14: *Comparison of total airtime cost for DA and SA schemes under non-uniform distribution of* 200 *MDs*

Table 3.3: Simulation parameters (Downlink delay)

Parameters	Values
Indoor environment (Dimensions)	Open space (20 m$\times 20$ m)
Number of CANs	16
Number of APs	8
MD traffic categories	VS, CBR, BE
MD Distribution	Uniform, Gaussian (10 m, 2.5 m)
Transmit power at CAN	10 dBm
VS shape parameter (s)	3.066
$T_{SIFS}, T_{DIFS}, T_{ACK}$	10 μs, 50 μs, 248 μs
Header transmission time	192 μs
$\nu_{CBR}, \nu_{VS}, \nu_{BE}$	($[75-125], [200-256], [150-180]$) kbps

are performed under two different MD scenarios, as portrayed in Table 3.4 [9].

---

[9]Note that, although we chose to illustrate our findings w.r.t. two MD scenarios, It is sufficient to portray the advantages of the DA scheme over the SA scheme, as the DA scheme provides a load balanced assignment over the SA scheme, when there are more than one MDs connected to the network.

Table 3.4: Traffic scenarios

Scenario 1	(10 MDs, 51 MDs, 25 MDs) with VS, BE and CBR traffic respectively
Scenario 2	(15 MDs, 30 MDs, 30 MDs) with VS, BE and CBR traffic respectively

Uniform MD distribution

Fig. 3.15 compares the DA and SA schemes for a uniform distribution of MDs. We can observe that the DA scheme achieves lower aggregate downlink delay across all APs, and the maximum decrease in downlink delay across sorted AP 1 is 20%.

Non-uniform MD distribution

Fig. 3.16 compares the DA and SA schemes for a non-uniform distribution of MDs. Here we also considered a Gaussian distribution of the x and y positions of MDs with a mean of 10 m and a variance of 2.5 m.

From Fig. 3.16 we can observe that the decrease in maximum downlink delay time across sorted AP 1 is a massive 66% (for Scenario 1). This is because less number of MDs lie in the corner grid areas of CANs $13, 1, 4$ and 6. Thus we have more opportunity to balance the highly congested APs by shifting CANs from those APs with the ones from the corner. We can also notice that for both uniform and non-uniform distributions the sorted APs of lower index share the congestion level of sorted APs with higher index thus providing a more balanced load level among APs at the HCC.

From Fig. 3.15 and Fig. 3.16 we can also see that the higher numbered sorted APs (less congested) experience a higher delay time for the DA scheme as compared to the SA scheme. This is because the delay time across the lower sorted APs (highly congested) are shared by the higher numbered sorted APs due to the shifting of CANs from highly congested APs to less congested APs. But the interesting thing to note is that the overall network delay of the whole network is reduced from the SA to the DA scheme.

3.9 Conclusion

We utilized the flexibility in RoF CE-WLAN connections, between CANs and APs (colocated at the HCC), to perform load balancing between APs, to reduce the overall congestion of the whole indoor network. We discussed metrics of uplink delay (approximated using airtime cost) and downlink delay to represent congestion in the network. We then formulated the congestion control problem using both uplink delay and downlink delay. Since the problem addressed is NP-

Figure 3.15: *Comparison of total downlink delay for DA and SA schemes under uniform distribution of MDs*

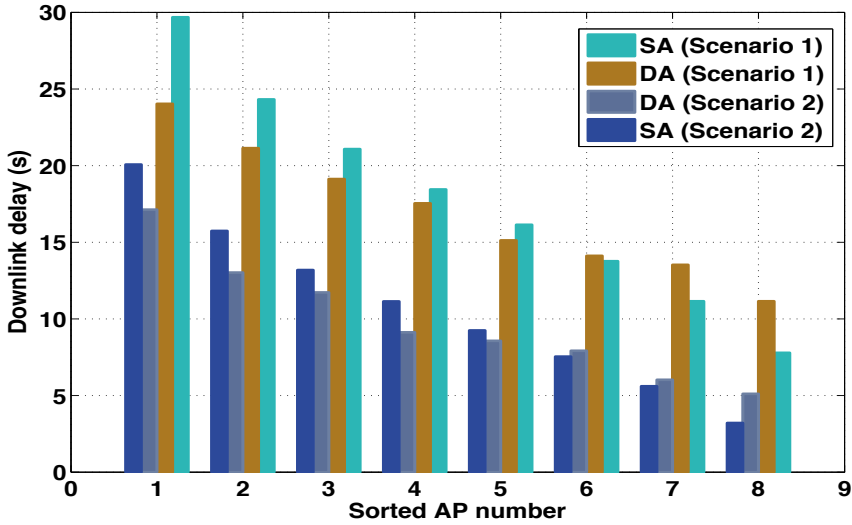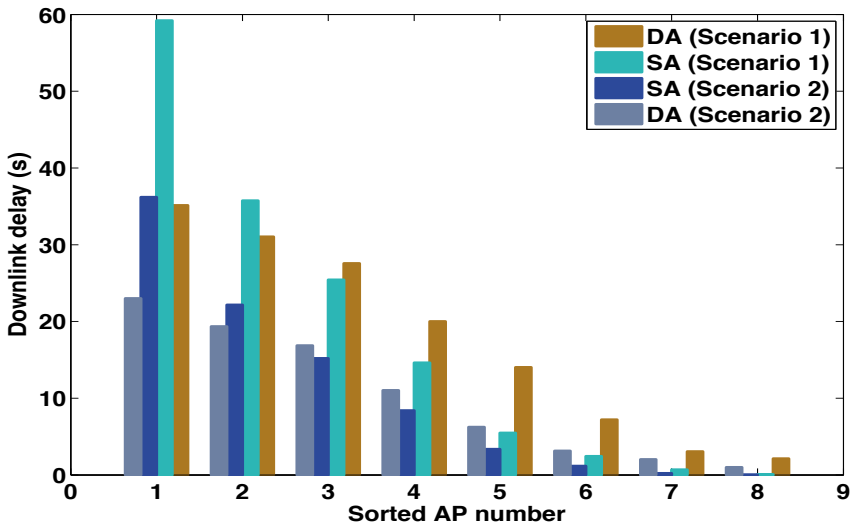**Figure 3.16:** *Comparison of total downlink delay for DA and SA schemes under non-uniform distribution of MDs*

complete, we proposed a DA algorithm that achieved both lower uplink delay and downlink delay as compared to the SA case for traditional CE-WLAN deployment.

Using coalition game theory, we also proved in Appendix A that the DA algorithm results in a stable partition that achieves minimum aggregate delay (either uplink or downlink) for the network.

Finally, we presented our simulation results, which show that the DA algorithms outperforms the SA scheme by reducing the uplink delay (airtime cost). As illustrated, by Fig. 3.14, 45.7% reduction of airtime cost, across an AP was achieved for non-uniform distribution of 200 MDs. Similarly, the study of the DA algorithm, considering downlink delay under heterogeneous MD category was shown to outperform the SA scheme by reducing the maximum downlink delay time by a massive 66% for non-uniform MD distribution, as illustrated by Fig. 3.16.

3.9.1 Limitations and future work:

- **Non-overlapping cell areas:** The congestion control DA algorithm was proposed under the assumption that the cell areas served by the CANs are non-overlapping. This was done to isolate the problem of congestion control from the problem of frequency channel allocation. But in real life, the channel allocation of APs plays an important part, and thus it would be interesting to study the combined problem of congestion control along with frequency channel allocation.

- **Reconfiguration cost:** In a CE-WLAN the RNM is the central part which decides on the re-assignment. As discussed before, the RNM maintains information about the AP and its connections. Some information at the RNM requires to be dynamically updated, e.g., the set of MDs associated and aggregate throughput of each AP. The RNM can send periodic requests to each AP connected to it to keep the dynamic state updated. This requires a total of 40 bytes of state per AP, in which only 8 bytes are needed for dynamically varying states [84]. Thus periodic updating does not cause serious overhead in terms of storage or communication overhead.

- **Reconfiguration delay & reconfiguration frequency:** The next important aspect is the delay that the MDs face because of the re-configuration. The work in this chapter does not talk about the reconfiguration delay faced by the MDs due to the dynamic re-assignment of CANs to APs. The MDs, when moved from one AP to another, have to initiate the association process with the new AP before sending or receiving traffic and even with the IEEE 802.11r [85] fast roaming approach it takes in the order of few tens of ms [86]. This is fairly small as compared to the uplink and downlink delays faced by MDs in an AP. But performing re-assignments too frequently

may be quite disruptive for the MDs. Thus one needs to investigate how frequent one needs to perform the re-assignment of CANs to APs. As discussed previously, we can see that the re-configuration cost due to communication overhead and storage is pretty small and so we could think of performing the re-assignment frequently. But this could lead to heavy disruption for MDs because of AP roaming. Also, since the traffic across MDs is varying over time and can be quite bursty, we can intuitively predict that the re-configuration will likely happen with a frequency of the order of once every several minutes. Further investigations to determine the frequency of network re-allocation are needed and might be a topic for future research.

4

Energy Efficient Indoor Communication Networks

4.1 Introduction

An exponential increase of WLANs is foreseen in the coming years [87] with a projected compound annual growth rate of 32%, and an estimated penetration of 800 million households globally by 2016 [88]. The trend of WLAN access from coverage-oriented to high-density deployment (in offices, university buildings, hospitals, etc.), for increasing capacity, is leading to an over-dimensioned deployment of APs. This over-dimensioning is necessary to meet the requirements of the most critical situations when bandwidth hungry or delay-sensitive applications running on a large number of high-end MDs, start accessing the network at the same time. Most indoor environments are thus opting for a centralized enterprise-WLAN (CE-WLAN)[1]. CE-WLAN supports numerous non-interfering light-weight APs (LWAPs)[2] with overlapping cell areas. The number of LWAPs to be deployed are determined by the network topology, usage characteristics and budget restrictions of the network.

In [29] it has been pointed out that peak demands occur only for a relatively short time. Moreover, the AP usage over a day, week, month and also throughout the year varies. The APs in such enterprise scenarios are thus frequently in idle mode. We portray in the later part of this chapter (Section 4.8), through a case study, that a considerable number of these APs remains idle for time intervals of the order of several hours. The number of idle APs are bound to increase as

---

[1]Please refer to Chapter 2 for the description of CE-WLAN

[2]Note that in CE-WLAN, IEEE 802.11x functions are implemented across multiple entities instead of a single entity, as discussed in Chapter 2. The APs in CAPWAP are referred to as light-weight APs, see Fig. 2.2, in Chapter 2, providing a simplified attachment point for WLAN MDs.

enterprises add more redundancy in their networks. Idle WLAN resources signify wastage of energy. This is a major issue, which has received little attention.

Thus energy consumption as a fundamental design goal should be included in the implementation of such CE-WLANs. An RoF-based hybrid Fi-Wi network architecture provides the opportunity to realize considerable energy saving because of the following two reasons:

- The APs[3] (colocated at the HCC) can flexibly connect to any number of CANs (because of the RoF-based DAS implementation). This allows changing their serviced cell areas dynamically over time. In the traditional CE-WLAN, this is not possible. Thus energy wastage can be minimized, as many CANs can be attached to a single AP until the capacity offered by that AP reaches its maximum.

- It costs more energy to keep the APs switched on as compared to the energy consumed in keeping the CANs powered on[4].

Thus efficient resource management strategies to reduce the energy consumption using RoF CE-WLANs become important. These strategies must enable RoF CE-WLANs to scale their energy consumption w.r.t. the MD demand, without hampering coverage or QoS. To ensure minimal energy consumption, resources should be switched off in those areas that are serviced by multiple CANs and APs while maintaining complete coverage at all times throughout the network. In this chapter, we, therefore, focus our attention on resource-on-demand (RoD) strategies, for attaining energy efficiency and compare the performance of traditional and RoF-based CE-WLANs.

The remainder of the chapter is organized as follows. Section 4.2 reviews existing literature about energy saving techniques in WLAN. Section 4.3 provides an overview of our research contributions. Section 4.4 introduces a power consumption model for RoF CE-WLAN. In Section 4.5 we describe our energy saving problem. Section 4.6 presents our heuristic algorithm, the On-Demand strategy. The MATLAB simulation results are presented in Section 4.7. Section 4.8 provides a case study on a large-enterprise WLAN network at the Dartmouth campus. In Section 4.9 we describe network scenarios that reflect different real-life CE-WLAN deployment. Section 4.10 compares the performance of traditional and RoF CE-WLAN for the On-Demand strategy under different network scenarios. Section 4.11 presents our power-managed load-balancing algorithm that reduces

---

[3]Note that an AP module in the RoF CE-WLAN consists of the LWAP and an O/E -E/O converter, as shown in Fig. 2.3 of Chapter 2.

[4]Please refer to Section 4.4 for approximate power consumption values across the CAN and AP.

the overall energy consumption of the CE-WLAN and balances the load among APs. The conclusions from the chapter are presented in Section 4.12.

4.2 Literature survey

There is a lot of work that discusses energy saving in WLAN. The major techniques that have been explored in the literature are discussed below.

Energy saving across MDs: Energy saving techniques can be formulated to reduce energy consumption across MDs or the network entities, e.g., APs. The reduction of energy consumption for MDs was studied in [89], [90]. They were based on making the MDs alternate between an active mode and sleep mode, depending on packets addressed to them from the AP. But the power of the MDs was reduced by a small amount of around 100 mW as compared to switching off APs, which saves approximately 5 W [91]. Also, none of the schemes discussed in [89], [90] are applicable for APs, as an AP needs to stay active to acknowledge the connection requests and receive packets from active MDs in the network.

Transmission power control: It is used to minimize the energy consumption of an AP when active MDs are located close to the AP [92]. This approach does not save much for CE-WLAN as compared to switching off APs that are used to provide redundant coverage.

RoD policies for switching off APs: Redundant coverage for CE-WLAN with multiple APs, is often used to meet MD demands in critical situations. But this leads to higher energy consumption. Thus switching off unnecessary APs can provide considerable energy saving. In [29], clusters of APs colocated in a small area were used to turn off all the APs except one to provide coverage. When the number of MDs increased, the scheme would turn on more APs by utilizing a technique called as Wake-on-WLAN [93]. Wake-on-WLAN uses the local information at the APs that are already switched on. In [94] the authors proposed to turn off 40% more active APs than the scheme in [29] without shrinking the coverage area. The scheme discussed a so-called sleeping cluster. The effective distance between clusters of APs was used to estimate the relative position of the clusters. A cluster was then categorized as sleeping cluster if the surrounding neighboring clusters could provide full coverage for any cluster. RoD policies were then studied in [29, 95]. While in [29] the authors investigated the energy saving (up to 54%) by switching APs off during the low traffic period. The authors in [95] provided a very simple analytical model assessing the effectiveness of the RoD policies for such CE-WLAN.

The aforementioned literature provides a comparative understanding of the

RoD policies to achieve energy efficient communication while maintaining acceptable MD performance. But none of those techniques provided the flexibility offered by the RoF-based DAS architecture. This unique flexibility allows us to utilize the maximum capacity offered by an AP by connecting multiple CANs to a single AP. Thus the number of APs needed to be switched on, to satisfy the MD traffic demands, is less as compared to the traditional CE-WLAN. As we will see, this achieves a much higher energy efficiency.

Energy saving using RoF-based DAS: In [96] the power consumption of different RoF links was compared. It was shown that centralized architectures using RoF technology are energy efficient when networks are designed with small cell sizes (< 5 m) and an AP has a higher energy consumption in comparison to a remote antenna unit. In comparison to distributed processing using base-band over fiber, centralized and dedicated analog processing and shared digital processing for digitized RoF and analog RoF were found to be approximately 60% and 33.33% more energy-efficient. In [97], deployment of energy efficient RoF-based DAS was studied. The authors proposed methods to find the position of distributed antennas to optimize the network capacity for a given deployment scenario. The results reveal that there is an optimal number of distributed antennas for a given indoor topology.

But the aforementioned work does not discuss network scenarios where the RoF-based technology deployment is indeed helpful as compared to the traditional deployment of APs, nor do they devise any RoD strategies for such RoF-based indoor deployment.

4.3 Contribution

The contributions of this chapter can be summarized as follows,

- We propose a power consumption model for RoF-based CE-WLAN and formulate the network energy saving problem as an optimization problem.

- We propose an RoD policy, the On-Demand strategy, that provides techniques for switching CANs and APs on and off, based on quantified MD demand, and we study its performance using MATLAB simulations.

- We provide a case study of a large enterprise network at Dartmouth campus, using their real life trace sets [98], which shows the extent of energy wastage in a large WLAN deployment.

- We define different network scenarios: (a) the colocated network entity scenario and (b) the clustered network entity scenario, that are used to compare the energy saving characteristics of the RoF and the traditional CE-WLAN.

- We compare the performance of the On-Demand strategy (based on channel utilization of the LWAPs), for both the traditional and the RoF CE-WLAN, under different network scenarios by utilizing the trace sets of [98].

- Finally, we discuss a unique power-managed load-balancing algorithm that not only reduces the total power consumption of the network but also provides load balancing, by shifting connections between the CANs and APs that are switched on.

4.4   Power consumption model
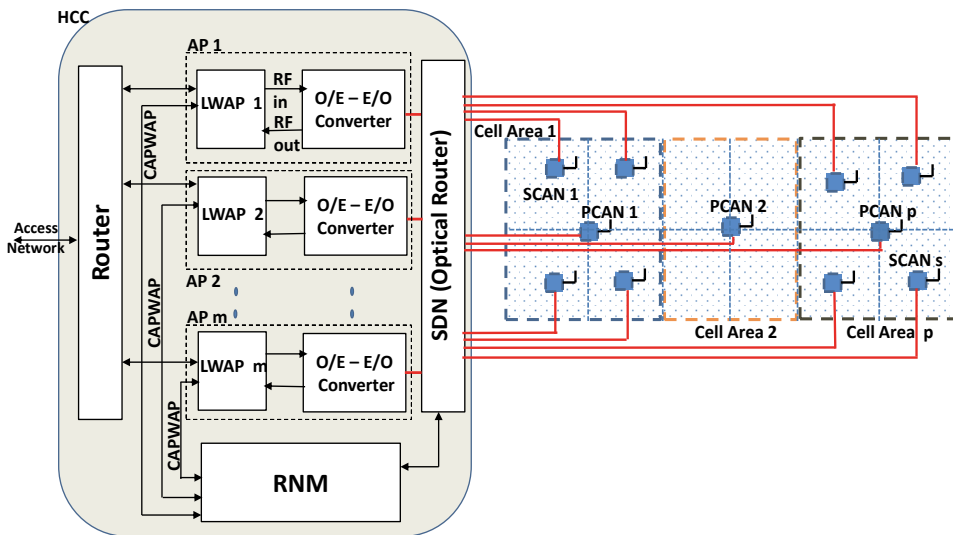
LWAP : Light-Weight AP; CAPWAP : Control and Provisioning of Wireless APs; PCAN : Primary Cell Access Node; SCAN : Secondary Cell Access Node.

Figure 4.1: *Hybrid Fiber-Wireless (Fi-Wi) LAN architecture*

The RoF-based CE-WLAN network can be divided into three parts, namely the HCC, the CAN and the optical fiber. We will discuss the power consumed in each of them individually.

HCC: The HCC (Fig. 4.1) is composed of four integral parts, namely the APs, the RNM, the SDN (Optical router), and the Router. The different elements of HCC and their functions have already been explained in Section 2.1 of Chapter 2.

AP: The AP module consists of the LWAP and the optical/electrical and electrical/optical (O/E - E/O) converter. The O/E - E/O converter module in the AP consists of an automatic gain controller amplifier and a laser source in the downlink. The automatic gain controller amplifier is used to provide controlled radio signal amplitude and DC bias in the linear modulation regime to avoid saturating the laser. The laser source then converts the electrical signal to an optical signal. While in the uplink, the O/E - E/O converter makes use of a trans-impedance amplifier and a photo-diode. The photodiode converts the optical signal back to an electrical signal, which is then fed to the trans-impedance amplifier that serves as a current to the voltage converter, before being fed to the reception port of the LWAP.

The power of an AP, $p_{\{AP\}}$, can thus be given as:

$$
\begin{aligned}
p_{\{AP\}} \quad = \quad & \underbrace{\left(p_{\{LWAP\ Tx.mode\}} + p_{\{AGC\}} + p_{\{Laser\}}\right)}_{AP\ Transmission} \\
+ \quad & \underbrace{\left(p_{\{LWAP\ Rx.mode\}} + p_{\{TIA\}} + p_{\{PD\}}\right)}_{AP\ Reception}
\end{aligned}
$$

where $p_{\{AGC\}}$, $p_{\{LWAP\ Tx.mode\}}$ and $p_{\{Laser\}}$ represent the power of the automatic gain controller amplifier, the LWAP during transmission mode and the laser source respectively. $p_{\{TIA\}}$, $p_{\{PD\}}$ and $p_{\{LWAP\ Rx.mode\}}$ represent the power of the trans-impedance amplifier, photo-diode and the LWAP during reception mode respectively.

The power of the SDN [41], the Router [91] and the RNM[5] is assumed to be of the order of a few Watts (see Table 4.1), which is a constant value, as the RNM, the Router, and the SDN are always switched on. Let us represent the power for the routing, computation and maintenance operations performed by the Router, the RNM, and the SDN as $p_{\{C/M\}}$.

CAN: We classify the CANs into two different types (see Fig.4.1),

---

[5]The value for power at the RNM depends on several factors, e.g., the number of APs and CANs in the network (which will determine the number of computations needed) etc. Thus for simplicity, we assume that the normal power consumption at the RNM is of the order of a few Watts.
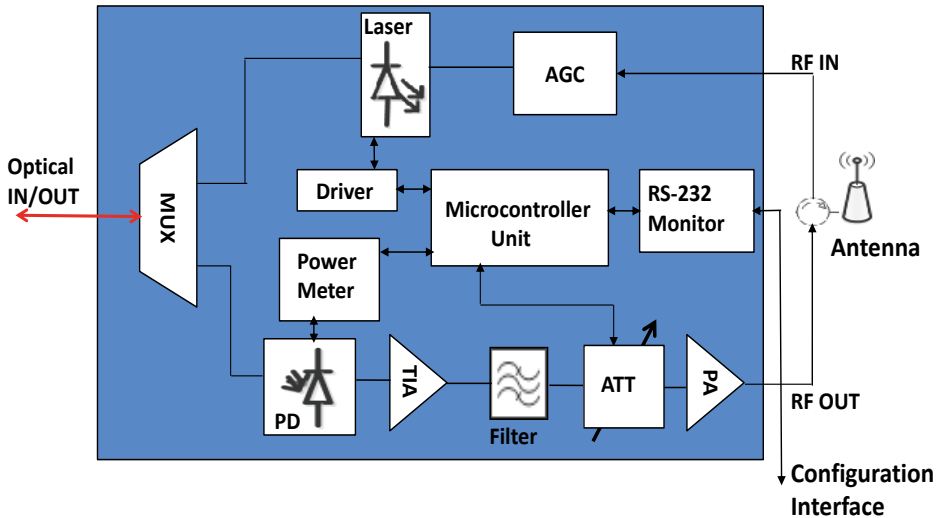
TIA : Trans-impedance Amplifier; AGC : Automatic Gain Controller; ATT :
Attenuator; PA : Power Amplifier; PD : Photodiode.

Figure 4.2: *Schematic of cell access node (CAN) in MEANS*

- **Primary CANs (PCANs):** Primary CANs (PCANs), are used to ensure basic coverage of the whole indoor network. Basic coverage means that the total indoor area is fully covered by the PCANs and their connection granting APs, such that all the MDs in the indoor network are able to associate with at least one AP.

- **Secondary CANs (SCANs):** Secondary CANs (SCANs), are switched on and connected to new APs only if the MD demand reaches a critical limit that cannot be satisfied using the PCANs and their connection granting APs.

The schematic of the CAN module (both PCAN and SCAN), used in the MEANS project [17], is shown in Fig. 4.2. For the downlink, the photodiode converts the optical signal back to an electrical signal, which is then fed to the trans-impedance amplifier which serves as a current to voltage converter. After that, the signal passes through a band-pass filter (matched to the frequency range of the ISM band), and amplified using a power amplifier before being transmitted on the wireless medium, using the antenna. The attenuator is used to provide controlled radio power transmission to vary the size of the cell covered by the WLAN signal. The power at the CAN for the downlink, $p_{\{CAN-down\}}$, can be given as below:

$$p_{\{CAN-down\}}=p_{\{PA\}}+p_{\{Filter\}}+p_{\{ATT\}}+p_{\{TIA\}}+p_{\{PD\}} \tag{4.1}$$

where $p_{\{PA\}}, p_{\{Filter\}}, p_{\{ATT\}}$ represent the power consumed at the power amplifier, the filter and the attenuator respectively.

The power consumed at the CAN in the uplink, $p_{\{CAN-up\}}$, can be given as:

$$p_{\{CAN-up\}} = p_{\{AGC\}} + p_{\{Laser\}} \tag{4.2}$$

where $p_{\{AGC\}}$ and $p_{\{Laser\}}$ represent the power consumed at the automatic gain controller amplifier and the laser source respectively.

Note that we have not included the power consumed by the control module, namely the RS 232 Monitor, the micro-controller unit, the driver and the power meter. This is because these components are not used unless the CAN module needs to be turned on or off by the RNM. Thus the energy they consume is minimal. The power consumption of the multiplexer/de-multiplexer (represented as MUX in Fig. 4.2) is also not included as it is usually very low or even zero for the case of passive coarse WDM [99].

The power consumed at the CAN, $p_{\{CAN\}}$, can thus be given as:

$$p_{\{CAN\}} = p_{\{CAN-down\}} + p_{\{CAN-up\}} \tag{4.3}$$

Optical fiber: Finally, let us also represent the power consumed by the optical fiber transmission as $p_{\{OL\}}$.

Since, a set of APs ($M = \{1, 2, ..., m\}$) are granting connection to a set of PCANs ($P = \{1, 2, ..., p\}$) and SCANs ($S = \{1, 2, ..., s\}$), located indoor (see Fig. 4.1). The total power consumed by the RoF-based CE-WLAN network, in any time-slot t, can be given as:

$$P_{\{rof-n/w\}}(t) = \underbrace{\sum_{j \in M} \sum_{i \in P} \delta_{ij}(t)(p_{\{AP\}} + p_{\{CAN\}} + p_{\{OL\}}) +}_{Primary\ connections}$$

$$\underbrace{\sum_{j \in M} \sum_{k \in S} \gamma_{kj}(t)(p_{\{AP\}} + p_{\{CAN\}} + p_{\{OL\}})}_{Secondary\ connections} + p_{\{C/M\}} \tag{4.4}$$

where $\delta_{ij}(t) \in \{0, 1\}$ and $\gamma_{kj}(t) \in \{0, 1\}$ are used to represent if PCAN $i \in P$ is connected to AP j, and if SCAN $k \in S$ is connected to AP j in any time slot t respectively. The typical power consumption of every component is provided in Table 4.1.

Table 4.1: Power consumption based on [23], [100], [41] and [91]

Component	Power
LASER	100 mW
Photodiode (PD)	10 mW
Filter	20 mW
Laser Drive Amplifier (AGC)	22 mW
Trans-impedance Amplifier (TIA)	22 mW
Power Amplifier (PA)	22 mW
AP Tx.-mode	2.71 W
AP Rx.-mode	1.88 W
SDN (MEMS switch)	< 1.8 W (Idle: 0.9 W)
Router	≈ 2 W

4.5 Optimization problem

Our main objective is to reduce the total energy consumption of the indoor RoF CE-WLAN network while ensuring that the traffic demands across the MDs are met. We utilize the aggregate channel utilization metric across each AP, and compare it to a predetermined threshold value (< 1), to ensure proper performance across all the MDs connected to it.

Why use aggregate channel utilization to quantify the traffic demand?

The simplest performance metric to quantify the traffic demand is the number of MDs. The problem however with the number of MDs is that it can over or under-estimate MD demand if many MDs generate little traffic or few MDs generate a lot of traffic respectively. Data rates of frames sent by MDs can also be used, as another metric, because low frame data rates indicate higher occurrence of frame collisions. But frame data rates are not a proper measure of the MD demand in the network. We, therefore, use aggregate channel utilization to estimate MD demand, as it takes into account both the number of MDs and the data rates [29].

Aggregate channel utilization across AP:

Aggregate channel utilization is used to represent the total number of bits sent and received over the channel by an AP from all the MDs. It does not only include the data bits but also the overhead bits. Each AP continuously sniffs MAC layer data and control frames transmitted by all the MDs, connected through the

CANs and compute their own aggregate channel utilization.

Note that, we have not talked about frequency planning of the cell areas served by PCANs and SCANs. We wanted to delineate the problem of network energy saving from the problem of channel allocation.

Assumption: The number of APs is assumed to be greater than or equal to the number of PCANs, i.e., $|M| \geq |P|$, and the total number of PCANs and SCANs is assumed to be greater than the number of APs, i.e., $|M| < |P| + |S|$. We make this assumption since the PCANs are always switched on and connected to an AP to guarantee complete coverage of the indoor area at all times. The SCANs, on the other hand, are intended to cover smaller cell areas than PCANs and are only switched on when the MD demand reaches a certain threshold. Thus offering more capacity by switching on more APs, connected to one or more SCANs.

Problem statement: Given a set of APs $M = \{1, 2, ..., m\}$, PCANs $P = \{1, 2, ..., p\}$ and SCANs $S = \{1, 2, ..., s\}$, where $|M| \geq |P|$ and $|M| < |P| + |S|$, we have to devise a strategy to minimize the total energy consumption of the RoF CE-WLAN by providing connectivity through the PCANs and a subset of the SCANs and the APs. We have to ensure that the **aggregate channel utilization** across each AP, that is used for connectivity, is less than a pre-defined threshold value to ensure proper QoS to the MD.

Let us represent the set of MDs already connected through the PCANs as $I = \{1, 2, ..., i\}$. The optimization problem can be formulated as an Integer Linear Programming (ILP) problem, which can be stated as follows[6]:

$$Minimize \qquad \sum_{j \in M} \sum_{i \in P} \delta_{ij}(t)(p_{AP} + p_{CAN} + p_{OL}) +$$

$$\sum_{j \in M} \sum_{k \in S} \gamma_{kj}(t)(p_{AP} + p_{CAN} + p_{OL})$$

$$= (p_{AP} + p_{CAN} + p_{OL})(\sum_{j \in M} \sum_{i \in P} \delta_{ij}(t) + \sum_{j \in M} \sum_{k \in S} \gamma_{kj}(t)) \text{ (4.5)}$$

subject to

$$\sum_{i \in P} \sum_{l \in I} \delta_{ij}(t)\alpha_{il}(t)\frac{r_{jl}^i(t)}{c_j} \leq \theta \ \forall j \in M; \qquad (4.6)$$

$$\sum_{k \in S} \sum_{l \in I} \gamma_{kj}(t)\beta_{kl}(t)\frac{r_{jl}^k(t)}{c_j} \leq \theta \ \forall j \in M; \qquad (4.7)$$

---

[6]In the minimization we have not included the $p_{\{C/M\}}$ term as it is assumed to have a constant value of the order of a few Watts.

where

$\alpha_{il}(t) \in \{0, 1\}$ if MD l is connected to PCAN $i \in P$ at time slot t.

$\beta_{kl}(t) \in \{0, 1\}$ if MD l is connected to SCAN $k \in S$ at time slot t.

θ represents the channel utilization threshold of each AP, which is kept at a value less than 1.

c_j represents the maximum physical layer capacity of the AP j.

$r^i_{jl}(t)$ and $r^k_{jl}(t)$ represent the total number of bits sent and received by the AP j from MD l connected using the PCAN i or the SCAN k respectively.

The problem described is a minimal set cover problem, which was shown to be NP-hard [101]. Hence, in Section 4.6 we provide a heuristic algorithm for the optimization.

4.6 Demand driven RoF CE-WLAN: On-Demand strategy

For the ILP problem described above, we provide an algorithm, On-Demand strategy, that provides resources to MDs only when there is a demand for it. The algorithm can be divided into three parts: (a) connection-guaranteeing coverage, (b) MD-demand quantification and (c) switching on-off CANs and APs. The steps are described in detail below,

4.6.1 Connection-guaranteeing coverage

The foremost important thing in a RoD strategy implementation is to guarantee complete coverage of the cell area. For this, we keep the PCANs always switched on and connected to individual APs so that the basic coverage for the whole area is ensured.

4.6.2 MD-demand quantification

Accurate MD-demand quantification forms another important part in devising any demand-driven RoD strategy. It serves as an important factor in maintaining QoS to the MD while optimizing network energy saving. Thus a metric, which quantifies the MD demand, plays a significant role. As discussed, in Section 4.5, we chose to utilize the aggregate channel utilization metric.

4.6.3 Switching on-off CANs and APs

Initially, all the PCANs are connected to individual APs, to ensure a complete basic coverage of the indoor network. We monitor the aggregate channel utilization,

θ, for each of those APs. If it exceeds a certain threshold value (> 1), that is set by the network administrator, the traffic load across that AP is higher than the capacity available to support the connected MDs. So, to reduce congestion, the On-Demand strategy should re-configure the MD traffic load from the congested AP. It powers on unused[7] APs and SCANs to provide coverage to a subset of MDs across the congested AP.

Switching on SCANs and APs: At reconfiguration time intervals, t_{reconf}, the algorithm switches on unused SCANs and APs based on sensed energy across the SCANs, located in the region of the congested PCAN.

Spectrum Sensing: The SCANs when they are not connected to any AP (i.e., when data connections are not used at the SCANs) keep on sensing the spectrum (across their respective cell area) for a particular time interval, t_{sense}. Spectrum sensing can be performed in many ways, e.g., we can think of another low power-costing link from the SCANs that connects to the RNM, where a sensor receiver is located. Each SCAN can sense the spectrum alternatively for a specific short time interval. The RNM keeps track of the energy sensed by all of the SCANs and then arranges the SCANs, located in the region of the PCAN, in a descending order of the sensed energy level.

The On-Demand strategy then powers on an unused AP and SCAN, with the highest sensed energy, after t_{sense} interval to meet the demand across that congested PCAN. Multiple numbers of SCANs can be connected to the same AP until the aggregate channel utilization of that AP is less than the pre-defined threshold.

Switching off SCANs and APs: If any SCAN connected to an AP remains idle for a period t_{idle}, it is switched off. If all the SCANs connected to an AP are switched off then that AP is switched off by the RNM.

The pseudo-code for the On-Demand strategy is given in Algorithm 2.

Let us analyze the On-Demand strategy,

- The proposed On-Demand strategy requires a differentiation between the PCANs and the SCANs. So it requires proper planning of placement for PCANs and their subsequent SCANs. This can be achieved using indoor radio planning tools. For situations, e.g., old buildings, where the positions of PCANs and SCANs are not properly planned using radio planning tools, they can also be sorted out, on the fly, using the techniques that we describe in [102] based on clustering.

- The On-Demand strategy neglects the load balancing that could be performed between the subset of switched on APs to improve the network

---

[7]Here unused APs and SCANs refers to APs and SCANs whose WiFi RF chains are powered off.

Algorithm 2 On-Demand strategy

---

1 Initialize:

PCANs $P = \{1, 2, ...p\}$; SCANs $S = \{1, 2, ...s\}$ and $M = \{1, 2, ...m\}$ APs.

2 Ensure coverage:

All $|P|$ PCANs are connected to $|P|$ out of $|M|$ APs to ensure basic coverage. SCANs are in switched off mode.

3 Monitor:

Monitor the aggregate channel utilization of the APs connected to $|P|$ PCANs, $\{\theta_1, \theta_2, ..., \theta_p\}$, and arrange them in descending order. Find the set M_p of APs with aggregate channel utilization greater than θ. Monitor the power received across the SCANs.

4 Resource-on-demand:

Select one AP in M_p in each round and shift the load by switching on the SCANs and connect them to the unused APs $\{M/P\}$.

4.1 Find the SCAN S_1 with the maximum sensed power. Turn it on and connect it to a new AP.

4.2 Check if $\theta_1 < \theta$. If not repeat **1** and connect the SCAN S_2 with the same AP as S_1 and calculate $\theta_{S_1} + \theta_{S_2}$. If $\theta_{S_1} + \theta_{S_2} > \theta$ then connect S_2 to new AP.

4.3 Repeat **4.2** and **4.1** until $\theta_1 < \theta$.

5 Repeat:

Repeat Step **4** for $|M_p|$ rounds, until each of the AP's in the set M_p has aggregate channel utilization value $\leq \theta$.

---

performance further. In the later part of this chapter, we therefore, propose techniques to incorporate load balancing along with energy saving.

- MD re-association due to the change in connectivity with different APs requires that the AP implements the IEEE 802.11v standard, where the APs can direct MDs to re-associate with an alternate AP using a different SCAN. This has not been tackled in describing the On-Demand strategy, but can be easily performed without changing the standard.

4.7 Simulation results

In this section, our objective is to compare the proposed On-Demand strategy to the Always-On strategy, where all the network entities are kept switched on at all times. The performances of both schemes are compared on (a) power saving and (b) throughput, for both uniform and non-uniform MD distribution over the network topology. Uniform and non-uniform MD distribution represent different simulation scenarios where every region in the simulated network topology has an almost similar amount of traffic to serve, and also the case where the traffic is dense in some areas and sparse in others.

In the simulations, we considered an open office space of size $10 \text{ m} \times 10 \text{ m}^8$ (see Fig. 4.3). We compared the performance of two different schemes,

- **On-Demand strategy:** There is only one PCAN located at the center of the square space area (see Fig. 4.3), which is connected to an AP at all times to ensure complete basic coverage. We have four more SCANs, which can be connected to other APs if the MD demands exceed the capacity that is being offered by the AP connected to the PCAN.

- **Always-On strategy:** Here all the SCANs are kept switched on and connected with individual AP. Thus for the Always-On strategy, the total cell area across the network is covered by four SCANs connected with four APs.

We perform Monte Carlo simulations in MATLAB to obtain the numerical results. In our figures, we plot the average values of the data rates, power and the energy per bit goodput obtained over all the simulation runs. The simulation parameters are given in Table 4.2. In the simulation, we assume that the SCANs

---

[8]Note that each of the SCANs is intended to provide coverage inside a square grid cell area of size $5 \text{ m} \times 5 \text{ m}$. A PCAN is placed at the center of the overall indoor area and is intended to provide basic coverage over the whole indoor area of $10 \text{ m} \times 10 \text{ m}$. These are typical femto-cell sizes, which usually are of the order of 10 m or less [62].
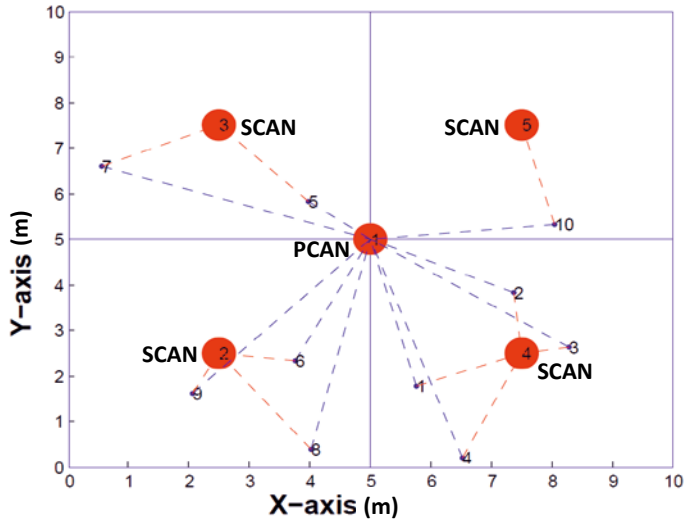
Figure 4.3: *Simulation scenario*

Table 4.2: Simulation parameters

Parameters	Values
Carrier Frequency	2.4 GHz
Indoor Environment (Dimension)	Open space ($10\,\text{m} \times 10\,\text{m}$)
Number of [PCANs, SCANs]	[1, 4]
Number of APs	4
Channel Bandwidth across AP	20 MHz
Path loss model	ITU office model [103]
Number of MDs	10
MD Distribution	Uniform, Gaussian (7.5 m, 2.25 m)
Channel utilization threshold	0.85 [104]
Transmit Power across [PCANs, SCANs]	[20 dBm 10 dBm]

serve non-overlapping cell areas, which allows us to disregard the problem of frequency planning and yet provide evidence of the energy saving of the RoF CE-WLAN network. In the network area, there are 10 MDs that are covered by the PCAN. We studied the On-Demand strategy and Always-On strategy under uniform and non-uniform distribution of the MDs. The channel utilization threshold is kept at 0.85 [104]. It also agrees with the value which WLAN vendors like Aruba

Networks set as their default threshold [105]. For the non-uniform distribution of MDs, their positions are assumed to be drawn from a Gaussian distribution whose mean is kept at $7.5\,m$ and the standard deviation is taken to be $1.5\,m$. This assumption can be justified from real life scenarios, as MDs tend to visit certain areas of an indoor network more often than others because of the arrangement of the indoor space. One important thing to note is that the simulation runs are independent, i.e., there are no temporal correlations among the MD locations. However, this has no significant impact on our performance evaluation.
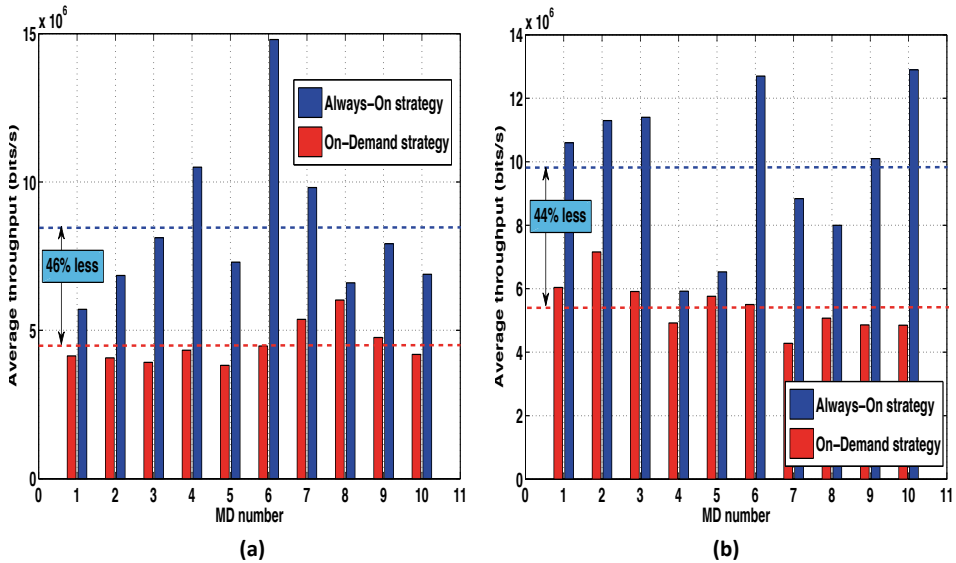
Figure 4.4: *Average throughput for (a) uniform distribution of MDs (b) non-uniform distribution of MDs*

Throughput

From the simulation results (see Fig. 4.4) we can observe that the average throughput for the On-Demand strategy suffers as compared to the Always-On strategy. For uniform distribution, the On-Demand strategy achieves 46% less total average throughput as compared to the Always-On strategy, and for the non-uniform distribution it is 44% less for the On-Demand strategy. This is because for the Always-On strategy the distance between the MDs and the SCANs is much smaller than for the On-Demand strategy. Moreover, between the case of uniform and non-uniform distribution of MDs, the later garners higher average data rates than the former as the probability of finding MDs with larger distance w.r.t. the CANs is much higher.
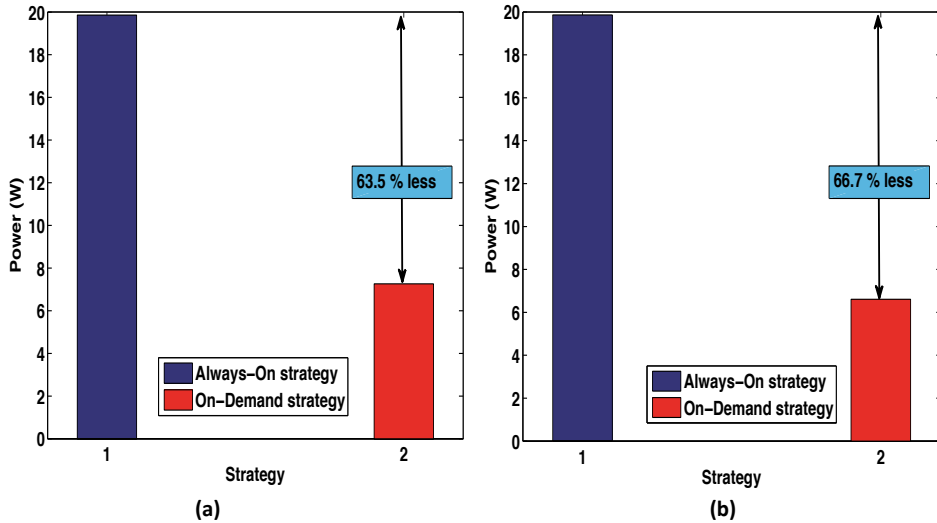
Figure 4.5: *Power consumption of the RoF CE-WLAN network for (a) uniform distribution of MDs (b) non-uniform distribution of MDs*

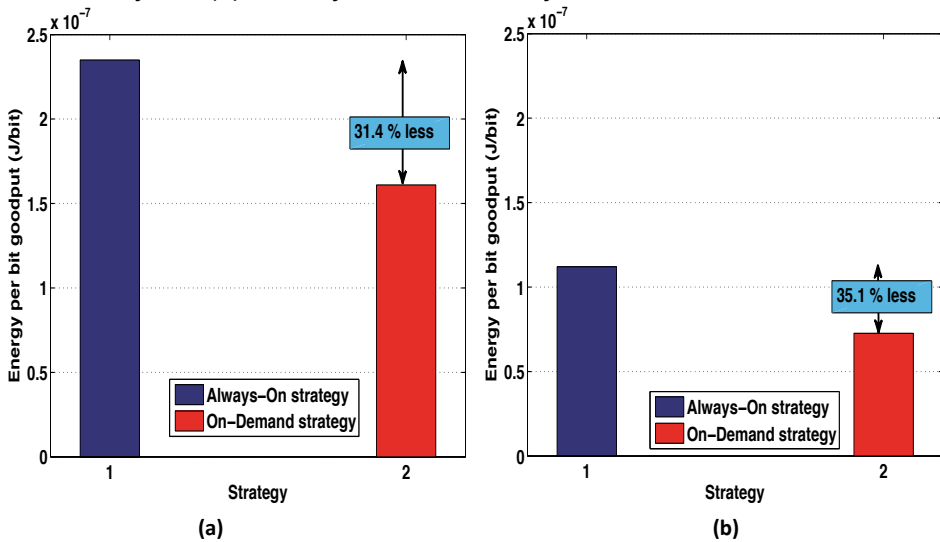**Figure 4.6:** *Energy per bit goodput (EBG) of the RoF CE-WLAN network for (a) uniform distribution of MDs (b) non-uniform distribution of MDs*

Power saving & Energy per bit goodput

Let us compare the power (see Fig. 4.5) consumed by both the strategies, by keeping APs or CANs powered on, for the uniform and non-uniform distribu-

tion of MDs. We can observe that the On-Demand strategy as compared to the Always-On strategy achieves a power saving of 63% and 67% respectively for the uniform and non-uniform MD distribution. Note, that for calculating the power saving, we calculated the average power difference between both the schemes over all simulation runs.

Energy per bit goodput (EBG) tells us how much energy the CE-WLAN network has to spend to transmit one bit of MAC payload data [106]. Thus for the RoF CE-WLAN network, the total EBG can be computed as below, in J/bit,

$$EBG = \frac{P_{rof-n/w}}{R} \tag{4.8}$$

where R and $P_{rof-n/w}$ represent the total throughput obtained by all MDs in the network and the total power consumed by an RoF CE-WLAN respectively. Thus if we compare the EBG, as shown in Fig. 4.6, we can see a large reduction for the On-Demand strategy as compared to the Always-On strategy: 31% and 35% for uniform and non-uniform MD distribution respectively.

4.8   Case study: Dartmouth campus

We examined the large-scale enterprise WLAN deployed at the Dartmouth College campus [98]. The campus hosts over 190 buildings on 200 acres of land. Around 500 APs are installed inside the buildings to provide coverage to the MDs. All APs share the same SSID, allowing the MDs to roam seamlessly between APs. On the other hand, a building's APs are connected to the building's existing subnet. We are mainly interested in quantifying the usage pattern of the indoor WLAN APs. We used the simple network management protocol (SNMP) trace sets [98]. SNMP was used in [98] to poll each AP every five minutes, querying AP about MD-specific counters. The parameters we are interested are the AP number along with the building name to which they belong and also the number of MDs connected to the APs in each interval[9]. We are interested in computing two metrics from the trace set that would quantify the AP usage pattern, as explained below.

Fraction of average usage of APs:

A WLAN AP is considered to be in use when at least one MD is associated with that AP, and thus the AP is used to send or receive data traffic. For calculating the

---

[9]Note that the data obtained from the trace sets exhibit temporal correlation among the MDs. While in our previous simulations, in Section 4.7, we were devoid of such temporal correlations among the MDs.

fraction of average usage of APs in an indoor building, we first explore each AP inside the building and compute the number of time intervals during which each AP has an MD to serve. We perform the same process for all the APs located inside the building and take an average over all the APs, to provide the fraction of average usage of APs.

Average AP idle time duration:

The AP idle time duration metric is introduced to designate the average amount of time an AP is idle before at least one MD associates with the AP and tries to send and receive a packet. For this metric, we calculate the complementary cumulative distribution function (CCDF) of the period of time, over a day, during which APs remain idle with no MDs and averaged over a month. This metric gives us an idea about how long the APs in the buildings are unused.

(a) (b)
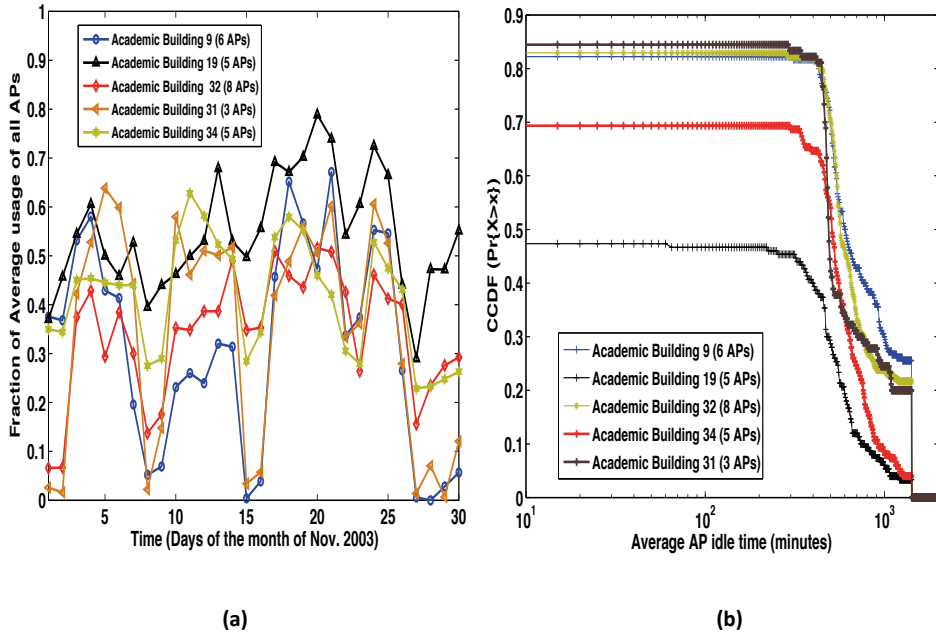
Figure 4.7: *(a) Fraction of average usage of APs in academic buildings (b) Average AP idle time in academic buildings*

From the SNMP trace set, we can observe that there are different kinds of buildings in the campus namely academic, administrative, social and residential buildings etc. We studied the pattern of usage in each building type and found that each type of buildings follows a different pattern of AP usage. In Fig. 4.7, and Fig. 4.8 we considered the academic buildings and the residential buildings re-

(a)   (b)
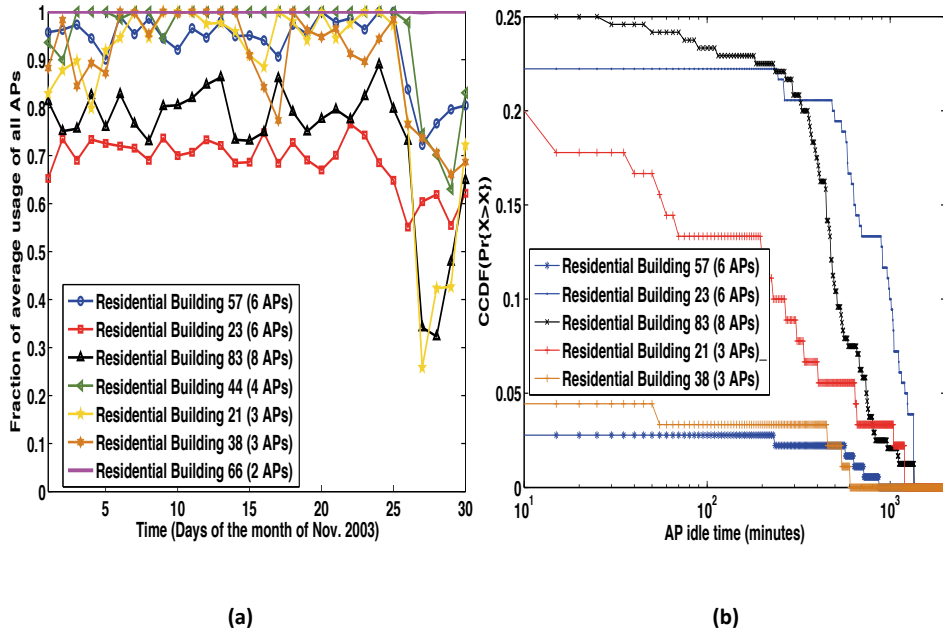
Figure 4.8: *(a) Fraction of average usage of APs in residential buildings (b) Average AP idle time in residential buildings*

spectively where we plotted the fraction of average usage of APs and the average AP idle time for the month of November 2003[10]. The fraction of average usage of APs in residential buildings was found to be much larger than for academic buildings. This is due to the fact that users tend to spend most of their time, in a day, at their residence. In Fig. 4.9(a), (b) the same metrics are studied over 71 APs located in different indoor buildings and we found that the maximum average usage of those APs was around 60% and the probability that an AP remains idle for at least 7 hours is 0.52.

Each AP consumes approximately 20 Wh [107]. Aruba networks, one of the major players in the WLAN market, reported 100 new customer acquisition with each customer requiring 75 APs per WLAN in 2009 [108]. Thus an approximate calculation about the energy that is wasted every week, during 7 hours daily idle time, sums up to a staggering amount of 3.8 MWh. Thus energy wastage in today's world, where there are tens of thousands of APs operating is massive.

We are aware that the case study presented here is relatively old, as the tracesets are from 2003, and presents a not so accurate picture because of the in-

---

[10]Due to the unavailability of any recent WLAN trace sets we used the ones that are freely available in [98].

(a)   (b)
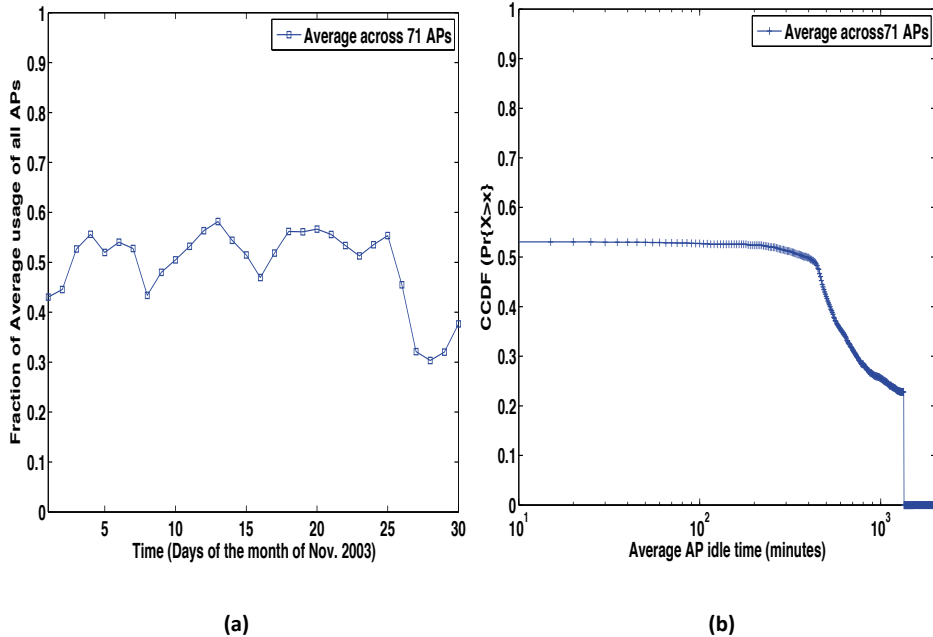
Figure 4.9: *(a) Fraction of average usage of* 71 *APs (b) Average AP idle time for* 71 *APs*

troduction of new wireless applications and devices in today's market. But the problem is still relevant because of the trend of over-dimensioned deployment of APs in an indoor environment. Thus with the growing deployments of larger centralized enterprise WLANs, in indoor, to support varied data rate and latency requirements of different applications and also due to the growing number of communication devices, we expect that our algorithms for energy efficient Fi-Wi network deployment can only perform better, in-terms of energy saving, resource utilization, and energy efficiency, as compared to the results discussed in our forthcoming sections.

4.9   Network scenarios

In this section we will characterize network scenarios to compare RoF-based CE-WLAN and the traditional CE-WLAN, when the energy saving On-Demand strategy is employed. We can contemplate two different scenarios that reflect all of the different real life possibilities.
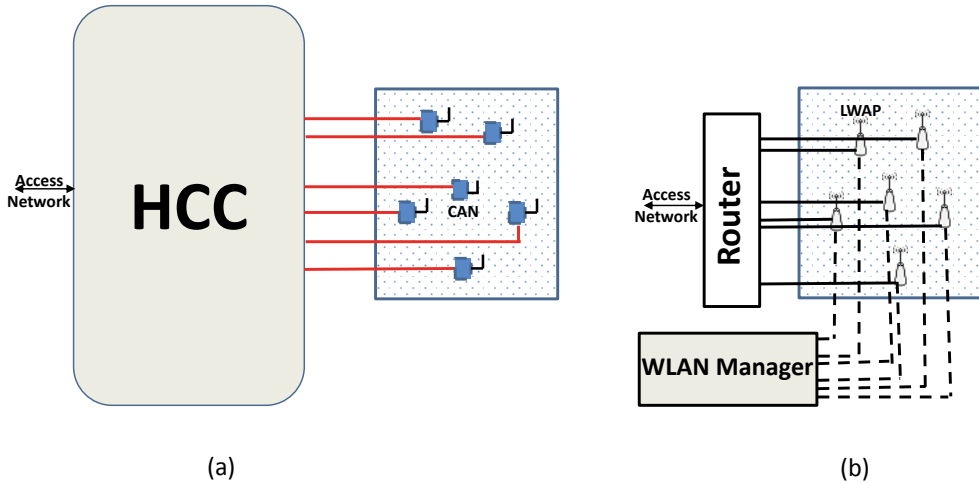
(a)   (b)

HCC : Home Communication Controller; CAN : Cell Access Node;
LWAP: Light-Weight Access Point.

Figure 4.10: *(a) RoF CE-WLAN colocated network entity scenario (b) Traditional CE-WLAN colocated network entity scenario*

- **Colocated network entity scenario**: Fig. 4.10(a) represents the colocated network entity scenario under the RoF CE-WLAN. Here all the CANs are deployed such that they have overlapping cell areas. Thus one CAN connected to an AP is sufficient for providing basic coverage over the whole cell area. Similarly in Fig. 4.10(b) we can observe the colocated network entity scenario for the traditional CE-WLAN, where one LWAP is sufficient to ensure basic coverage over the whole area.

- **Clustered network entity scenario**: Fig. 4.11(a) and (b) represent the cluster network entity scenario for both the RoF and the traditional CE-WLAN respectively, whereas an example, two individual cluster groups of network entities (CANs or LWAPs) are formed. Each of the different cluster group needs one individual network entity (CAN or LWAP) to provide full coverage in its cluster area. Thus for a clustered network entity scenario, there are non-overlapping clusters of network entities.

Our next step is to compare, in the next section, the performance of the **On-Demand strategy** for traditional and RoF CE-WLAN and for the discussed network scenarios.

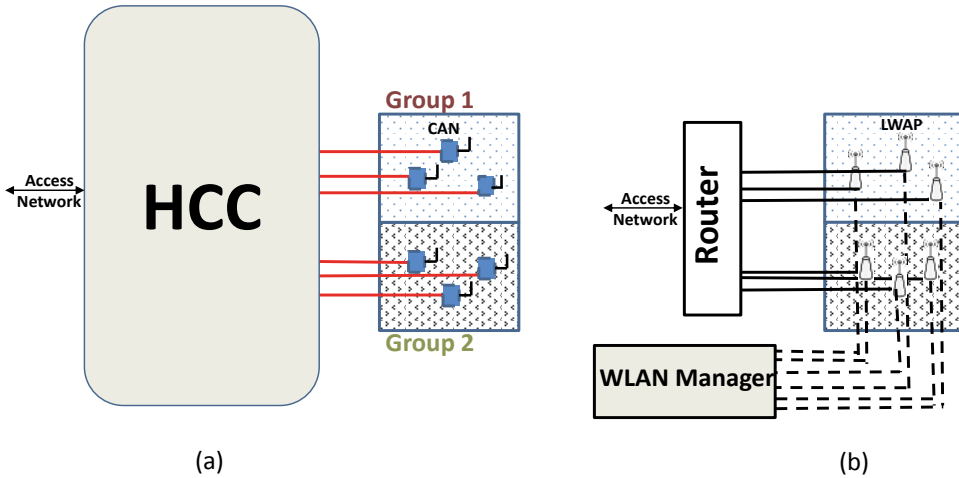(a)   (b)

HCC : Home Communication Controller; CAN : Cell Access Node;
LWAP: Light-Weight Access Point.

Figure 4.11: *(a) RoF CE-WLAN clustered network entity scenario (b) Traditional CE-WLAN clustered network entity scenario*

4.10   Comparison of On-Demand strategy for RoF and Traditional CE-WLAN

In Section 4.6, we proposed the On-Demand strategy and evaluated its performance for RoF CE-WLAN using MATLAB (Section 4.7). The results showed energy saving w.r.t. the Always-On strategy. But we did not evaluate the performance of the On-Demand strategy for traditional CE-WLAN and RoF CE-WLAN. In this section, we, therefore, utilize the WLAN SNMP trace sets of Dartmouth campus [98], to evaluate their performance. Note that, previously the results in Section 4.7, lacked temporal correlation among MD positions. In this section, since we employ real life trace sets, we take into account both temporal and spatial MD correlation.

Simulation set-up:

From the trace sets [98], we consider a residential and an academic building with 6 APs in each building. Fig. 4.12(a) and (b) portray the number of MDs connected to those 6 APs in that academic building on a Monday, and the residential building on a Saturday. We chose Monday and Saturday as they are the busiest days in the academic and residential buildings respectively. Fig. 4.13(a) and (b) represents the total throughput of 6 APs for the same academic and residential buildings, on the same day.

Note that, since SNMP was used in [98] to poll each AP every five minutes, querying AP about MD-specific counters, so each of the five minutes intervals serves as a time-slot for our simulations.

Total throughput: The term total throughput represents a number of bits sent and received by each AP per time-slot.
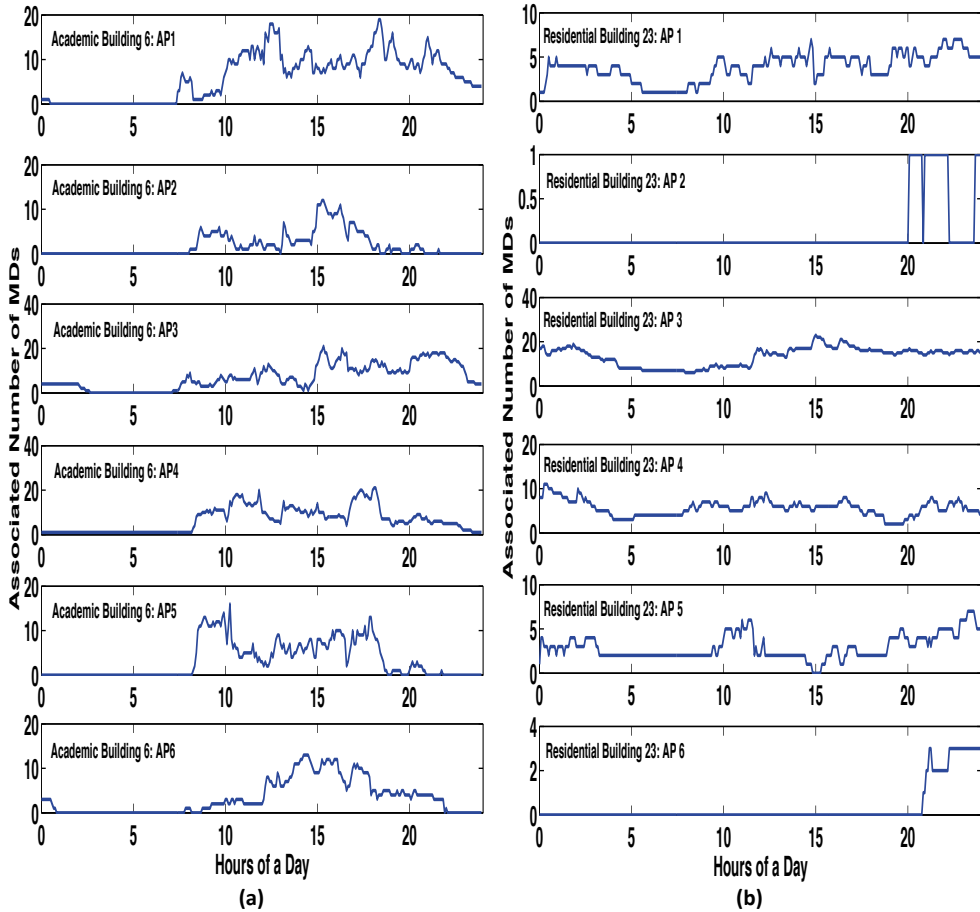
Figure 4.12: *Associated number of MDs to different APs in (a) academic building on Monday (b) residential building on Saturday*

In our simulations, we determine the set of CANs and APs needed to be switched on or off over a day. We assume that we have knowledge of the physical layer ca-
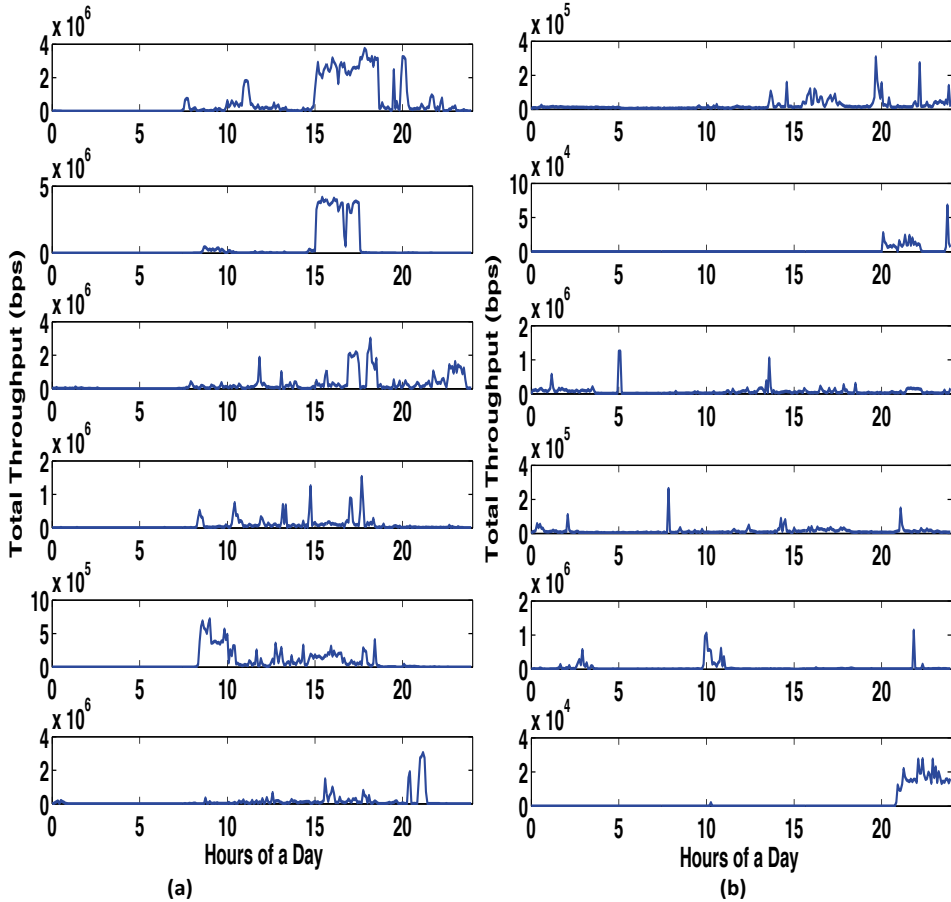
Figure 4.13: *Total throughput of different APs in (a) academic building on Monday (b) residential building on Saturday*

pacity (C) of the APs. For the simulations, we assume that $C = 100$ Mbps[11].

We compare our On-Demand RoF and Traditional CE-WLAN scheme against the Always-On strategy, where all the LWAPs in the coverage area are kept switched on all the time.

4.10.1   On-Demand strategy for colocated network entity scenario

Energy saving

---

[11]We also conducted our simulation runs with different values of C which portray similar findings. Note that the source code and the results of all the related algorithms and simulations can be obtained by contacting the author via email celusddb@gmail.com.

We compute the percentage of energy saving attainable during the whole day. If we look at Fig. 4.14(a)[12], the maximum and the minimum energy saving[13] obtained for the academic building was 83% and 20% respectively. Similarly looking at Fig. 4.14(b) we can see that the energy saving for the residential building was 83% at all time, thus proving that the network achieves higher energy saving gains from On-Demand strategy as compared to the Always-On strategy.

(a)   (b)
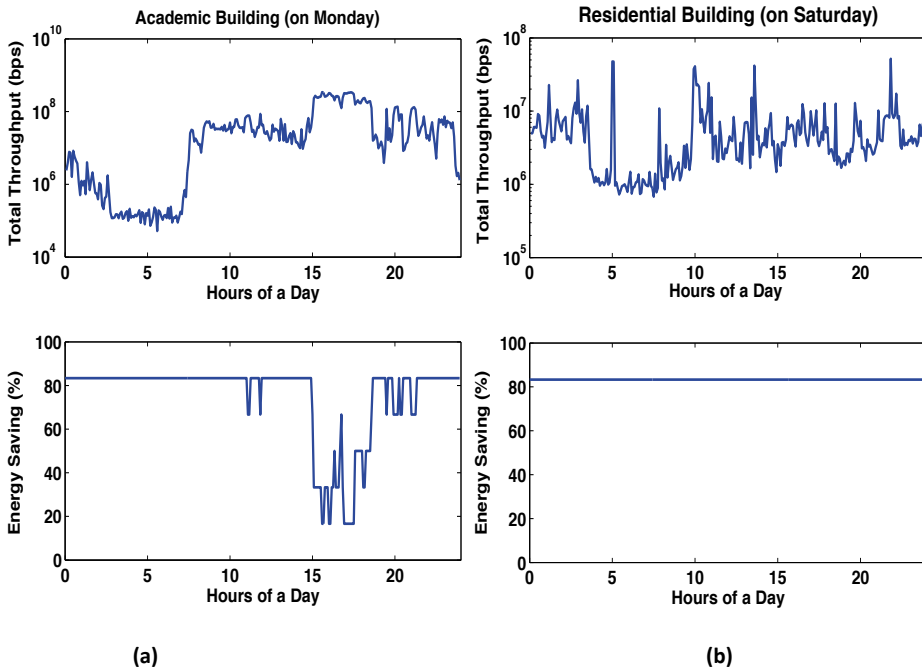
Figure 4.14: *Percentage of energy saving for colocated scenario (On-Demand RoF CE-WLAN strategy), over a day, for (a) academic building (b) residential building*

For a comparison of the energy saving attainable by the On-Demand strategy for both the traditional and the RoF CE-WLAN (compared against the Always-On strategy) let us look at Table 4.3. We can observe that using the On-Demand strategy results in large energy savings (6.05 daily kWh for the RoF scheme in the academic building). But the RoF CE-WLAN scheme consumes more energy

---

[12]For the sake of clarity of the results, our uppermost plots in Fig. 4.14 (a), (b) provide the total throughput across all 6 APs over the hours of a day.

[13]Note that the energy saving was computed for the On-Demand RoF CE-WLAN by comparing against the Always-On strategy where all the LWAPs are kept switched on at all times.

than the traditional CE-WLAN scheme because the network has to switch on more entities (CANs) compared to the traditional scheme (only LWAPs). However, the difference for both schemes is marginal (see Table 4.3).

Table 4.3: Energy saving (academic building)

Scenario	Strategy	Scheme	Energy Saving (Daily kWh)
Colocated	On-Demand	Traditional	6.09
Colocated	On-Demand	RoF	6.05
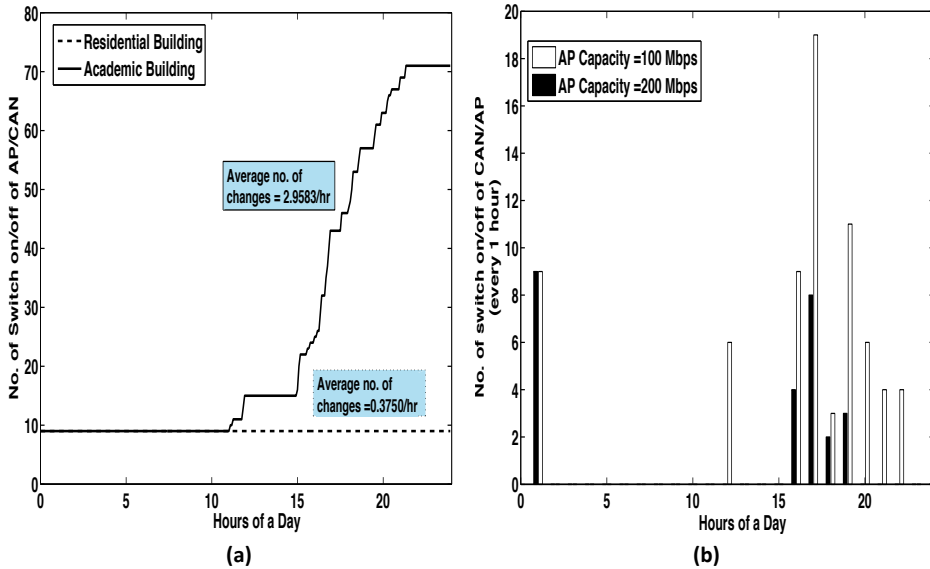
Figure 4.15: *(a) Cumulative number of switch on/off occurrences of CAN/AP (On-Demand RoF CE-WLAN strategy) over a day (b) Number of switch on/off occurrences of CAN/AP (On-Demand RoF CE-WLAN strategy) over 1 hour interval for the academic building*

Switching changes

One more important metric to compare is the cumulative number of switching changes of CANs and LWAPs, needed over a day, and also the maximum number of switching changes over an hour. These metrics help us understand if the MDs will face heavy disruption in the network, which can degrade the quality of the service perceived. From Fig. 4.15(a)) we can observe that the average number of changes per hour in the case of the academic building on Monday was found to be 2.96. Now if we look at Fig. 4.15(b) we can see that the maximum

number of changes on the peak hour for an academic building was 19 (AP capacity $C = 100$ Mbps), which indicates that MDs associated with the LWAPs during peak hour were highly active. We can also notice that (see Fig. 4.15(b)) increasing the physical layer capacity of the LWAP two times can decrease the number of changes more than two times, during peak traffic hour.
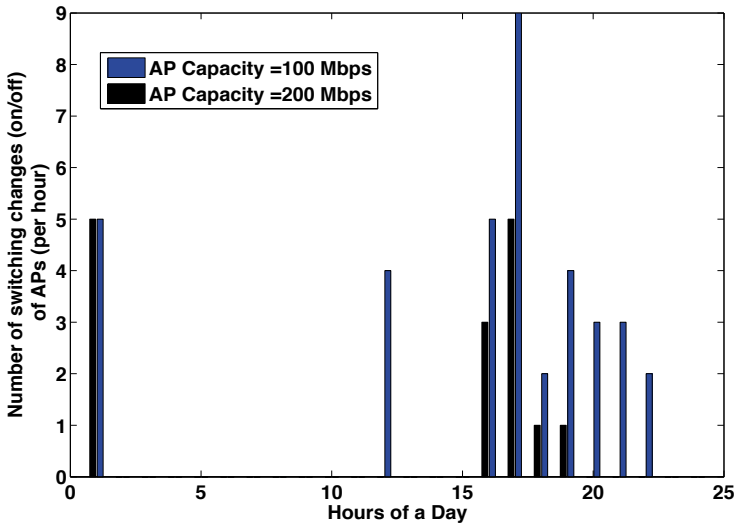
Figure 4.16: *Number of switch on/off of AP for On-Demand RoF CE-WLAN strategy over 1 hour interval for academic building*

But the actual disruption faced in the network is only gauged by the number of switching changes that the LWAPs has to undergo. This is because of the fact that the MDs have to re-associate themselves with new LWAPs. Fig. 4.16 depicts the number of switching changes that have to be performed every hour. One interesting fact to note is that, for the colocated network scenario, the number of switching changes for the On-Demand strategy for both RoF and traditional CE-WLAN is the same. Thus the disruption perceived by the MDs will be of the same magnitude for both the traditional and RoF CE-WLAN while employing On-Demand strategy.

Energy efficiency

Energy efficiency refers to the amount of energy utilized to transmit a bit per Hertz (Hz). Note that, in calculating the energy efficiency, we utilized the AP's bandwidth of 20 MHz, used in [98].

The energy efficiency of a network is another important parameter to judge the performance. The trend is shifting from spectral efficiency to energy effi-

ciency [109].

While for the academic building, in the colocated RoF scenario, we can ob-
serve that for off-peak hours the energy spent to transmit a bit is large (Fig. 4.17(a)),
but for the residential building (Fig. 4.17(b)) it is far less. This can be explained
by the fact that, in a residential environment the traffic difference between the
peak and the off-peak hour is not as massive as in the academic building. A similar
trend is observed for the On-Demand colocated traditional CE-WLAN. The differ-
ence between the On-Demand traditional and the RoF energy efficiency is very
marginal (maximally 2% for the residential building), which is why we chose not
to plot the On-Demand traditional CE-WLAN in Fig. 4.17.

(a)   (b)
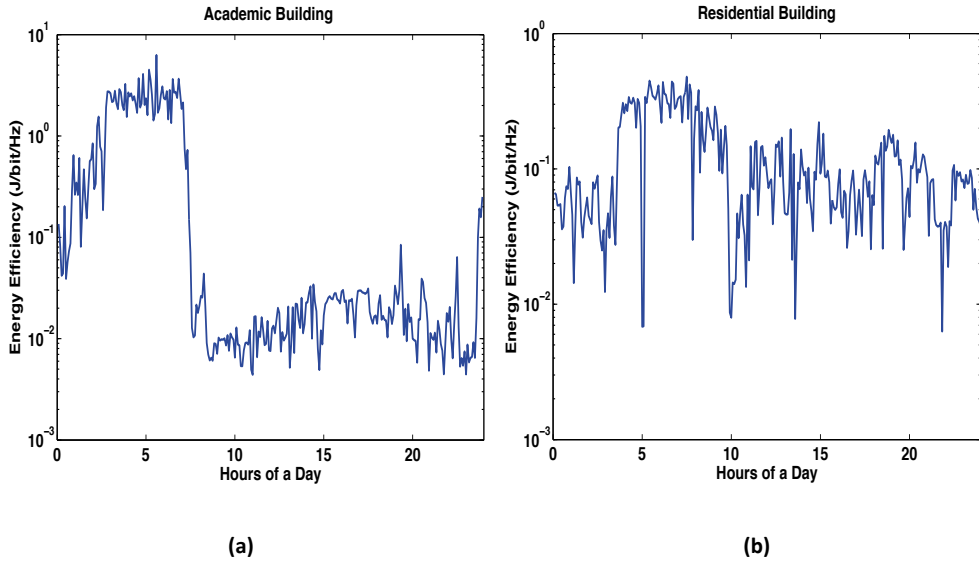
Figure 4.17: *Energy efficiency for colocated scenario (On-Demand RoF CE-WLAN)
over a day for (a) academic buildings (b) residential buildings*

4.10.2   On-Demand strategy for clustered network entity scenario

In a dense CE-WLAN network, the cluster-based network deployment is much
more realistic, as not all the LWAPs (or CANs) will have overlapping cell areas be-
cause of their transmit power limitations, thus forming different clusters of LWAPs
(or CANs). The results obtained below show that the RoF scheme allows for higher
gains in terms of energy saving, energy efficiency, and resource utilization.

Energy saving

In the uppermost plots of Fig. 4.18(a) and (b), variations in total throughput across the LWAPs associated in two different cluster groups (Group 1 and 2), over a day, are shown. Each group consists of 3 LWAPs or CANs. Thus either 1 CAN or one 1 LWAP is always needed to be switched on to ensure full coverage of a single cluster area. From Fig. 4.12 we can also get the number of MDs associated with the two clusters by grouping the first three LWAPs as Group 1 and the last three LWAPs as Group 2.

(a)   (b)
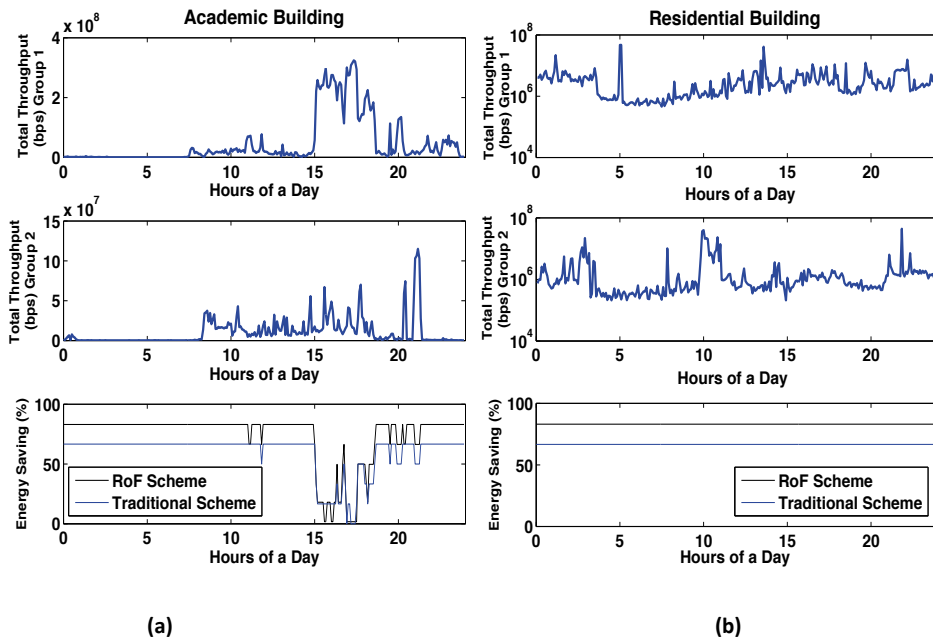
Figure 4.18: *Throughput and energy saving for clustered scenario (On-Demand strategy) over a day for (a) academic buildings (b) residential buildings*

In the bottom plots of Fig. 4.18 we can observe a comparison of the percentage of energy saving that is achievable by using the On-Demand strategy based traditional and the RoF-based CE-WLAN. In Fig. 4.18(a) we can observe that the maximum energy saving, for the academic building, for the traditional CE-WLAN is 66%. Whereas for the RoF-based CE-WLAN (see Fig. 4.18(a)), we can observe that the maximum energy saving is 83%. We also observe an anomaly at two different time intervals, the energy saving of the RoF scheme is less than the traditional approach and this can be accounted by the extra energy consumption due to the use of CANs which could lead to less saving, in cases where an equal

number of LWAPs are sufficient for both the traditional and the RoF CE-WLAN. Similarly, if we look at Fig. 4.18(b) we can see the energy saving that is achievable for the residential building. For the traditional CE-WLAN, the residential building achieves an energy saving of 66% as compared to 83% energy saving achieved by the RoF CE-WLAN. If we calculate the energy saving for a whole day, for the academic building (see Table 4.4), the RoF scheme saves 6.04 daily kWh as compared to the traditional CE-WLAN which saves 4.85 daily kWh. Thus, for the clustered network scenario (academic building), the RoF CE-WLAN is approximately 25% more energy efficient.

Table 4.4: Energy saving (academic building)

Scenario	Strategy	Scheme	Energy Saving (Daily kWh)
Clustered	On-Demand	Traditional	4.85
Clustered	On-Demand	RoF	6.04

Switching changes

(a)   **(b)**
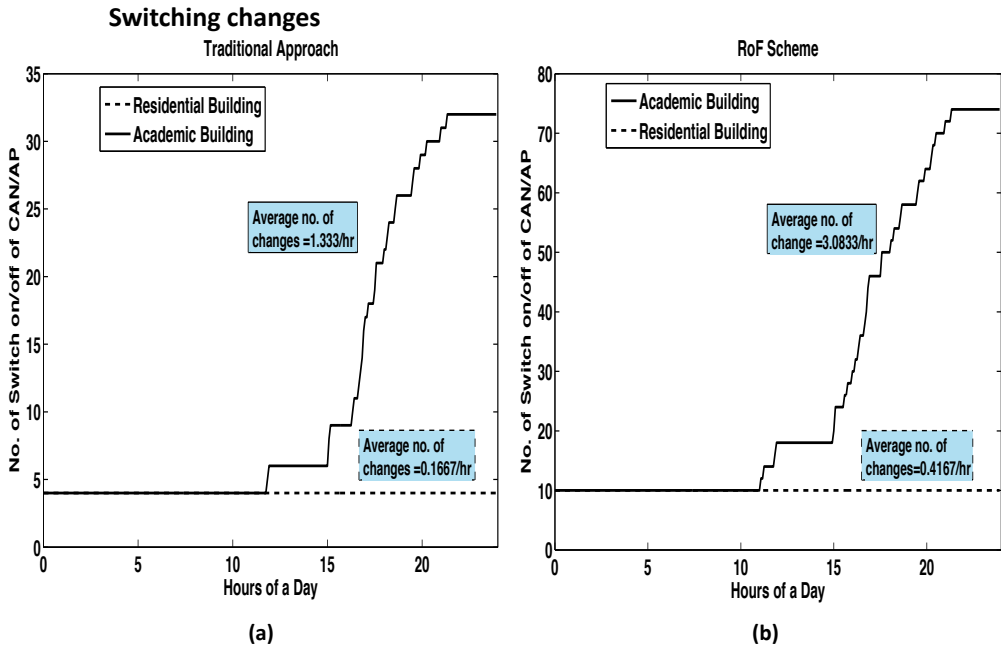
Figure 4.19: *Cumulative number of switch on/off of CAN/AP for clustered scenario (On-Demand strategy) for (a) Traditional approach (b) RoF approach*

Now let us compare the number of switching changes that the network has to

perform. Looking at Fig. 4.19 we can observe that the average number of changes per hour for traditional CE-WLAN in an academic building is 1.33, whereas for RoF CE-WLAN is 3.0833. The traditional CE-WLAN requires less number of switching changes of network entities as compared to the RoF scheme. Although the number of changes in RoF scheme is greater than the traditional approach, it is interesting to study how it impacts the performance of the MDs. For this, we can see Fig. 4.20, where we computed the number of switching changes for LWAPs that are needed. This number represents how many times MDs have to initiate the association and authentication procedure. From Fig. 4.20 we can observe that for the RoF CE-WLAN the maximum number of switching changes, for LWAPs, in an hour is 9, whereas for the traditional scheme it is 7. We can also compare the number of LWAPs, which are kept on during the different time intervals of the day, and we can see that more LWAPs are kept on for the traditional than for the RoF-based CE-WLAN. Thus the RoF CE-WLAN helps in minimizing the wastage of resources by keeping more LWAPs switched off than the traditional CE-WLAN.
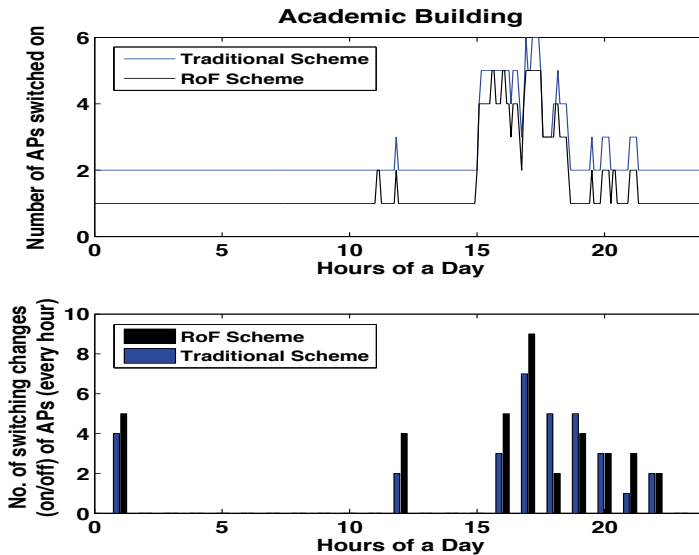
Figure 4.20: *Number of APs switched on and number of switching changes (on/off) of APs, every hour, for On-Demand strategy*

Resource utilization and Energy efficiency

Resource utilization refers to the ratio of the number of bits that are sent and received from all the switched on LWAPs to the total capacity offered by them.

(a)   (b)
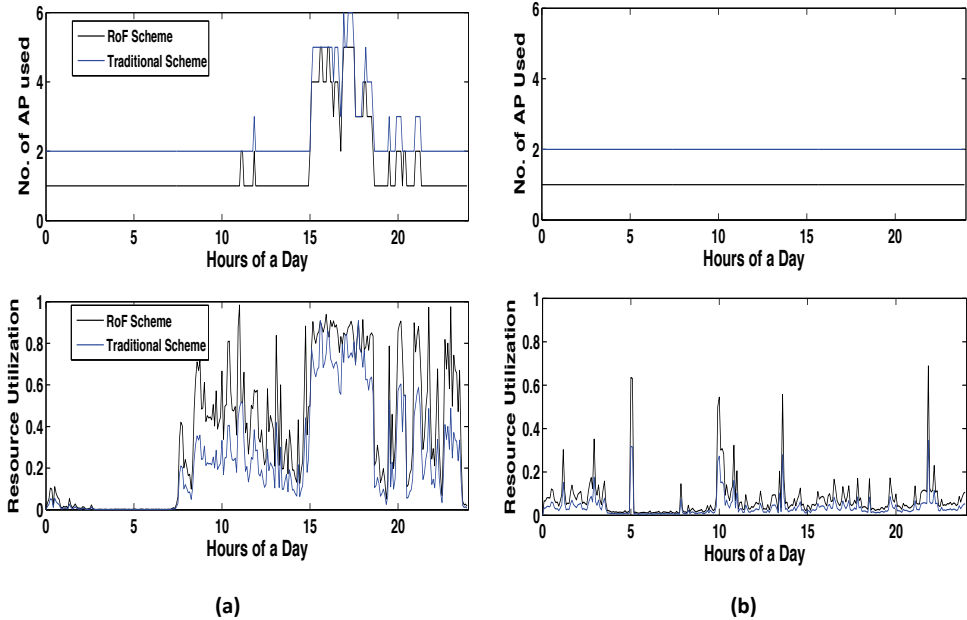
Figure 4.21: *No. of APs used and resource utilization for clustered scenario (On-Demand strategy) (a) Traditional CE-WLAN (b) RoF CE-WLAN*

Comparing the results obtained in Fig. 4.21(a) and Fig. 4.21(b) for both the RoF and the traditional CE-WLAN (for both academic and residential building), we can see that a higher resource utilization is obtained for the RoF CE-WLAN as compared to the traditional CE-WLAN, in every time interval. If we look at the number of LWAPs used (for the RoF CE-WLAN) in the peak period for the academic case it can be found out to be 5. Whereas, the maximum number of LWAPs used for the traditional CE-WLAN is 6. This can be attributed to the DAS implementation in the RoF CE-WLAN. Next, we compute the energy efficiency metric. As is evident from Fig. 4.22(a) and (b), the RoF CE-WLAN results in better energy efficiency as compared to the traditional CE-WLAN, at all time intervals.

Thus we saw that using the On-Demand strategy and DAS-based RoF CE-WLAN achieved higher energy saving, resource utilization, and energy efficiency. The penalty we pay for the RoF CE-WLAN as compared to the traditional CE-WLAN is the number of switching changes we have to make. Although we should note that the number of switching changes of only LWAPs is comparable for both the RoF and the traditional CE-WLAN. Thus the disruption of MDs due to switching changes of LWAPs is also envisioned to be similar.
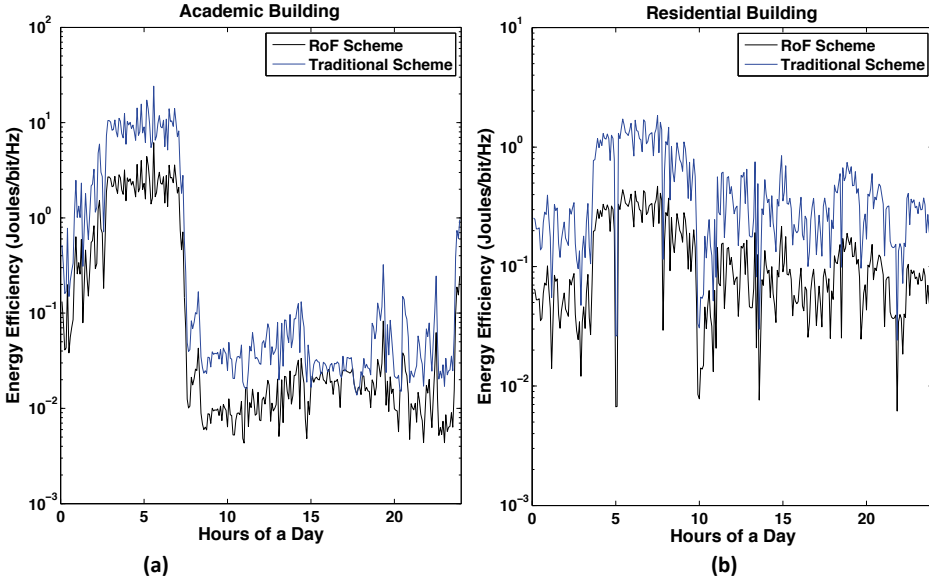
Figure 4.22: *Energy efficiency for clustered scenario (On-Demand strategy) (a) Traditional CE-WLAN (b) RoF CE-WLAN*

4.11 Power-managed Load-balanced RoF CE-WLAN

The indoor network should be both: (a) energy efficient and (b) load balanced, for optimal performance. Therefore we combine both techniques of dynamic radio resource management (proposed in Chapter 3) and energy efficient communication, to propose a unique power-managed load-balanced (PMLB) algorithm for indoor RoF CE-WLAN.

4.11.1 System description

The RoF-based CE-WLAN architecture (see Fig. 4.1), consists of m WiFi APs (represented by the set $M = \{1, 2, ..., m\}$). They are providing connectivity to a set of PCANs ($P = \{1, 2, ..., p\}$) and SCANs ($S = \{1, 2, ...s\}$) located in indoor spaces. $I = \{1, 2, ..., i\}$, represents the set of MDs already connected through the PCANs. Let us represent the set of CANs that connects to an AP m by N_m. We also denote the set of MDs associated with a CAN n by I_n. We assume that the locations of the PCANs and the SCANs are properly assigned using radio planning tools, which is usually the case for newly constructed office buildings. While the PCANs are used to provide basic coverage, the SCANs are used to provide granular

QoS refinement by the dynamic shifting of MD traffic. Thus as mentioned previously, if the PCANs are not able to handle the traffic demand arising from more than one MD in its coverage area, the RNM can decide to turn on the SCANs (in the coverage area of the congested PCANs) and connect them to other APs to satisfy the MD demand. We make the same assumptions as discussed in Section 3.4 and Section 4.5. The reasoning behind the assumptions and the impact they have on system performance have been discussed before. To characterize the load level at individual APs, we use the metric of total downlink delay (as discussed in Section 3.6). The justification for using the total downlink delay metric can be found in Chapter 3.

4.11.2   Optimization problem

Problem statement: Given a set of APs $M = \{1, 2, .., m\}$, PCANs $P = \{1, 2, .., p\}$ and SCANs $S = \{1, 2, .., s\}$, where $|M| \geq |P|$ and $|M| < |P| + |S|$, we have to devise a strategy to minimize the total energy consumption of the RoF CE-WLAN by providing connectivity through the PCANs and a subset of the SCANs ($\hat{S}$) and the APs ($\hat{M}$). We have to ensure that the **aggregate channel utilization** across each AP, that is used for connectivity, is less than a predefined threshold value to ensure proper QoS. We also have to balance the load between the $\hat{M}$ AP subset that is switched on by shifting connectivity of SCAN $\hat{S}$, such that the **total downlink delay** of the network is reduced.

Our optimization problem is thus twofold,

- Firstly, reduce the total energy consumed by the RoF CE-WLAN, by providing connectivity through a subset of APs and CANs (PCANs and SCANs).

- Next perform load balancing among the subset of switched-on APs, by changing connectivity between them such that the overall network performance (total downlink delay) is improved.

The first optimization problem (*Optimization problem* 1), to minimize the total energy consumption of the RoF CE-WLAN network, was formulated as an ILP problem in Section 4.5.

The network performance, characterized by the total downlink delay experienced by the MDs, can be further improved by switching the connections between the SCANs and APs that are switched on ($\hat{S}$ and $\hat{M}$, which are obtained as a solution to the *Optimization problem* 1). The *Optimization problem* 2 for load

balancing can thus be formulated similarly, as in Section 3.6.3:

$$\text{Minimize} \sum_{\forall m \in \hat{M}} \sum_{n \in \hat{S}_m} \sum_{i \in \hat{I}_n} V_{mi}^{nD}$$

$$= \sum_{\forall m \in \hat{M}} \sum_{n \in \hat{S}_m} \sum_{i \in \hat{I}_n} (D_i + \frac{L_i}{b_{mi}^{nD}})$$

subject to

$$b_{mi}^{nD} \le p_{mi}^{D} \frac{P_m R_{mi}^{n}}{T_m}, \ \forall i \in \hat{I}, n \in \hat{S}, m \in \hat{M}. \tag{4.9}$$

$$p_{mi}^{D} \le \sum_{j \in \{BE,VS,CBR\}} (1 - \vartheta_j)^{\sum_{n \in N_m} \sum_{j \in \{BE,VS,CBR\}} i_{n_j}} \quad \begin{matrix} \forall i \in \hat{I}, \\ n \in \hat{S}_m, \\ m \in \hat{M} \end{matrix} \tag{4.10}$$

$$D_i = \begin{cases} \dfrac{\nu_{i_{CBR}} \sigma^2_{\overline{T_i}_{CBR}}}{2(1 - \nu_{i_{CBR}} \overline{T_i})} & \text{CBR MDs} \\[2ex] \dfrac{\nu_{i_{VS}} (\sigma^2_{\overline{T_i}_{VS}} + \frac{s}{\nu_{i_{VS}}})}{2(1 - \nu_{i_{VS}} \overline{T_i})} & \text{VS MDs} \quad \forall i \in \hat{I}. \\[2ex] \dfrac{\nu_{i_{BE}} (\sigma^2_{\overline{T_i}_{BE}} + \sigma^2_t)}{2(1 - \nu_{i_{BE}} \overline{T_i})} & \text{BE MDs} \end{cases} \tag{4.11}$$

where
$\hat{I}$ represents the MDs located in the region of the switched on SCANs,
$\hat{S}_m$ represents the set of SCANs connected to AP m,
V_{mi}^{nD} represents a packet downlink delay from AP m to MD i, using SCAN n,
D_i represents the average queue waiting time for MD i,
$\frac{L_i}{b_{mi}^{nD}}$ represents the downlink packet transmission time from AP m to MD i.
Constraint (4.9) concerns the downlink throughput for MD i connected to AP m using any CAN n. Constraint (4.10) concerns the probability of successful transmission in the downlink. Constraint (4.11) refers to the average queue waiting time for MD i's packet, which can belong to any category (VS, BE, CBR).

4.11.3 Proposed heuristic: Power-Managed Load-Balanced strategy

The Power-Managed Load-Balanced (PMLB) algorithm consists of two parts:

- **Energy Efficient Assignment:** The first and the foremost important part of the PMLB strategy is the RoD technique to minimize the total energy consumption of the whole network.

- **Performance Management:** During the performance management phase, the connection of the SCANs with the APs are reviewed and then dynamically changed such that the total downlink throughput of the network can be maximized or, in turn, the total downlink delay across the MDs can be reduced.

Optimization 1: *Energy efficient assignment*

We proposed a heuristic algorithm in Section 4.6, On-Demand strategy, that provides resources to MDs, only when there is a demand for it. The algorithm was divided into three main parts (a) connection-guaranteeing coverage, (b) MD-demand quantification and $c)$ switching on-off CANs and APs. Please refer to Section 4.6 for a detailed description of the strategy.

Optimization 2: *Performance management*

The channel utilization metric used in *Optimization* 1, is an incomplete measure of the congestion level in the network and requires throughput and goodput measurements of the channel to describe it accurately. So we propose to utilize the total downlink delay measure, which is obtained based on the calculations of downlink throughput as a measure of network congestion. Thus shifting the connectivity between the switched-on APs and the SCANs, that are connected to them, can improve the network performance by decreasing the total downlink delay. The algorithm for performance management is similar to the one discussed in Chapter 3 (see Section 3.7 for a detailed description).

The pseudo-code for PMLB is provided in Algorithm 3.

Algorithm 3 Power-Managed Load-Balanced strategy

1-5 Perform Algorithm 1.
6 Initialize: Get $\hat{S} \subset S$; $\hat{M} \subset M$.
7 Assess Load Level: Find set $M_c = max_{m \in \hat{M}} V_m^D$ with maximum downlink delay.
8 Crossover payoff: Compute $(t, X) = max_{t \in \hat{S}_z, X \in \hat{M} - M_c} \{V_Z^D - V_{X \cup \{t\}}^D\} \forall t \in Z$, where Z is an AP in M_c with lowest ID.
9 Swap: check if $\{V_Z^D - V_{X \cup \{t\}}^D\} > 0$
check if there exists (Y, j) that satisfies swap condition then swap SCAN t to AP Y and SCAN j to AP X.
10 Crossover: Else crossover SCAN t to X.
11 Repeat Steps **8** till **10** until no more APs in M_c has SCAN to perform crossover operation.

4.11.4 Results and discussion

In this section our motivation is to compare three different schemes:

- Always-On strategy

- On-Demand strategy

- PMLB strategy

The performance of the schemes is compared on (a) power saving, (b) total downlink throughput and delay, and (c) the impact on MD power consumption, for both uniform and non-uniform MD distribution over the network coverage area. The simulations consider an indoor open office space of size $20m \times 20m$
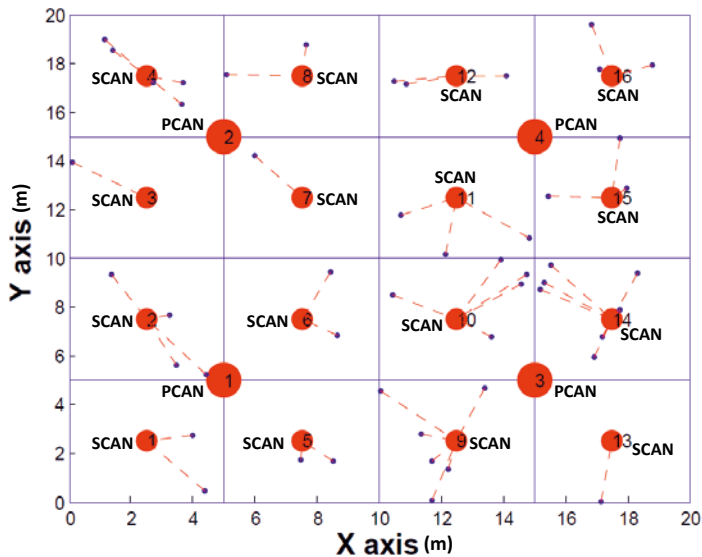
Figure 4.23: *Simulation scenario PCAN and SCAN layout*

(see Fig. 4.23). There are 4 PCANs (see Fig. 4.23) connected to 4 different APs. The area across each PCAN is divided further into 4 SCAN cell areas that are non-overlapping. We vary the number of total MDs from 10 to a max of 70. For the simulations, we only consider the BE traffic. We have chosen to use only BE traffic because the energy saving gain, downlink throughput etc., become more prominent than when using different classes of traffic. We perform the simulation under both uniform and non-uniform distributions of MDs (see Table 4.5). For the

non-uniform distribution, the MDs are distributed according to a Gaussian distribution across the x and the y coordinates with a mean of 10 m and a variance of 3m. For the association of MDs to APs, we assume RSSI based association for both cases. We perform Monte Carlo simulations in MATLAB to obtain the simulation results. In our figures, we only plot the average values of the downlink throughput per MD, downlink delay per MD, power per MD and the energy per bit goodput obtained over all the simulation runs. The same random waypoint mobility model is employed for the mobility of the MDs. Please refer to Section 3.8 for the description of the mobility model and the remarks on it.

Table 4.5: Simulation parameters

Parameters	Values
Carrier Frequency	2.4 GHz
Channel Bandwidth across AP	20 MHz
Path loss model	ITU office model [103]
Indoor Environment (Dimensions)	Open Office space ($20\,\text{m} \times 20\,\text{m}$)
Number of [PCANs, SCANs]	[4, 16]
Number of APs	16
Number of MDs	[10-70]
MD Distribution	Uniform, Gaussian (10 m, 3 m)

Power saving

Let us take a look at the figures to understand our findings. For the case of the PMLB and the On-Demand strategies, the power saving is the same. This is because PMLB is performed after executing similar power saving steps as in the On-Demand strategy. For a uniform distribution of MDs, we see a max of 74.1% power saving (see Fig. 4.24 (a)). The power saving observed by the schemes for non-uniform 10 MDs case is 74.6% (see Fig. 4.24(b)). As the number of MDs increases, we can see that the percentage of power saving increases for the non-uniform distribution as compared to the uniform distribution case (69.5% and 68.1% for non-uniform and uniform distribution respectively). This is because, as the number of MDs increases, for the uniform distribution more network entities need to be switched on in comparison to the non-uniform MD distribution case.

Downlink throughput and delay

But the power saving comes at a cost of downlink throughput achievable at the MDs (see Fig. 4.25). The throughput degradation gap reduces as the number
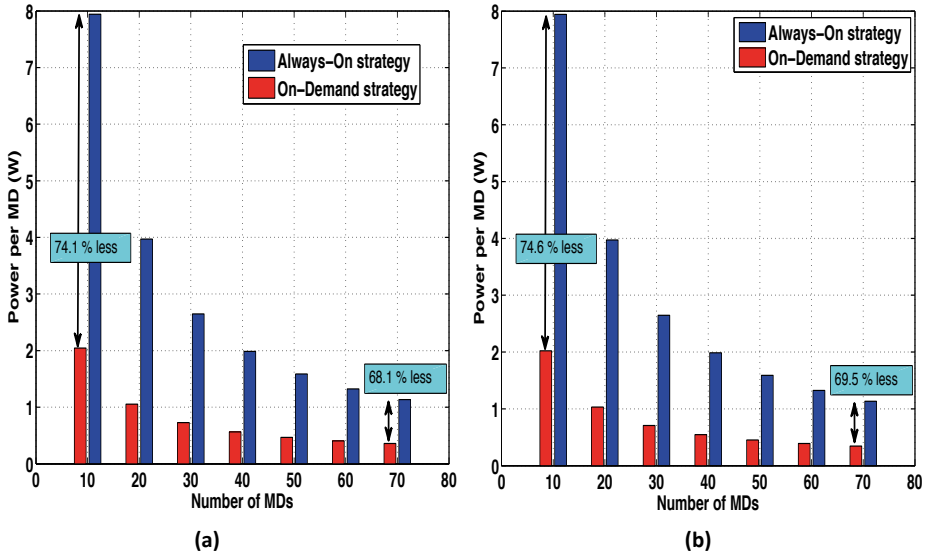
Figure 4.24: *Power per MD for (a) uniform distribution of MDs (b) non-uniform distribution of MDs*
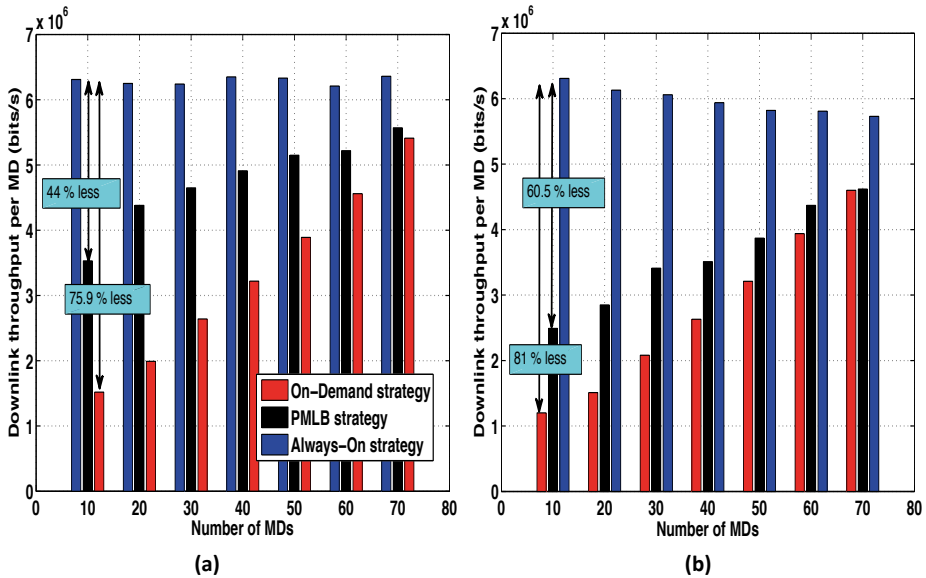
Figure 4.25: *Downlink throughput per MD for (a) uniform distribution of MDs (b) non-uniform distribution of MDs*
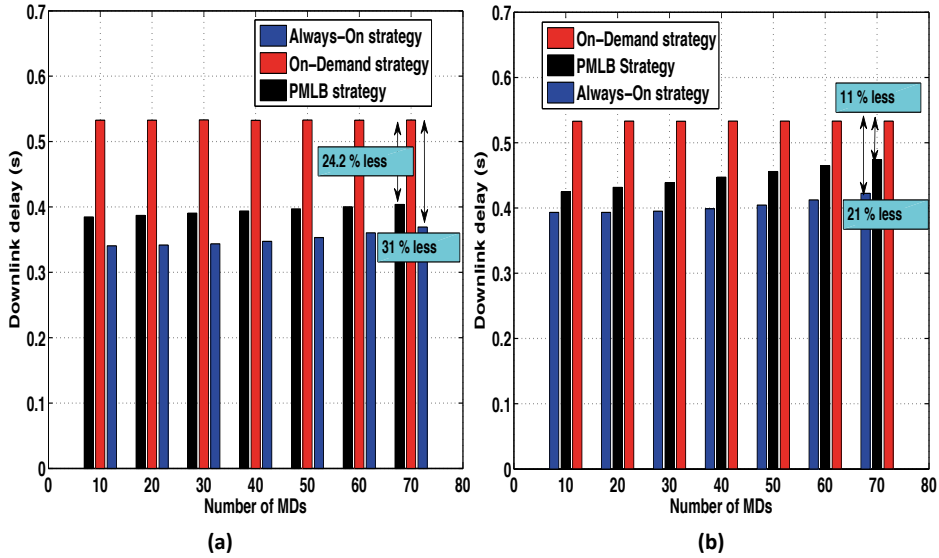
Figure 4.26: *Downlink delay for (a) uniform distribution of MDs (b) non-uniform distribution of MDs*

of MDs increases. This is because of the fact that as the number of MDs increases, more SCANs gets switched on and get connected to other APs thus reducing the congestion across the PCANs. Moreover, the distance of the MD from the PCAN can take larger values than when the MDs are very close to the SCANs, thus the rate obtained across the MDs, when using the SCANS, increases. If we look at the downlink throughput achievable for the non-uniform distribution case, we observe a larger gap (see Fig. 4.25 (b)) between the Always-On strategy and the PMLB strategy owing to the fact that the MDs are more concentrated around a few PCANs and thus causing uneven probability of success values, which increases the overall downlink throughput gap. Similarly, we can observe the downlink delay achievable (see Fig. 4.26) for both the cases.

Energy per bit goodput

We also studied the energy per bit goodput (EBG). We observe that for a uniform distribution of MDs, the EBG is minimized for both On-Demand and PMLB strategy as compared to the Always-On strategy (see Fig. 4.27 (b)). For the non-uniform distribution case we observe that the EBG is reduced only for the PMLB case (e.g., 52% lower than the On-Demand strategy for 10 MDs) as compared to the Always-On strategy. But for the On-Demand strategy with a lower MD count, its performance degrades compared to the Always-On strategy (see Fig. 4.26 (b)).

Impact on MD power consumption
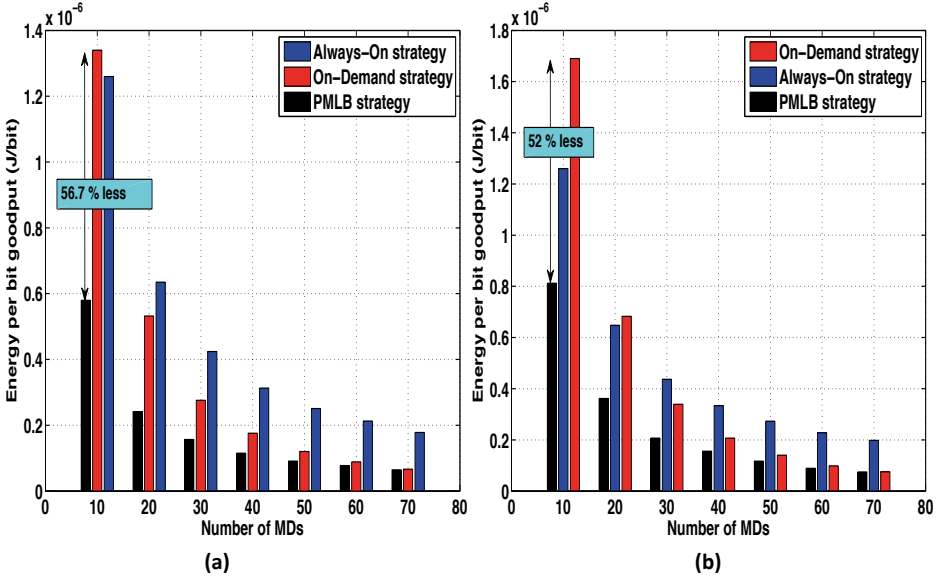
Figure 4.27: *EBG for (a) uniform distribution of MDs (b) non-uniform distribution of MDs*

The impact of the PMLB algorithm on the MD power consumption can be obtained from [110] $P_T \propto d^n$, where P_T, d, n refers to the transmit power, the distance between the MD and the CAN and the path-loss coefficient respectively. Thus employing transmission power control at the MDs results in a reduction of the transmit power proportionally to the distance. But the power that is saved at the MD is of the order of few mWs, which is negligible compared to the power consumed at the network side.

The difference of the distance between MDs and CANs, for both PMLB strategy and Always-On strategy, using $P_T \propto d^n$, can thus be given by [110]:

$$\zeta = \sum_{\forall i \in I} ((\log(d_1^i) - \log(d_2^i))) = \frac{\sum_{\forall i \in I} (\log(P_{T_1}^i) - \log(P_{T_2}^i))}{n} \qquad (4.12)$$

where

d_1^i represents the distance between MD i and the associated CAN under Always-On strategy,

d_2^i represents the distance between MD i and the associated CAN under PMLB strategy,

$P_{T_1}^i$ represents the transmit power for MD i under Always-On strategy strategy,

$P_{T_2}^i$ represents the transmit power for MD i under PMLB strategy.

From Fig. 4.28 we can observe that the difference of the logarithmic distances for the non-uniform case and for a higher number of MDs is smaller than for a uniform distribution of MDs. This is because as more MDs are in the network the non-uniform distribution of MDs packs more MDs in a smaller area and thus the probability that the distance between the MD and the CANs is larger for PMLB strategy is small as compared to the case of uniform distribution of MDs. Thus the power saved for a non-uniform distribution of MDs is more than for a uniform distribution.
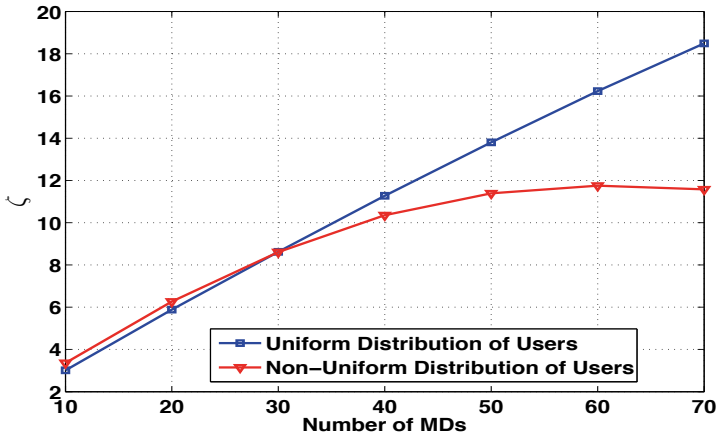
Figure 4.28: *Logarithmic difference of the distances between PMLB strategy and Always-On strategy w.r.t. number of MDs*

4.12 Conclusion

Our focus in this chapter was to make the indoor CE-WLAN network more energy efficient. We advocated the implementation of RoF CE-WLAN that takes advantage of the RoF-based DAS for minimizing the energy wastage in the network. The RoF-based DAS architecture allows for many CANs to be connected to a single AP, which allows for higher utilization of the AP's offered capacity as compared to the traditional deployment. For the RoF CE-WLAN, we provided a detailed power consumption model and formulated the problem of minimizing the total energy

consumption in the network such that the channel utilization across the APs, that are switched on, are below a threshold value.

We then proposed a MD demand driven RoD strategy namely, the On-Demand strategy, that minimizes the overall power consumption in the network while providing measures for (a) ensuring basic coverage of the whole indoor network, (b) providing MD demand quantification and (c) switching off unused APs and CANs. We used MATLAB simulations to show that the RoF CE-WLAN can provide high power savings as compared to the Always-On strategy where all the network entities are kept powered on at all times. For uniform distribution of MDs, the power saving of RoF CE-WLAN was found to be 63% while the EBG gain was 30%.

We then discussed the amount of energy wastage in a large enterprise WLAN using the Dartmouth campus as an example. The study points out that large numbers of APs remains idle over a period of the day, wasting a lot of energy. The AP usage also varies spatially and over time. Thus pointing out that we can indeed take advantage of this varied AP usage pattern and save a large amount of energy. We then pointed out the different network scenarios that are possible in CE-WLAN. The network entities could either have colocated or clustered coverage.

The channel utilization for the On-Demand strategy was then studied for different network scenarios, using the trace sets from Dartmouth. Our finding points out that traditional CE-WLAN fairs marginally better than the RoF CE-WLAN in terms of energy saving and switching changes, for the colocated network entity scenario. While for the clustered network entity scenario, the RoF-based CE-WLAN gains extensively as compared to the traditional CE-WLAN. Although a penalty to be paid is the total number of switching changes that have to be performed for both APs and CANs. One more interesting point to note is that the APs switching changes are almost the same for both, resulting in similar disruptions faced by the network MDs due to re-association to a new AP. The results show that RoF CE-WLAN indeed achieves higher energy savings, energy efficiency, and resource utilization.

Finally, we proposed a PMLB strategy, that switches on CANs and APs in a RoF-based CE-WLAN, such that the total MD demand is satisfied. Then the load across each AP is balanced by shifting the connections between the SCANs and the APs connected to them. We observed the power consumed in the network is reduced by nearly 76% (for 10 MDs) for the non-uniform MD distribution case. We also observed that the PMLB technique also improved the downlink throughput and delay for the RoF CE-WLAN as compared to the On-Demand strategy.

4.12.1   Limitations and future work

This chapter provided an overview of the energy efficient RoF-based CE-WLAN indoor but there are various areas that need further investigation:

- **Channel allocation:** The On-Demand strategy was proposed based on the channel utilization observed at the APs. Although the strategy provides details about various aspects of the implementation of such RoD strategy, the algorithm does not provide any answers as to how the frequency channel allocations across the APs should be performed. The areas of the PCANs and he SCANs are bound to have overlapping cell area and thus frequency allocation across APs, serving those PCANs and SCANs, is an important area that has not been discussed in this dissertation.

- **Lack of new WLAN trace sets:** In this chapter, due to the unavailability of recent data sets from a CE-WLAN, the simulations justifying the RoD policies were carried out using the freely available trace sets of Dartmouth campus [98]. The introduction of new applications and devices has a significant impact on the way the CE-WLAN network is accessed by the MDs nowadays. Thus it is necessary to conduct experiments to gather recent WLAN trace sets. The study of RoD strategies on such trace sets will lend valuable insights into the present day energy saving capabilities.

- **SCAN and PCAN selection:** We also made the assumption that the PCANs and the SCANs are selected beforehand based on indoor radio planning. However, the selection of the PCANs and the SCANs can be done on the fly. We have also discussed some schemes regarding this selection in our work [102].

- **Frequency planned PMLB:** The PMLB strategy proposed utilizes the load balancing technique discussed earlier in Chapter 3. The load balancing technique was proposed for non-overlapping cell areas to avoid the complexity of frequency planning. Thus investigations on how to combine frequency planning techniques with PMLB strategy is also an area that should be looked into.

- **Reconfiguration cost, delay and frequency:** Finally one important limitation of the work in this chapter is that we did not discuss the cost, delay, and frequency of reconfiguration. Their impact and ways to optimize them are described briefly in Section 3.9.1. But they require further investigations.

5

Fi-Wi Uplink

5.1 Introduction

The RoF architecture provides the network with two important degrees of free-
dom (a) multiple optical wavelengths to carry the RF signals to different CANs,
and (b) radio channels that can be reused spatially at each CAN. For WiFi, the
medium access contention mechanism is CSMA/CA. If mobile devices (MDs) served
by different CANs, using the same radio channel, try to access that channel, there
is a chance that there will be a collision at the AP located at the HCC, because
they are hidden to each other. These MDs at different CANs are deaf to each
other's ongoing transmission as they are outside each other's sensing range. So,
when they transmit their messages, these messages can collide at the AP. In IEEE
802.11, the hidden node problem has been extensively studied [48, 111--114].
This problem will cause a reduced throughput over the Fi-Wi channel, compared
to collision free access. The request-to-send/clear-to-send (RTS)/(CTS) mecha-
nism, to deal with the hidden node problem, can also adversely impact the per-
formance of the system. They can hamper the transmission of MDs, communi-
cating with different APs, that are using the same frequency channel. Moreover
using the RTS/CTS mechanism makes sense only if the data packet length is larger
than a threshold value. Hence it is not a generic solution for all sizes of data pack-
ets [115]. The use of the point coordinated function (PCF) access at the HCC could
in principle help to avoid the hidden node problem, but hardly any manufacturer
has implemented PCF today.

In this chapter, we investigate how we can resolve the hidden node collision
problem. We propose a novel multi-user multiple input multiple output (MU-
MIMO) uplink scheme that takes advantage of both the spatial and the optical

multiplexing. We compare the MU-MIMO uplink scheme with a multi-user detection technique called successive interference cancellation (SIC). SIC serves as a comparative benchmark. A SIC receiver [116] implementation at the HCC makes it possible at the physical layer to decode messages from the MDs across different CANs, that arrive simultaneously, and, in principle, avoids the loss due to hidden node collisions. The proposed MU-MIMO technique can be used to provide even higher network capacity gains. A huge amount of literature is available about conventional MU-MIMO techniques (e.g., [117--119]). Our proposed MU-MIMO scheme takes advantage of the spatially distributed MDs communicating with the MU-MIMO-enabled CANs. Different optical wavelengths are used to transport the messages to the HCC where the decoding is done. The optical fiber provides a huge bandwidth and has no (for our purpose) significant bit error rate. For the communication scenarios we consider, the propagation delay introduced by the optical fiber is negligible, which allows for the WiFi protocol to stay within the operating range specified by the IEEE 802.11 standards.

In this chapter we model and compare three different cases for uplink access:

- No modifications to the normal WiFi standard, i.e., independent MDs transmission where collisions are allowed.

- The use of SIC at the AP in the HCC.

- The use of a novel opto-spatial MU-MIMO uplink scheme.

This chapter is organized as follows. Section 5.2 describes the Fi-Wi system architecture. Section 5.3 provides an overview of SIC. We then analytically find the capacity that is achievable by using SIC and compare it against the unmodified system. In Section 5.4 we propose our MU-MIMO architecture for Fi-Wi networks and determine the capacity achievable. Section 5.5 compares the bit error probability, for the three cases. Section 5.6 presents the simulation results and finally in Section 5.7 we highlight our achievements and provide a future outlook.

5.2 System architecture

The RoF-based Fi-Wi architecture has been described extensively in Chapter 2. However, for the clarity of understanding, we would like to repeat the important parts of the architecture in this section. The architecture described here is a centralized architecture controlled by the HCC. RoF is used to distribute radio signals throughout the building using CANs, which act as distributed antenna elements. The red lines in Fig. 5.1 represent the optical fibers. There is a single
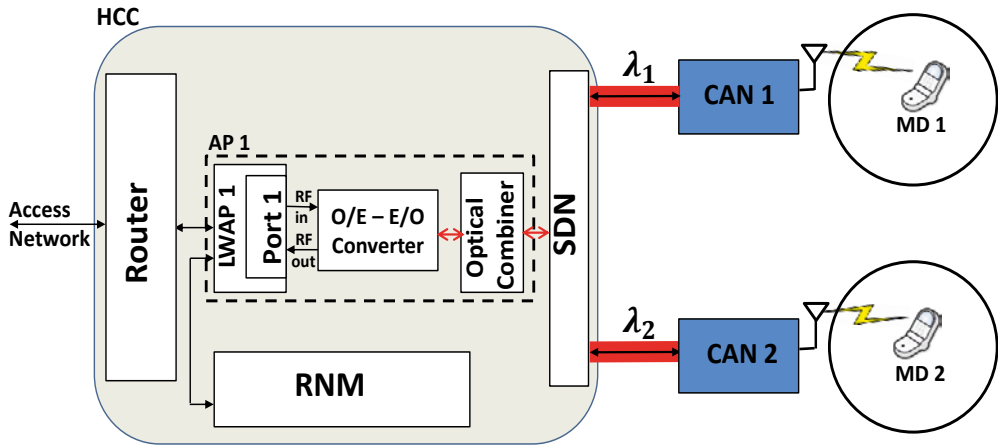
HCC : Home Communication Controller; CAN : Cell Access Node; AP : Access Point;
RNM : Radio Network Manager; SDN : Signal Distribution Network; LWAP : Light-
Weight AP; MD : Mobile Device.

Figure 5.1: *Overall system architecture*

CAN per room or living space. Each radio cell is confined to the room or living space, where WiFi is supported. We assume that there is no overlap between the radio cells. The number of CANs is assumed to be more than the number of non-overlapping channels in WiFi. Thus many CANs use the same radio channel. However, for our analysis, we consider two such CANs, each with a single antenna element, operating at the same radio channel, in different rooms, trying to communicate with a single WiFi AP[1] located in the HCC. In Fig. 5.1, CAN 1 and CAN 2 are operating at the same radio channel. We also use two different optical wavelengths, λ_1, λ_2, across the CANs to transport the signal in the uplink. The optical signals, transmitted from different CANs on different wavelength, are combined, by an optical combiner, before feeding them to an O/E - E/O converter at the HCC for optical to electrical conversion.

The electrical to optical conversion used at the CANs, in the uplink, consists of an amplifier and a laser diode for amplifying the RF signals received from the MDs and converting them to optical signals.

The system architecture described in this section is applicable for the cases of independent transmissions and SIC as described in Section 5.1. For MU-MIMO, the system architecture is a bit different and is explained later in Section 5.4.

---

[1]Note that LWAP in the AP module has a single port for transmission and reception of radio signals.

5.3 Successive interference cancellation

A well-known technique in cellular networks for decoding messages that arrive simultaneously is successive interference cancellation (SIC). It is the ability of the receiver to receive and decode two or more messages concurrently, which otherwise would have been lost due to the collision. The recent advances in software-defined radio like GNU radios [120], [121] have led us to think that SIC is implementable for indoor system architecture. SIC receivers have been shown to be practically implementable in [120] for Zigbee (which operates in the same ISM band as that of WiFi employing CSMA/CA as the MAC contention mechanism) using software radios for the wireless environment.

With SIC the trick of decoding the messages lies in decoding the message from the MD with higher received signal strength (RSS) where all other MDs messages are treated as interference. Subtracting the reconstructed signal of that decoded MDs message from the mixed signal allows for possible decoding of other weaker signal from the residue. The use of a SIC receiver at the HCC thus helps to deal with the problem of the hidden nodes. We defer from going into the implementation part of SIC receiver and focus on the physical layer aspects of using SIC for our architecture.

Assumption: *We assume that for implementing SIC, without any power control across the CANs (described later in Section 5.3.2), the MDs in different cells operate with different RSS.*

MDs are heterogeneous in nature. Depending on the capability of the MD and the radio link between the MD and the AP, different MDs may operate with different modulation schemes, e.g., complementary code keying (CCK) for IEEE 802.11 b and OFDM for IEEE 802.11 g/n/ac, and so on. The transmit power limit, set by ETSI, for OFDM is 20 dBm and for CCK its 18 dBm [122]. This, in turn, may result in different RSS for different MDs. Moreover, other reasons that can cause different RSS received from different MDs are [123] (a) different hardware used at the MDs, (b) spatial variation due to difference in distance between MDs and the receiving AP, (c) RF interference from other devices operating in the same frequency band, (d) human presence/absence, and (e) environment, e.g., wall type, the material used and so on.

5.3.1 System model

Let x_1 and x_2 (see Fig. 5.2) be two messages that are being transmitted from the two independent MDs (MD 1 and MD 2 respectively). The receiver at the HCC thus receives an amplified version of the signals received across the two different
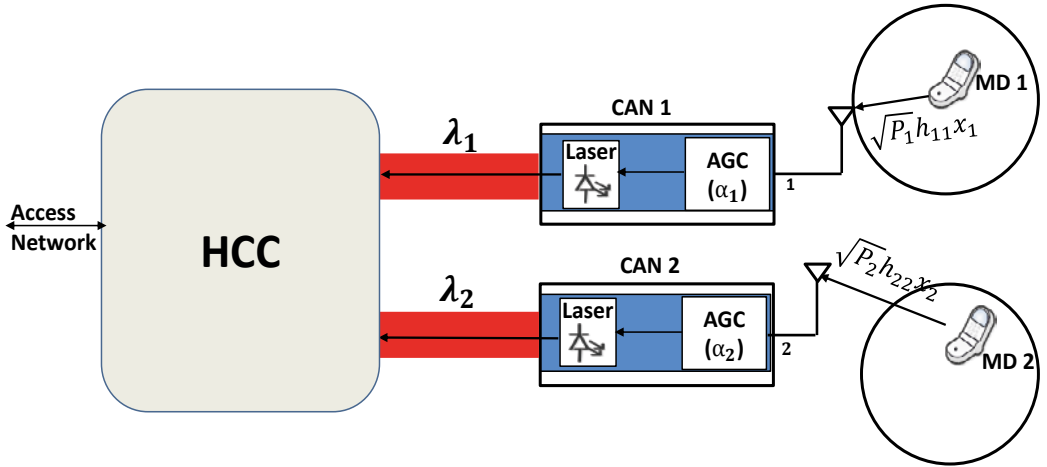
HCC : Home Communication Controller; CAN : Cell Access Node;
MD : Mobile Device; AGC : Automatic Gain Controller.

Figure 5.2: *System model*

CANs, and can be given as below:

$$y = \alpha_1 y_1 + \alpha_2 y_2, \tag{5.1}$$

where y_j and α_j (see Fig. 5.2[2]) represent the signal received from MD i across the CAN j and the amplification factor with which MD i's received signal at CAN j is amplified. y_j can be expressed as:

$$y_j = \sqrt{P_i} h_{ij} x_i + n_j, \tag{5.2}$$

where
h_{ij} represents the respective channel gain from MD i to CAN j,
x_i is the message transmitted from MD i,
n_j represents the noise across the CAN j that receives MD i's signal,
P_i represents the transmission power at MD i.

---

[2]Note that we only represented the AGC and laser source, as the only components, in the O/E -E/O Converter as we consider only the uplink scenario.

Thus, (5.1) can be rewritten as:

$$
\begin{aligned}
y &= \alpha_1 y_1 + \alpha_2 y_2 \\
&= \alpha_1 \sqrt{P_1} h_{11} x_1 + \alpha_2 \sqrt{P_2} h_{22} x_2 + \underbrace{\alpha_1 n_1 + \alpha_2 n_2}_{n_0} \\
&= \alpha_1 \sqrt{P_1} h_{11} x_1 + \alpha_2 \sqrt{P_2} h_{22} x_2 + n_0,
\end{aligned}
\tag{5.3}
$$

where $n_0 = \sqrt{N_0} = \sqrt{|\alpha_1 n_1 + \alpha_2 n_2|^2}$. N_0 represents the noise variance. The amplification factors (α's) can be calculated as follow:

$$
\bar{P} = \alpha_j^2 E[y_j]^2.
\tag{5.4}
$$

$\bar{P}$ represents the relative constant power level, of the received radio signal (after amplification), that is needed to feed the laser source at the CAN[3]. $E[\cdot]$ represents the expected value of a random variable.

Let B be the bandwidth of the operating wireless channel. The decodability of the two messages with SIC depends on the RSS and the transmission bit rates. When the two MDs, as shown in Fig. 5.1 as MD 1 and MD 2, are transmitting concurrently to the HCC, the HCC must decode the message with the strongest RSS first. Without loss of generality, let us assume it to be x_1, treating the other one, x_2 in our case, as interference. Thus the rate achieved by MD 1 is:

$$
\begin{aligned}
r_1 &= B \log_2 \left(1 + \frac{P_1 |h_{11}|^2 |\alpha_1|^2 |x_1|^2}{P_2 |h_{22}|^2 |\alpha_2|^2 |x_2|^2 + N_0} \right) \\
&= B \log_2 \left(1 + \frac{X_1}{X_2 + N_0} \right),
\end{aligned}
\tag{5.5}
$$

X_1, X_2 represents the RSS of the different MDs at the HCC after optical to radio conversion. Only if MD 1 transmits at rate r_1 or below, it can be decoded successfully by the HCC. After that, HCC can attempt to decode MD 2's signal. The best feasible bit rate r_2 for MD 2, assuming perfect cancellation of MD 1's message, can thus be given as:

$$
r_2 = B \log_2 \left(1 + \frac{X_2}{N_0} \right).
\tag{5.6}
$$

To facilitate SIC, MD 1 with the strongest RSS may achieve a lower rate than MD 2, which has a weaker RSS. This is due to the fact that the signal from MD 1 is decoded in the presence of noise and interference from MD 2 but MD 2 signal is decoded only in the presence of noise.

---

[3]The amplification at the CAN in the uplink is done by the Automatic Gain Controller, which is needed because of the fading propagation variations of the received radio signal from the MD.

5.3.2 Capacity without and with SIC

The basic measure of performance of a system is capacity. The hybrid Fi-Wi capacity of a given Fi-Wi channel is the limiting information rate that can be achieved with arbitrarily small error probability. Let us now compare the capacity of the hybrid Fi-Wi channel both without and with SIC.

Without SIC

As there is no packet capture technique applied at the physical layer therefore, without SIC, only one of the two MDs can transmit at the same time. Their transmissions will collide at the HCC if both of them transmit at the same time. Let τ represent the probability of collision at the HCC, for the messages transmitted from MDs at different CANs. So the capacity of the channel without SIC can be given as:

$$
C_{\text{withoutSIC}} = \max \left\{ (1 - \tau) B \log_2 \left(1 + \frac{X_1}{|\alpha_1 n_1|^2} \right), \right.
$$

$$
\left. (1 - \tau) B \log_2 \left(1 + \frac{X_2}{|\alpha_2 n_2|^2} \right) \right\} \quad (5.7)
$$

With SIC

It is possible to simultaneously receive two messages. The highest bit rates at which MD 1 and MD 2 can successfully transmit concurrently are r_1 and r_2 respectively, assuming perfect rate adaptation. Correspondingly, hybrid Fi-Wi channel capacity with SIC can be given as [121]:

$$
\begin{aligned}
C_{\text{withSIC}} &= B \log_2 \left(1 + \frac{X_1}{X_2 + N_0} \right) + B \log_2 \left(1 + \frac{X_2}{N_0} \right) \\
&= B \log_2 \left(1 + \frac{X_1 + X_2}{N_0} \right).
\end{aligned} \quad (5.8)
$$

Let us assume the channel to be time varying. The ensemble average of all these instantaneous capacity over all possible channel matrices is the *ergodic* capacity. So it makes more sense to calculate the ergodic capacity. Thus, the capacity gain with SIC for the Fi-Wi environment is said to be the gain in ergodic capacity that we achieve using SIC over the case when we do not implement SIC

and is given by:

$$\begin{aligned}
\varpi &= \frac{E[C_{\text{withSIC}}]}{E[C_{\text{withoutSIC}}]}, \\
&= \frac{E\left[B \log_2\left(1 + \frac{X_1 + X_2}{N_0}\right)\right]}{E\left[(1-\tau)B \log_2\left(1 + \frac{X_1}{|\alpha_1 n_1|^2}\right)\right]}
\end{aligned} \tag{5.9}$$

The maximum capacity gain is attained at the point where both of $X_1 > X_2$ and $X_2 > X_1$ cases attain the same capacity gains. Thus equating both the cases we obtain the respective RSS at which the maximum of the relative capacity gain is achieved. This can be given as below:

$$\frac{E\left[B \log_2\left(1 + \frac{X_1 + X_2}{N_0}\right)\right]}{E\left[(1-\tau)B \log_2\left(1 + \frac{X_1}{|\alpha_1 n_1|^2}\right)\right]} = \frac{E\left[B \log_2\left(1 + \frac{X_1 + X_2}{N_0}\right)\right]}{E\left[(1-\tau)B \log_2\left(1 + \frac{X_2}{|\alpha_2 n_2|^2}\right)\right]} \tag{5.10}$$

So for maximizing the relative capacity gain, we need to operate at RSS's given by:

$$X_1 = X_2 \left(\frac{|\alpha_1 n_1|^2}{|\alpha_2 n_2|^2}\right). \tag{5.11}$$

Therefore, if we assume that we have full channel state information (CSI) at the HCC, then the HCC can control the amplification factors (α_2, α_2) of the AGC, employed at the CANs, to vary the power received at the CANs from the MDs. This we refer to as the power control scheme with SIC. This, in fact, always makes sure that the RSS's of the MDs are different.

The average *packet transmission time* needed to send the messages from the

MDs to the HCC with and without SIC can be given as follows:

$$
T_{\text{withoutSIC}} = \frac{L}{E\left[(1-\tau)B\log_2\left(1+\frac{X_1}{|\alpha_1 n_1|^2}\right)\right]} +
$$

$$
\frac{L}{E\left[(1-\tau)B\log_2\left(1+\frac{X_2}{|\alpha_2 n_2|^2}\right)\right]} \tag{5.12}
$$

$$
T_{\text{withSIC}} = \max\left\{\frac{L}{E\left[B\log_2\left(1+\frac{X_2}{N_0}\right)\right]},\right.
$$

$$
\left.\frac{L}{E\left[B\log_2\left(1+\frac{X_1}{X_2+N_0}\right)\right]}\right\}. \tag{5.13}
$$

Here, L represents the average packet length. The transmission rates of the two transmissions, with SIC, from the MDs, are different. So we are faced with the problem of disparity in the different rates, which leads to a disparity in transmission time. We can have equal average transmission time with SIC for both the MDs. This will improve the MAC throughput as suggested in [121].

An interesting fact to note here is that there is a fine balance between increasing MAC throughput and physical layer capacity. We can choose to operate at the maximum physical layer capacity or achieve maximum MAC throughput. We can either be greedy, i.e., choose to maximize the systems ergodic capacity, or we can provide equal average transmission time to both MDs and be fair to all.

If the MDs have access to full CSI of both MDs in the Fi-Wi network, then they can vary their transmission powers as below:

$$
P_1 \approx \frac{\bar{P}|h_{22}|^4 E[y_1]^2 P_2^2}{|h_{11}|^2 E[y_2]^4}. \tag{5.14}
$$

Thus (5.14) helps to achieve maximum MAC throughput. Assuming that the HCC has full CSI knowledge, which it can use to calculate the optimal transmit power levels for the MDs, it can direct them to operate at that power level.

5.4 Multi-User Multiple Input Multiple Output

Multi-User Multiple Input Multiple Output (MU-MIMO) is an advanced MIMO technology that exploits the availability of multiple independent data streams from different MDs in order to enhance the communication capabilities of each

individual MD. To the best of our knowledge, this is the first work in the Fi-Wi domain that exploits a unique optical-spatial multiplexing scheme to attain MU-MIMO gains in the uplink.

5.4.1 System architecture

Let us look at the system architecture for MU-MIMO, as given by Fig. 5.3. It follows the same structure as that explained in Fig. 5.1 with some differences. Here, we assume, for the sake of simplification, that there are two different wavelength sets (e.g., λ_1, λ_2 for CAN 1, and λ_3, λ_4 for CAN 2) that can carry the signals from the two antennas at each CAN. We also assume, as in Section 5.2, that the coverage areas of the CANs do not overlap. So if we consider the uplink, MD 1 at CAN 1 is assumed to get two different views of the channel as there are two antennas at each CAN. MD 1 will be sending message x_1 and similarly, MD 2, connected to CAN 2, will send message x_2. At the HCC, the message set (x_1, x_2) carried on the different wavelengths, belonging to different CANs, are combined in the optical domain, using the optical combiner, and are converted back to radio signals using an O/E converter. These are then fed into the LWAP1 at different ports (see Fig. 5.3). Thus, we are able to combine multiple messages from the MDs across different antennas in the CANs to take advantage of MIMO. This scheme takes advantage of the optical wavelength multiplexing for the spatially multiplexed sig-
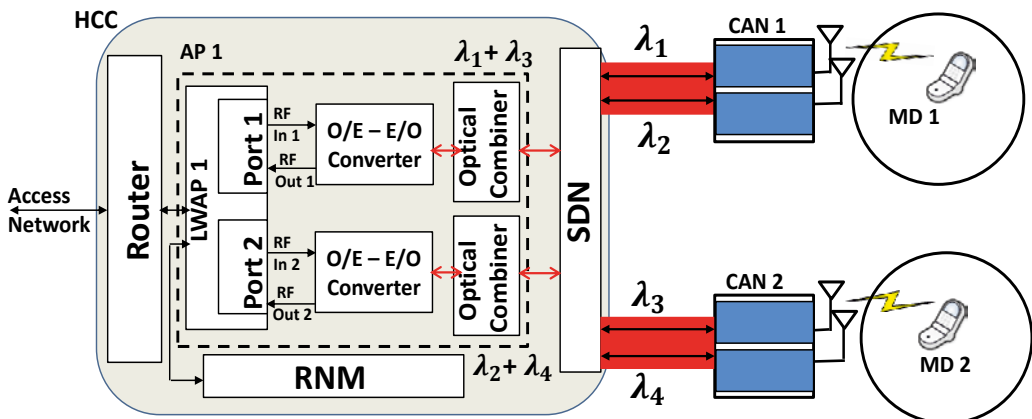
HCC : Home Communication Controller; CAN : Cell Access Node; AP : Access Point; RNM : Radio Network Manager; SDN : Signal Distribution Network; LWAP : Light-Weight AP; MD : Mobile Device.

Figure 5.3: *MU-MIMO system architecture*

nals, from the different CANs, to attain MU-MIMO capabilities. This architecture described can be generalized for larger MU-MIMO systems.

5.4.2 MU-MIMO capacity

The receiver located at the HCC receives two inputs, which can be written into matrix form as:

$$\mathbf{y} = \mathbf{Hx} + \mathbf{n} \tag{5.15}$$

where

$\mathbf{H} = \begin{bmatrix} \alpha_{11'}h_{11'} & \alpha_{21}h_{21} \\ \alpha_{12'}h_{12'} & \alpha_{22}h_{22} \end{bmatrix}$ represents the amplified channel gain matrix,

h_{ij} and α_{ij} (see Fig. 5.4) represent the channel gain and amplification factor respectively, from MD i to antenna j of the CAN under consideration,

$j\epsilon(1', 2')$ represents the antennas across CAN 1,

$j\epsilon(1, 2)$ represents the antennas across CAN 2,

$\mathbf{x} = \begin{bmatrix} \sqrt{P_1}x_1 \\ \sqrt{P_2}x_2 \end{bmatrix}$ represents the messages transmitted,

P_i represents the transmission power across MD i,

$\mathbf{n} = \begin{bmatrix} N_1 \\ N_2 \end{bmatrix}$ represents the noise vector at the HCC, $N_1 = (\alpha_{11'}n_{1'} + \alpha_{21}n_1)$,

$N_2 = (\alpha_{12'}n_{2'} + \alpha_{22}n_2)$,

(n_1, n_2) represents the noise added across the two different antennas at CAN 2,

$(n_{1'}, n_{2'})$ represents the noise added across the two different antennas at CAN 1.

The value of the amplification factors α_{ij} (see Fig. 5.4) can be computed as (5.4), and can be given as below:

$$
\begin{aligned}
\bar{P} &= \alpha_{ij}{}^2(|h_{ij}|^2 P_i|x_i|^2 + |n_j|^2) \\
&= \alpha_{ij}{}^2 E[x_{ij}]^2
\end{aligned} \tag{5.16}
$$

where $E[x_{ij}]^2 = |h_{ij}|^2 P_i|x_i|^2 + |n_j|^2$ is the received signal power from MD i to antenna j across the CAN under consideration. $\bar{P}$ represents the relative constant power level, of the received radio signal (after amplification), that is needed to feed the laser source at the CAN.
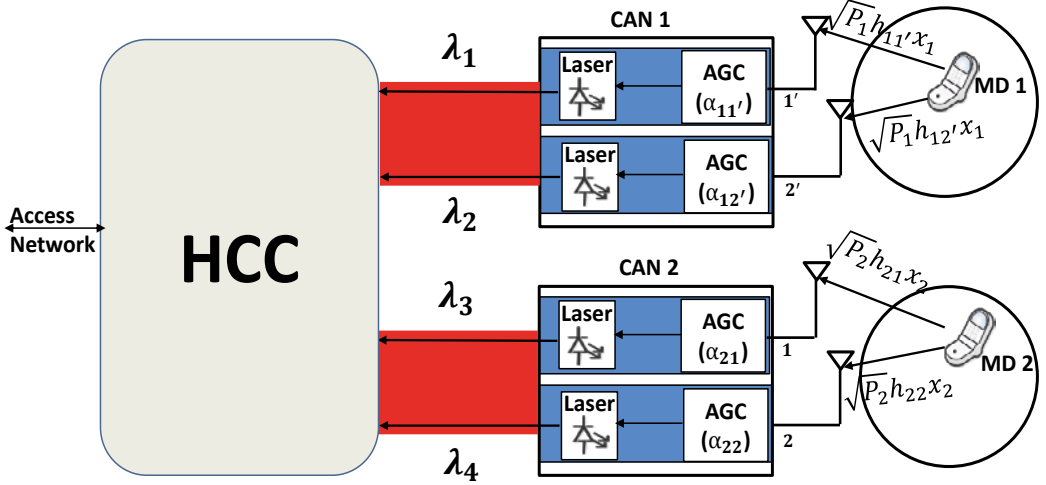
HCC : Home Communication Controller; CAN : Cell Access Node;
MD : Mobile Device; AGC : Automatic Gain Controller.

Figure 5.4: *MU-MIMO system model*

The expression for capacity can thus be given by [124]:

$$C_{\text{MU-MIMO}} = E_{\mathbf{H}} \left[B \log_2 \| \mathbf{I} + (\mathbf{H}) \mathbf{K}_x (\mathbf{H})^H \mathbf{Cov}^{-1} \| \right] \qquad (5.17)$$

where $\mathbf{K}_x$ is the signal variance matrix given by $\mathbf{K}_x = \begin{bmatrix} P_1 & 0 \\ 0 & P_2 \end{bmatrix}$ assuming independent messages and **Cov** is the covariance matrix of the noise, **I** refers to the identity matrix and $\| \cdot \|$ represents the determinant.

The message transmission time for the MU-MIMO case can thus be given as:

$$T_{\text{MU-MIMO}} = \frac{2L}{C_{\text{MU-MIMO}}} \qquad (5.18)$$

where $2L$ accounts for the fact that MU-MIMO decodes messages from both the MDs at the same time.

The capacity gain that we get with MU-MIMO in comparison with SIC and without SIC implementation can thus be written as:

$$\zeta = \frac{C_{\text{MU-MIMO}}}{E[C_{\text{withSIC}}]} \qquad (5.19)$$

$$\delta = \frac{C_{\text{MU-MIMO}}}{E[C_{\text{withoutSIC}}]} \qquad (5.20)$$

5.5 Bit error probability

The bit error probability [124] serves as a basic parameter in judging the performance of a system. It represents the probability that the bit transmitted is in error due to the noise and interference introduced by the channel. We now calculate the bit error probability for the different cases discussed above.

5.5.1 Without SIC

The bit error probability is the expectation over the value of the bit error rate. IEEE 802.11 employs different modulation techniques, e.g., DBPSK, QPSK, and QAM to support different data rates. We can, therefore, choose to study the bit error probability, for our schemes, for any of the above modulation techniques. We chose to study the bit error probability using the simplest modulation scheme of DBPSK, as it is supported by all the MDs, and is often used as a fallback when the received signal strength at the MDs is low.

In order to obtain the bit error probability, assuming a Rayleigh fading channel [125, 126], we first obtain its instantaneous signal to noise ratio (SNR), γ_j, at CAN j, as:

$$\gamma_j = h_{ij}^2 \frac{E_{b_i}}{|n_i|^2} \qquad (5.21)$$

h_{ij} represents the channel gain from MD i to CAN j, which is assumed to be a Rayleigh distributed random variable. E_{b_i} represents the bit energy across MD i and n_j represents the noise at CAN j.

The average SNR for Rayleigh faded channel at CAN j can thus be computed as:

$$\bar{\gamma}_j = E[h_{ij}]^2 \frac{E_{b_i}}{|n_j|^2} = 2\sigma^2 \frac{E_{b_i}}{N_0} \qquad (5.22)$$

where $2\sigma^2$ represents the variance of the channel. The probability distribution function of the Rayleigh distribution can be given as [124]:

$$P(h_{ij}) = \begin{cases} \frac{h_{ij}}{\sigma^2} exp\left(-\frac{h_{ij}^2}{2\sigma^2}\right) & \text{if } 0 \leq h_{ij} \leq \infty \\ 0 & \text{if } h_{ij} < 0 \end{cases}$$

The $P(h_{ij})$ can be expressed with respect to instantaneous SNR, γ_j as:

$$
\begin{aligned}
P(\gamma_j) &= \frac{P(h_{ij})}{|\frac{d\gamma_j}{dh_{ij}}|} \\
&= \frac{1}{\bar{\gamma}_j} exp\left(-\frac{\gamma_j}{\bar{\gamma}_j}\right) \quad 0 \leq \gamma_j \leq \infty
\end{aligned}
\tag{5.23}
$$

Therefore, the bit error probability for a single MD's transmission, received by CAN j, as shown in [125], can be given as:

$$
P_{\text{BER}} = \int_0^\infty \frac{1}{2} exp(-\gamma_j) \frac{1}{\bar{\gamma}_j} exp(-\frac{\gamma_j}{\bar{\gamma}_j}) d\gamma_j.
\tag{5.24}
$$

where $\frac{1}{2} exp(-\gamma_j)$ represents the bit error rate for a DBPSK system. The bit error probability, as shown in [125], for MD i received by CAN j, can thus found out to be:

$$
P_{\text{BER}} = \frac{1}{2(1 + \bar{\gamma}_j)}.
\tag{5.25}
$$

Bit error rate, without SIC, for both MDs is the summation of the bit error rate from MD 1 (received by CAN 1) and MD 2 (received by CAN 1) and can be given as below:

$$
P_{\text{BER}}^{\text{(withoutSIC)}} = \frac{1}{2(1 + \bar{\gamma}_1)} + \frac{1}{2(1 + \bar{\gamma}_2)}.
\tag{5.26}
$$

5.5.2 With SIC

With SIC, decoding is done successively in the presence of interference from other messages. Thus the instantaneous SNR for the first message can be given as:

$$
\gamma_1 = \frac{\alpha_1^2 h_{11}^2 E_{b_1}}{\alpha_2^2 h_{22}^2 E_{b_2} + N_0}.
\tag{5.27}
$$

$N_0 = |\alpha_1 n_1 + \alpha_2 n_2|^2$ represents the noise variance at the HCC. After decoding the first message, the second message can be decoded after subtracting the first message's signal from the mixed signal combination. The instantaneous SNR of the second message can be written as:

$$
\gamma_2 = \frac{\alpha_2^2 h_{22}^2 E_{b_2}}{N_0}.
\tag{5.28}
$$

The average signal to interference noise ratio can be obtained by taking the expectation over (5.27) and (5.28) as:

$$\bar{\gamma}_1 = \frac{\alpha_1^2 2\sigma^2 E_{b_1}}{\alpha_2^2 2\sigma^2 E_{b_2} + N_0} \tag{5.29}$$

$$\bar{\gamma}_2 = \frac{\alpha_2^2 2\sigma^2 E_{b_2}}{N_0}, \tag{5.30}$$

where we assume that the variance of both channels are the same, i.e., $E[h_{11}^2] = E[h_{22}^2] = 2\sigma^2$. Thus $P(h_{11})$ can be expressed with respect to the instantaneous SNR, γ_1 as:

$$
\begin{aligned}
P(\gamma_1) &= \frac{P(h_{11})}{|\frac{d\gamma_1}{dh_{11}}|} \\
&= \frac{a}{b\bar{\gamma}_1} exp\left(-\frac{\gamma_1 a}{\bar{\gamma}_1 b}\right) \quad 0\le \gamma_1 \le\infty,
\end{aligned}
\tag{5.31}
$$

where $a = \alpha_2^2 h_{22}^2 E_{b_2} + N_0$ and $b = \alpha_2^2 E[h_{22}^2] E_{b_2} + N_0$. Thus the bit error probability, for MD 1 is:

$$P_{\text{BER-MD 1}} = \frac{a}{2(a + b\bar{\gamma}_1)} \tag{5.32}$$

Similarly, for MD 2, $P(h_{22})$ can be expressed with respect to the instantaneous SNR γ_2 as:

$$
\begin{aligned}
P(\gamma_2) &= \frac{P(h_{22})}{|\frac{d\gamma_2}{dh_{22}}|} \\
&= \frac{1}{\bar{\gamma}_2} exp\left(-\frac{\gamma_2}{\bar{\gamma}_2}\right) \quad 0\le \gamma_2 \le\infty
\end{aligned}
\tag{5.33}
$$

Thus the bit error probability for MD 2 would be:

$$P_{\text{BER-MD 2}} = \frac{1}{2(1 + \bar{\gamma}_2)} \tag{5.34}$$

Thus the bit error probability can be given by:

$$P_{\text{BER}}^{(\text{withSIC})} = \max\left(\frac{a}{2(a + b\bar{\gamma}_1)}, \frac{1}{2(1 + \bar{\gamma}_2)}\right) \tag{5.35}$$

5.5.3 MU-MIMO

For finding the bit error probability for our special MU-MIMO uplink scheme we need to know how the decoding is done. The simplest decoder is the Zero-Forcing (ZF) decoder. We use it for our analysis. We have two MDs namely MD 1 and MD 2 and two receiving ports in HCC. The channel matrix is represented as:

$$\mathbf{H} = \left[\begin{array}{c} \mathbf{h}_1, \mathbf{h}_2 \end{array} \right]^T \tag{5.36}$$

where $\mathbf{h}_1 = (h_{11'}, h_{12'})$ and $\mathbf{h}_2 = (h_{21}, h_{22})$, $[\sim]^T$ represent the transpose of the matrix and h_{ij} are Rayleigh with mean 0 and variance $2\sigma^2$. We assume for simplicity that the amplification factors are all set to unity. The post-detection SNR of the ith MD after ZF decoding, as given in [118] is:

$$\gamma_i = \frac{\gamma_0}{[(\mathbf{H}^H \mathbf{H})^{-1}]_{ii}} \tag{5.37}$$

where $\mathbf{H}^H$ represents the Hermitian of the matrix $\mathbf{H}$ and γ_0 is the transmitted SNR for each antenna pair.

If we look closely at the distribution of $\frac{1}{[(\mathbf{H}^H \mathbf{H})^{-1}]_{ii}}$ it turns out to be a Gamma distribution with two degrees of freedom and variance σ^2. Consequently the post detection SNR of the MD i has a pdf:

$$f_2(\gamma_i) = \frac{1}{2\sigma^2 \gamma_0} exp\left(-\frac{\gamma_i}{2\sigma^2 \gamma_0}\right) \tag{5.38}$$

Thus to find the average bit error rate we have to find $P[\gamma_i \leq \gamma_{th}]$, where γ_{th} represents the threshold value of the SNR, for the messages from the MDs, to be decoded properly. Thus we first find the cumulative distribution function (CDF) of the post-detection SNR as:

$$P[\gamma_i \leq \gamma_{th}] = \int_0^{\gamma_{th}} \frac{1}{2\sigma^2 \gamma_0} exp\left(-\frac{\gamma_i}{2\sigma^2 \gamma_0}\right) d\gamma_i \tag{5.39}$$

The BER of the MU-MIMO, which is the CDF, can be given as:

$$P_{\text{BER}}^{\text{(MU-MIMO)}} = P[\gamma_i \leq \gamma_{th}] = 1 - exp\left(-\frac{\gamma_{th}}{2\sigma^2 \gamma_0}\right). \tag{5.40}$$

The above equation (5.40) is true because the system decodes both the messages at the same time. Hence the system has the bit error probability which is the maximum of the two MDs bit error probability. As we set the parameters to be the same, it turns out to be equal to a single MDs bit error probability.

The goal of our analysis is to compare the performance of the SIC, with and without transmission power control, and the MU-MIMO scheme against the normal WiFi transmission. The results from the mathematical analysis are used to generate the graphs in MATLAB. We present our results on three broad categories (a) ergodic capacity gain, (b) packet transmission time, and (c) bit error probability.

Table 5.1: Simulation parameters

Parameters	Values
Rayleigh wireless channels parameters	Mean = 0, Variance = 1
Transmission power at MDs (P_i)	[1-10] mW
Probability of collision (τ)	0.34
SNR threshold (γ_{th})	0.5 mW
Noise (Gaussian distributed)	Mean = 0, Variance = 1
Packet length (L)	512 bytes, 2048 bytes

We perform Monte Carlo simulations in MATLAB to obtain the numerical results. In our figures, we plot the average values of the ergodic capacity gain, bit error probability, and the packet transmission time obtained over all the simulation runs. The simulation parameters and their values are given in Table 5.1.

The maximum transmit power level for smart phones, e.g., iOS devices, are in the range [127] of $[9-14]$ dBm which is between $[9.5-11.5]$ mW. This justifies our choice for the maximum transmission level at the MDs to be 10 mW. Moreover, choosing 0 dBm as the lowest transmission power is also justifiable for a small sized cell of the order of tens of meters or less. This is because the typical WiFi receiver sensitivity for proper reception is in the range [128] of -40 dBm to -80 dBm. Thus our choice of 0 dBm transmit power at MDs does not violate the limit of receiver sensitivity.

Observe that the probability of collision for the non-SIC case is kept to 0.34, which is high (see Table 5.1). This value is portrayed in [129], where collision probability was studied for saturated IEEE 802.11b networks for a contention window size of 8.

Ergodic capacity gain

Fig. 5.5 (a) compares the ergodic capacity achieved by different transmission schemes against the transmission power at the MDs. In this plot, the power

(a)   (b)
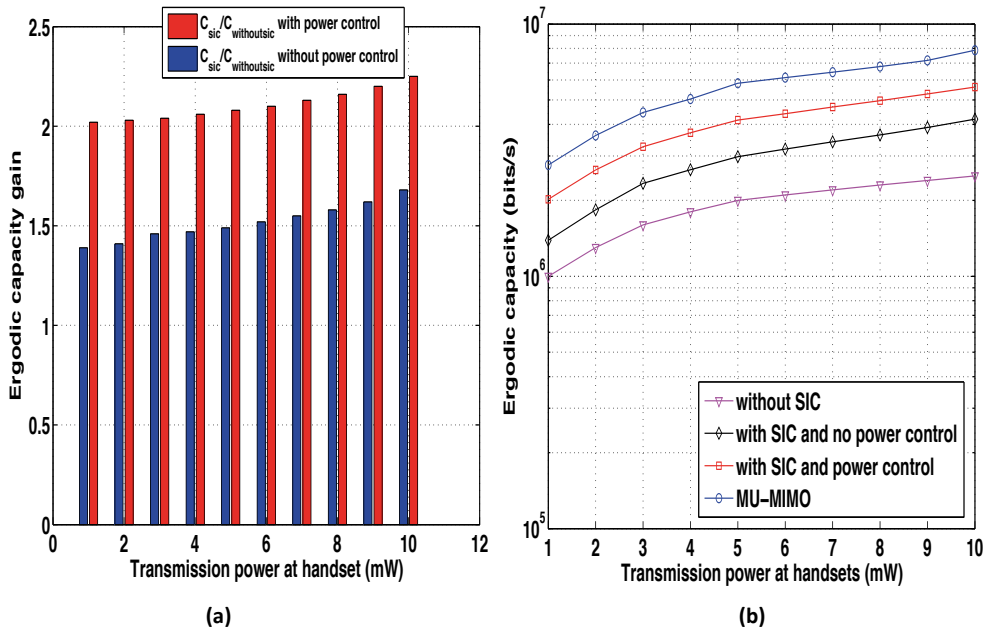
Figure 5.5: *(a) Ergodic capacity gain with and without SIC vs. transmission power at MDs (b) Capacity of different schemes vs. transmission power at the MDs*

across both the MDs are kept the same and are varied from $1 - 10$ mW (see Table 5.1). If we assume that, we have full CSI at the HCC, the way the transmit power control is done at the HCC is given by (5.11), as discussed in Section 5.3. The RSS's from the MDs can be controlled such that maximum capacity gain is achieved for SIC. In Fig. 5.5 (b) the ergodic capacity gains are plotted for the SIC and the non-SIC case with and without power control at different values of transmit power at MD 1. The capacity gain achieved for SIC with and without power control is higher than the capacity of without SIC (approximately double the non-SIC case in comparison to the SIC case with power control). This is true because of the assumption of perfect rate adaptation and high probability of collision for the non-SIC case.

Fig. 5.6 (a) shows the ergodic capacity gains that we can achieve while moving from non-SIC case to SIC case (with no power control) and finally to the MU-MIMO scenario. MU-MIMO garners more capacity gain, as compared to the other two schemes because of spatial-optical multiplexing of the data stream. Carrying different radio signals across different CANs, by different optical wavelength, allows for spatial-optical multiplexing. At the HCC the optical wavelengths, belong-
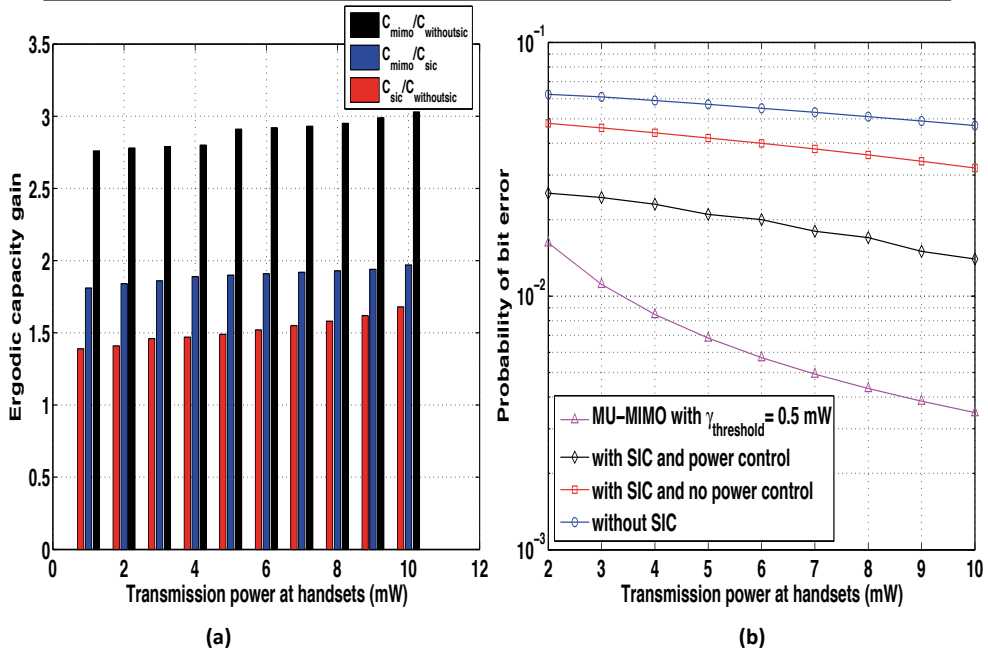
Figure 5.6: *(a) Capacity gain vs. the transmission power at MDs (b) Bit error probability vs. the transmission power at the MDs*

ing to different CANs, are combined in the optical domain to get superimposed messages from different MDs with different channel gains.

Bit error probability

In Fig. 5.6 (b) the bit error probability is plotted against the transmission power at the MDs. The interesting fact is that the first two schemes of without SIC and with SIC do not vary much with an increase in transmission power at the MDs. However, the MU-MIMO scheme varies greatly with the variation in transmission power at the MDs, which again can be attributed to the spatial-optical multiplexing of the messages. The parameter of $\gamma_{threshold}$ is set such that the signal power threshold is greater than or equal to 0.5 mW for individual messages to be assumed decoded.

Packet transmission time

Finally, Fig. 5.7 shows how the packet transmission time varies for the different schemes with respect to the transmission power at the MDs for different packet sizes. The MU-MIMO scheme takes the least packet transmission time and the normal WiFi transmission, without SIC, needs the highest packet trans-
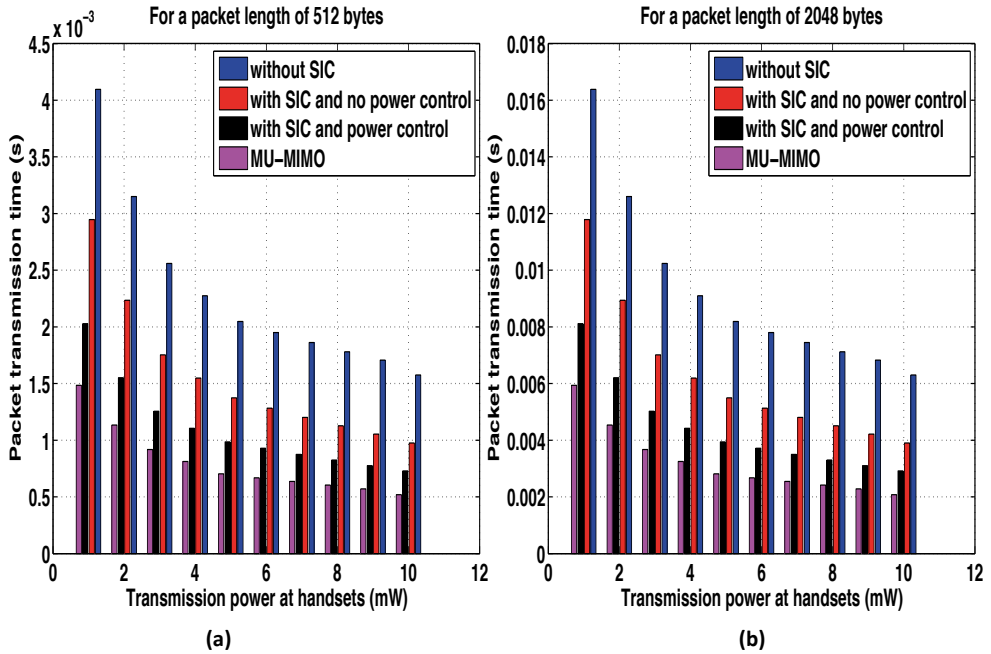
Figure 5.7: *Packet transmission time vs. transmission power for different packet lengths (*512 *bytes,* 2048 *bytes)*

mission time for both packet lengths.

Thus the analysis helps us to establish that by using the proposed MU-MIMO technique discussed in this chapter, we can get a much better performance for such a Fi-Wi uplink channel. Further, we alleviated the problem of hidden nodes in WiFi.

5.7 Conclusion

In this chapter, we proposed a novel MU-MIMO uplink scheme, for the Fi-Wi in-door environment, that takes advantage of both spatial and optical multiplexing to achieve high capacity. We also discussed the physical layer aspects of imple-menting SIC receivers, which served as a comparative benchmark for our MU-MIMO scheme. Thus increased data rate by joint decoding has been discussed. We presented a physical layer comparative study of the different transmission schemes (i.e., SIC, non-SIC and MU-MIMO case). Our SIC and novel MU-MIMO schemes resolved the problem of the hidden nodes caused due to the CSMA/CA contention mechanism at the MAC layer of WiFi, as discussed for the non-SIC

scheme. Apart from this, we have found a transmission power control scheme for SIC such that the maximum capacity gain is achieved. Our simulation results pointed out that, we can achieve almost triple ergodic capacity gain for the MU-MIMO scheme as compared to the non-SIC scheme, for a transmission power of 10 mW. Please note that the ergodic capacity gain calculation, included the factor of probability of collision for the non-SIC case. Furthermore, we also saw that MU-MIMO resulted in low bit error probability. But of course, the MU-MIMO scheme required double the resources (antennas, optical wavelengths etc.) as compared to the non-SIC and SIC case. Our results, also showed that SIC scheme performs better under power control, at the CANs, in terms of ergodic capacity gain and bit error probability.

5.7.1 Limitations and future work

- **Fiber dispersion and propagation delay:** In our analysis and simulations, we assumed that the optical channel is ideal. This was assumed because the fiber length in average homes would not exceed a few hundred meters and thus fiber dispersion would not be significant. We also neglected the added extra propagation delay of the signals due to the fiber lengths. We should, however, note that extra fiber propagation delay may have a negative impact on the performance of the MAC if it exceeds certain timeouts of the WiFi MAC protocol and the network performance could become worse. The extra propagation delay thus might not be negligible and might require adjustment of MAC parameters, e.g., acknowledgment time-out [69], whereas fiber dispersion, if not negligible, could worsen the bit error rate. However, a more realistic study would involve both the fiber dispersion and extra added propagation delay metric.

- **Cost:** From the cost perspective, the use of MU-MIMO results in a much larger need for resources (e.g., transmit/receive antennas at CANs, O/E - E/O converters and optical combiners) than SIC and non-SIC case. Thus an in-depth study is needed to outline the ergodic capacity gain vs. the cost.

- **Amplification:** The amplifications of the received radio signals were performed at the CANs, before sending them to the HCC, where the signals were decoded. But we could also possibly amplify the radio signals after reception at the HCC. This case can also lead to different findings than the ones discussed in our case and needs to be explored.

- **Non-overlapping cell areas:** In this chapter, we performed our analysis assuming that the cell areas of the CANs are non-overlapping. The analysis would, therefore, change if the cell areas of the CANs are overlapped. The overlapping cells could lead to the presence of overlapped MDs in the cell edge area, thus resulting in MD's signal reception via multiple antennas of different CANs, which could create interference.

6

Fi-Wi Downlink

6.1 Introduction

An important objective for the RoF-based hybrid Fi-Wi indoor network architecture is to maximize the downlink system throughput while providing the QoS requirements for the served MDs. Therefore, this chapter studies MU-MIMO schemes that help in maximizing the downlink throughput. We model a downlink MU-MIMO, for the Fi-Wi indoor environment, supporting signal-to-leakage-and-noise ratio (SLNR) precoding and scheduling at the HCC. For attaining individual QoS, for MDs, we propose a Fair-SLNR scheduling algorithm based on the throughput fairness metric proposed in [130].

The Fair-SLNR scheduling algorithm, with perfect channel state information at the transmitter (CSIT) (i.e., at the HCC), can significantly improve the indoor network performance. Information theoretic studies show that when accurate CSI of all the MDs is known at the transmitter, the broadcast channel capacity grows with the number of MDs at the rate of $N \log \log (MK)$, where N is the number of transmitting antennas at the base station, M is the number of receiving antennas at each MD and K is the number of all MDs [131]. The performance, however, is degraded by reduced SNR due to the deviation caused by imperfect CSIT. But obtaining perfect CSIT is difficult, because a large number of channel parameters needs to be estimated at the receivers (MDs) and then fed back to the transmitter (HCC). This can only be achieved by dedicating a significant amount of time resources to both downlink training (for frequency division multiplexing) and channel state feedback [132]. Thus considering MU-MIMO systems with imperfect CSI is a more relaxed and realistic assumption for today's networks. CSIT with error is a form of partial CSIT, which is caused by (a) a non-ideal estimation

technique, or (b) non-ideal feedback. This chapter, therefore, studies the precoding and scheduling scheme for such MU-MIMO Fi-Wi downlink, based on maximizing the so-called SLNR, in presence of channel estimation errors. To ensure overall Fi-Wi network improvement, we have to ensure improvement over each and every cell area supported by a single multi-antenna element CAN. Hence, in this chapter, we therefore only consider the case of a single cell area, served by a single multi-antenna CAN, supporting multiple MDs.

6.2 Contribution

The contributions, of this chapter, can be summarized as below,

- We model a downlink MU-MIMO scheme based on SLNR precoding and scheduling at the HCC. For supporting individual QoS requirements across the MDs we propose a Fair-SLNR scheduling algorithm based on the throughput fairness metric of [130].

- We compare our Fair-SLNR scheduling algorithm against random and greedy scheduling algorithms and quantify their fairness using Jain's fairness index.

- We study the performance of the Fair-SLNR scheduling under imperfect CSIT. Based on the minimum mean squared error (MMSE) alteration, on the imperfect CSIT, we obtain a close approximate estimate of the CSIT.

- We provide a mathematical bound on the maximum achievable sum-rate due to the imperfect estimation of CSIT.

- We compare our Fair-SLNR scheme under equal power allocation (EPA) and channel adaptive power allocation (CAPA) policy in terms of network capacity and average network bit error rate.

6.3 Downlink MU-MIMO: Perfect CSIT

For supporting high data rates indoor, MU-MIMO is definitely a prominent choice for many wireless technologies (e.g., IEEE 802.11ac, LTE-Advanced). QoS serves as an important feature that should be ensured among the MDs.

When perfect CSI is available at the HCC (i.e., channel state information at the transmitter (CSIT)) and the MDs (i.e., channel state information at the receiver (CSIR)), the dirty paper coding (DPC) [133] scheme is the optimal capacity attaining scheme for MU-MIMO downlink. However, DPC is impractical because of the

high computational complexity owing to non-linearity. Linear beamforming techniques are sub-optimal approaches, but they help to reduce the computational complexity. In [134], the authors proposed a precoding scheme based on the signal-to-leakage-and-noise ratio (SLNR).

Signal-to-leakage-and-noise ratio (SLNR) is a transmitter side performance metric. In comparison with co-channel interference (CCI), which represents the amount of signal power received from unwanted MDs to the desired MD, SLNR represents the amount of signal power from the desired MD leaked onto other MDs.

It has been shown in [134] that SLNR performs better than a simple zero forcing (ZF) scheme. However, with linear beamforming, the number of transmitting antennas should be greater than or equal to the number of receiving antennas across all MDs unless they are time shared. One of the driving objectives for any network is to maximize the system throughput. Signal-to-interference-and-noise ratio (SINR) scheduling, in this case, serves as the most intuitive objective, as maximization of SINR directly relates to maximizing system capacity. SINR is a receiver parameter. The calculation of SINR for determining the precoding vectors, before scheduling, is thus an interleaved problem for all the MDs. It increases the computational complexity. SLNR scheduling serves as a different objective, which is motivated from the SLNR based beamforming scheme. The diverse literature on MD scheduling based on SLNR has been proposed [135, 136]. Maximizing the network capacity served as the motivation for such schemes proposed earlier. But they overlooked the important issue of fairness across individual MDs. Especially for the indoor network, where vendors are trying to push their products into the market, the foremost interesting factor for an MD is the throughput guarantee that it can get, especially when multiple MDs with different throughput requirements want to download at the same time. Thus fairness plays a big role for such a scheduler based on SLNR. Round Robin (RR) scheduling has been suggested where MDs are served in a cyclic order irrespective of the channel condition. Proportional Fairness (PF) has been proposed [137] to provide long-term fairness across the MDs taking into account both the channel states and also the past throughputs. In [130] QoS-aware throughput fairness was proposed. We, therefore, study the downlink MU-MIMO schemes for improving the capacity of RoF-based hybrid Fi-Wi network while ensuring that each MD receives a guaranteed QoS using the metric proposed in [130].

6.3.1   System model
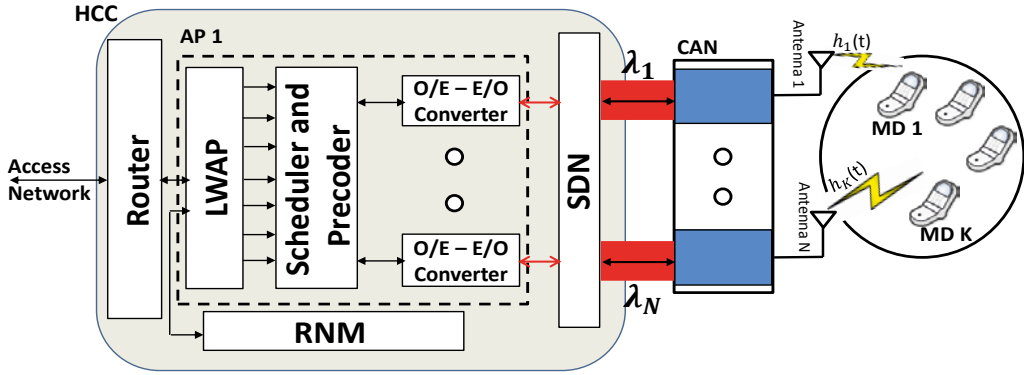
HCC : Home Communication Controller; CAN : Cell Access Node; AP : Access Point;
RNM : Radio Network Manager; SDN : Signal Distribution Network; LWAP : Light-
Weight AP; MD : Mobile Device.

Figure 6.1: *MU-MIMO downlink Fair-SLNR precoding for Fi-Wi indoor*

We consider a downlink MU-MIMO scenario for the Fi-Wi indoor environment (see Fig. 6.1). The HCC is trying to communicate with K MDs, having one antenna each, via a single CAN with N transmit antennas. As shown in Fig. 6.1, the signals for different MDs are generated at the LWAP in the HCC. After SLNR precoding and scheduling, the signals are optically modulated onto different wavelengths using individual E/O converters. The different optical wavelengths are then transported through the fiber to the CAN, where optical/ electrical conversion is done at each individual antenna of the CAN and the signal is radiated in the cell area. Different antenna elements across the CAN are thus accessed using different optical wavelengths making the system transparent. We make the following assumptions:

- **The total number of antennas across all the MDs, K, in the cell area of the CAN, is larger than the total number of antennas across the CAN, N (i.e., $K > N$).** This satisfies the condition for the application of linear beamforming techniques.

- **The optical channel introduces no bit error and the propagation delay is negligible**. This is a valid assumption because the fiber length in average homes would not exceed a few hundred meters, resulting in negligible propagation delay. Also, since the fiber lengths are limited to a few hundred meters, the fiber dispersion would not be significant to introduce any

bit error. We should, however, note that extra fiber propagation delay may have a negative impact on the performance of the MAC if it exceeds certain timeouts of the WiFi MAC protocol and the network performance could become worse. The extra propagation delay thus might require adjustment of MAC parameters, e.g., the acknowledgment time-out [69].

- **Quasi-static time-variant spatially uncorrelated Rayleigh fading channel**. A quasi-static time varying indoor radio channel is a good assumption which is validated by [138]. The Rayleigh fading channel assumption is reasonable because connectivity within indoor cell areas predominantly lacks strong line of sight signal paths because of furniture, walls, human movement, to name a few. The spatially uncorrelated channel assumption is true if the separation between the antenna elements in the CAN is at least half a wavelength.

Let $\mathbf{h}_k(t) \in \mathbb{C}^{1 \times N}$ denote the channel gain from the antennas, across the CAN, to MD k at time t. For a specific time-slot t, the transmitted symbol of MD k is given by $x_k(t)$. The transmitted symbol is pre-multiplied by a unit norm beamforming precoding vector $\mathbf{b}_k(t)$. The received signal vector at MD k can thus be written as:

$$
\begin{aligned}
\mathbf{y}_k(t) &= \mathbf{h}_k(t) \sum_{i=1}^{N} \mathbf{b}_i(t) x_i(t) + w_k(t) \\
&= \mathbf{h}_k(t) \mathbf{b}_k(t) x_k(t) + \\
&\quad \mathbf{h}_k(t) \sum_{i \neq k}^{N} \mathbf{b}_i(t) x_i(t) + w_k(t)
\end{aligned}
\tag{6.1}
$$

where $w_k(t) \sim N(0, \sigma^2)$ represents the additive white Gaussian noise. The power allocation across all the MDs is assumed to be equal. We also assume that the signal variance is equal to 1 and the signals for different MDs are not correlated. The SINR for MD k at time slot t can be given by:

$$
SINR_k(t) = \frac{|\mathbf{h}_k(t)\mathbf{b}_k(t)|^2}{\sigma^2 + \sum_{i=1, i \neq k}^{N} |\mathbf{h}_k(t)\mathbf{b}_i(t)|^2}
\tag{6.2}
$$

Similarly, SLNR for MD k at time slot t can be given as:

$$
SLNR_k(t) = \frac{|\mathbf{h}_k(t)\mathbf{b}_k(t)|^2}{\sigma^2 + \sum_{i=1, i \neq k}^{N} |\mathbf{h}_i(t)\mathbf{b}_k(t)|^2}
\tag{6.3}
$$

Reminiscing (6.3) and (6.2) we can observe the difference between leakage and CCI. CCI is used to represent the interference caused at the desired MD from all other MDs. Leakage refers to the interference caused by the desired MD to all other MDs. So intuitively a higher SLNR means a larger desired signal power than leakage caused by the desired MD onto other MDs.

While SINR serves as the benchmark criterion, the problem of finding maximum SINR is computationally complex as beam designing is interleaved. The level of complexity is too high for such beams to be implemented since the optimal solution is obtained by generalized eigenvalue decomposition implemented with an iterative algorithm. SLNR calculation for the MD only depends on the beam of that MD and hence it simplifies the problem. A closed-form solution maximizing the SLNR is shown to be achievable and hence finding the precoding vectors is computationally easier. The HCC offers centralized control and is assumed to have the CSI of all the MDs. So it is easier to precode and schedule the messages for the MDs.

Our goal is to maximize the network capacity based on SLNR precoding and scheduling while taking into account the QoS requirements, that each MD demands. We, therefore, propose our Fair-SLNR scheduling algorithm and compare it against the Greedy-SLNR algorithm as proposed in [135] and with the Random scheduling and SLNR precoding scheme.

6.3.2 Scheduling algorithms

Greedy-SLNR scheduling

In the Greedy-SLNR based scheduling, we compute the maximum SLNR across each MD at every time slot, assuming that all the MDs use leakage based precoded beamforming vector, which is used to maximize the SLNR metric.

From (6.3) and using the Rayleigh-Ritz quotient property as in [139] we can get SLNR for MD k at time slot t as:

$$SLNR_k(t) \leq maxev\left(\frac{\mathbf{h}_k^*(t)\mathbf{h}_k(t)}{\left(\sigma^2 I + \tilde{\mathbf{H}}_k^*(t)\tilde{\mathbf{H}}_k(t) \right)} \right) \tag{6.4}$$

where
$\tilde{\mathbf{H}}_k(t) = [\mathbf{h}_1^T(t).....\mathbf{h}_{k-1}^T(t)\mathbf{h}_{k+1}^T(t).....\mathbf{h}_N^T(t)]^T$, is the extended channel matrix and it excludes the MD k's channel vector.

$maxev$ denotes the largest eigenvalue. Since we have only one antenna per MD there is only one non-zero eigenvalue possible.

The precoding vector $\mathbf{b}_k(t)$ can hence be found out to be proportional to the eigenvector corresponding to the maximum eigenvalue, which is the same eigenvalue as given by (6.4):

$$\mathbf{b}_k^o(t) \propto max\boldsymbol{ev}\left(\left(\sigma^2 I + \tilde{\mathbf{H}}_k^*(t)\tilde{\mathbf{H}}_k(t) \right)^{-1} \mathbf{h}_k^*(t)\mathbf{h}_k(t) \right) \quad (6.5)$$

The leakage power is computed accurately on the fly for every time slot. The SLNR based successive scheduling algorithm is used to select the set of MDs to be served in each time slot. This scheme was proposed in [135], which we call the Greedy-SLNR algorithm as only the MDs maximizing the network capacity are chosen. The issue of throughput fairness among MDs is neglected.

At every time slot's first iteration, the scheduler in the HCC selects the MD with the largest channel gain, $\gamma_k(t)$, as given by:

$$\gamma_k(t) = |h_k(t)|^2 \quad (6.6)$$

The scheduler then adds MDs to the selected MD set, $S(t)$, in the successive iterations. The maximum number of iterations per time-slot is equal to the number of transmitting antennas at the CAN. Each iteration at every time-slot, the HCC adds only one MD with the largest SLNR. Only the leakage power to the MDs selected in the previous iteration is considered in the scheme as proposed in [135]. Since we assume that we have full CSI at the HCC, the computation of the SLNR for each MD is accurate. Thus the SLNR based precoding vector for MD k, $k = \{1, ..., N\}$, can be given by:

$$\mathbf{b}_k(t) \propto max\boldsymbol{ev}\left(\left(\sigma^2 \mathbf{I} + \tilde{\mathbf{H}}_k^*(t)\tilde{\mathbf{H}}_k(t) \right)^{-1} \mathbf{h}_k^*(t)\mathbf{h}_k(t) \right) \quad (6.7)$$

where $\tilde{\mathbf{H}}_k(t) = [\mathbf{h}_{s^1(t)}^T(t)...\mathbf{h}_{s^{k-1}(t)}^T(t)\mathbf{h}_{s^{k+1}(t)}^T(t)...\mathbf{h}_{s^N(t)}^T(t)]^T$.

The greedy-SLNR scheme fails to satisfy the MDs demand for throughput fairness. The algorithm only strives to maximize the network capacity and does not pay any attention to the individual MDs demand. So some MDs get lower data rate and a few get much higher data rates. Thus the scheme fails to satisfy the QoS demand per MD. The pseudo-code for the Greedy-SLNR scheduling is given in Algorithm 4.

Random scheduling

Random scheduling with an SLNR precoding scheme also serves as one more comparative scheme against our proposed Fair-SLNR scheduling. In this scheme, at

---

Algorithm 4 Greedy-SLNR based scheduling

TIME-SLOT (t=n,$n \geq 1$);
$Initialize : S(n) = \{\phi\}; \hat{S}(n) = \{1, 2, ..., K\}$;
$s^1(n) = argmax_{k \in \hat{S}(n)}|h_k(n)|^2$;
$S(n) = S(n) \bigcup \{s^1(n)\}; \hat{S}(n) = \hat{S}(n) - \{s^1(n)\}$;
for j=1:N-1 **do**
    $\tilde{H}_j(n) = [\mathbf{h}^T_{s^1(n)}......\mathbf{h}^T_{s^{|S(n)|}(n)}]^T$;
    while $for\ each\ k \in \hat{S}(n)$ **do**
        1. $find\ precoding\ vector\ \mathbf{b}^o_k(n)$;
        2. $normalize\ \mathbf{b}^o_k(n)\ to\ unity$;
        3. $find\ SLNR_k(n)$;
    end while
    $s^{j+1}(n) = argmax_{k \in \hat{S}(n)}\{SLNR_k(n)\}$;
    $S(n) = S(n) \bigcup \{s^{j+1}(n)\}; \hat{S}(n) = \hat{S}(n) - \{s^{j+1}(n)\}$;
end for

---

every time slot, the MDs are selected randomly from the MD set and they are multiplied with their SLNR precoded beamforming vectors before being transmitted. This scheme is used to showcase the importance of SLNR scheduling, to guarantee that the overall network capacity is improved.

Fair-SLNR scheduling

In the MU-MIMO downlink broadcast scenario, the HCC is likely to provide a variety of services to different MDs, each with different QoS requirements. Therefore, the main goal of the scheduler, in the Fair-SLNR based precoding and scheduling, is to maximize the network capacity while ensuring that at least the minimum individual throughput as demanded by the MD is attained. For supporting such heterogeneous throughput fairness among the MDs, a throughput fairness metric as proposed in [130] is used. The fairness metric for MD k at time $t > 1$ can be given as:

$$\mu_k(t) = exp\Big(\frac{\bar{C}(t) - a_k\bar{c}_k(t)}{\xi + a_k\bar{c}_k(t)}\Big) \tag{6.8}$$

Constant valued a_k allows for different demand of throughput among different MDs. A very small value of ξ is chosen for avoiding the denominator from being zero.

Algorithm 5 Fair-SLNR based scheduling

TIME-SLOT (t=1);
$Initialize : S(1) = \{\phi\}; \hat{S}(1) = \{1, 2, ..., K\};$
$s^1(1) = argmax_{k \in \hat{S}(1)} |h_k(1)|^2;$
$S(1) = S(1) \bigcup \{s^1(1)\}; \hat{S}(1) = \hat{S}(1) - \{s^1(1)\};$
for j=1:N-1 **do**
  $\tilde{H}_j(1) = [\mathbf{h}^T_{s^1(1)} ...... \mathbf{h}^T_{s^{|S(1)|}(1)}]^T;$
  while $for\ each\ k \in \hat{S}(1)$ **do**
    1. $find\ precoding\ vector\ \mathbf{b}^o_k(1);$
    2. $normalize\ \mathbf{b}^o_k(1)\ to\ unity;$
    3. $find\ SLNR_k(1);$
  end while
  $s^{j+1}(1) = argmax_{k \in \hat{S}(1)} \{SLNR_k(1)\};$
  $S(1) = S(1) \bigcup \{s^{j+1}(1)\}; \hat{S}(1) = \hat{S}(1) - \{s^{j+1}(1)\};$
end for
TIME-SLOT (t=n,$n > 1$**)**;
$Initialization : S(n) = \{\phi\}; \hat{S}(n) = \{1, 2, ..., K\};$
$s^1(n) = argmax_{k \in \hat{S}(n)} \mu_k(n)|h_k(n)|^2;$
$S(n) = S(n) \bigcup \{s^1(n)\}; \hat{S}(n) = \hat{S}(n) - \{s^1(n)\};$
for j=1:N-1 **do**
  $\tilde{H}_j(n) = [\mathbf{h}^T_{s^1(n)} ...... \mathbf{h}^T_{s^{|S(n)|}(n)}]^T;$
  while $for\ each\ k \in \hat{S}(n)$ **do**
    1. $find\ precoding\ vector\ \mathbf{b}^o_k(n);$
    2. $normalize\ \mathbf{b}^o_k(n)\ to\ unity;$
    3. $find\ Fair - SLNR_k(n) = \mu_k(n)SLNR_k(n);$
  end while
  $s^{j+1}(n) = argmax_{k \in \hat{S}(n)} \{Fair - SLNR_k(n)\};$
  $S(n) = S(n) \bigcup \{s^{j+1}(n)\}; \hat{S}(n) = \hat{S}(n) - \{s^{j+1}(n)\};$
end for

The moving average of MD $k's$ past throughput for time slot t as given by [130]:

$$\bar{c}_k(t) = (1 - \frac{1}{\kappa})\bar{c}_k(t-1) + \frac{1}{\kappa}C_k(t-1) \qquad (6.9)$$

κ denotes the smoothing factor, and $C_k(t-1)$ is the data rate of MD k at the previous last time-slot $t-1$. $\bar{C}(t)$, used in (6.8), is defined as:

$$\bar{C}(t) = (1/K)\sum_{k=1}^{K}\bar{c}_k(t) \qquad (6.10)$$

$\bar{C}(t)$ represents the moving average of past throughputs across all the MDs. Thus the MDs might be excluded from the selected scheduled set for transmission, even if they have a higher channel gain than other MDs, if they fail to meet the throughput fairness constraint. The main idea of using the metric, described in (6.8), is to incorporate the scaled deviation of throughput to the SLNR metric, for each MD k. Thus the Fair-SLNR metric for MD k, at time t, can be given as:

$$Fair - SLNR_k(t) = \frac{\mu_k(n)|\mathbf{h}_k(t)\mathbf{b}_k(t)|^2}{\sigma^2 + \sum_{i=1,i\neq k}^{N}|\mathbf{h}_i(t)\mathbf{b}_k(t)|^2} \qquad (6.11)$$

So we only choose an MD when it has a maximum value of Fair-SLNR among all other MDs. The pseudo-code for the Fair-SLNR scheduling is shown in Algorithm 5. In the first time-slot, the MDs are scheduled as discussed in the previous section of Greedy-SLNR scheduling (see Fig. 6.2 (a)). From time-slot two onwards (see Fig. 6.2 (b)) the scheduling algorithm also takes into account the throughput fairness metric as described by (6.8). So as it is evident from the algorithm proposed, for the first iteration the scheme searches to maximize the throughput fair largest channel gain of the MD. Once the first MD is chosen in the first iteration, then the algorithm tries to include a single MD in every other iteration based on the maximization of the throughput Fair-SLNR criterion. In the calculation of throughput Fair-SLNR, the leakage power to MDs selected in the previous iteration is considered. The throughput fairness metric takes into account the QoS demanded by the MDs. SLNR precoding is used to precode the selected MDs signal and is sent to the CAN using optical transmission employing different optical wavelengths.

6.3.3   Comparison of Fair-SLNR, greedy-SLNR and random scheduling

We compare our proposed Fair-SLNR scheduling scheme against the Greedy-SLNR scheduling and Random scheduling. The performance of the schemes are compared for (a) downlink network capacity, and (b) fairness. We choose to compare
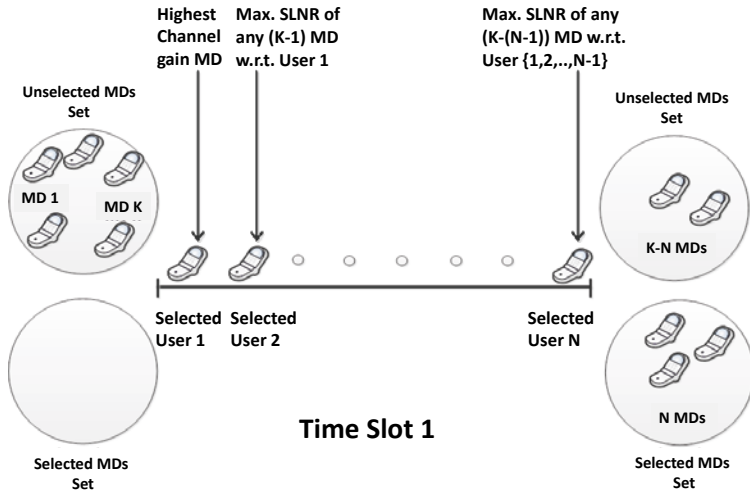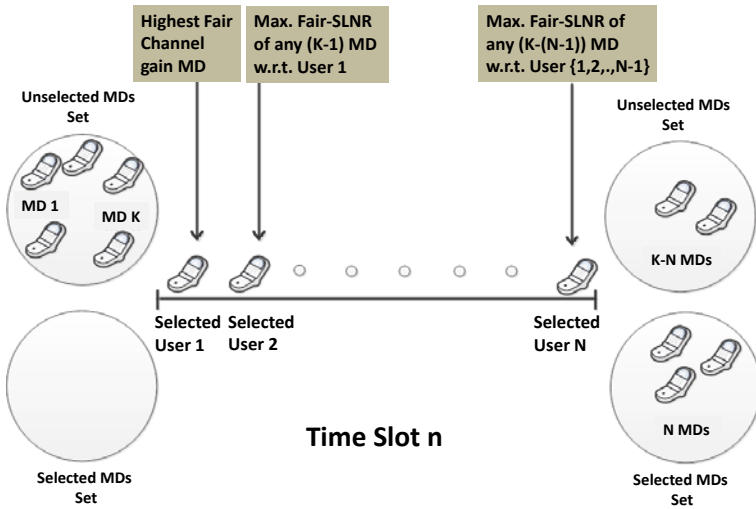
Figure 6.2: *Fair-SLNR algorithm for: (a) Time-slot $(t = 1)$ (b) Time-slot $(t = n, n > 1)$*

these two parameters as our motivation was to provide high downlink through-put while satisfying every MD's QoS requirements.

Table 6.1: Simulation parameter

Parameter	Value
ξ, a_k	0.1, 1
κ (smoothing factor)	2
SNR-per MD	[0,5,10,15,20,25] dB
N (number of Tx. antenna at CAN)	3
K (number of MDs)	10

We use MATLAB to generate the simulation results. The simulation parameters are provided in Table 6.1. The wireless channels are modeled as a Rayleigh random variable with mean 0 and variance 1. The choice of wireless channel is explained in our assumptions before. The value of the smoothing factor is taken to provide equal weight to both the immediate past value of data rate for MDs as well as the past moving average throughput for MDs. The value of ξ is chosen to avoid the zero denominator case, as mentioned earlier. The value of a_k is kept at 1 to provide equal throughput fairness across all the MDs. It is the easiest case, assuming that all MDs demand the same throughput. It provides us an opportunity to calculate the Jain's Fairness Index, discussed later in this section, for our proposed scheme. As we assume that the channels are quasi-static time varying, in the simulations, after every 4 time-slots the channel gains are changed. We schedule 3 MDs after every 4 time-slots and these MDs transmit their message during those time-slots.

Network capacity

We perform Monte Carlo simulations in MATLAB to obtain the numerical results. In our figures, we plot the average values of the network capacity obtained over all the simulation runs. We compare the network capacity in bits/s/Hz for the schemes w.r.t. per MD SNR, which is given by $1/\sigma^2$. The Fair-SLNR scheme achieves almost the same network capacity compared to the Greedy SLNR scheme as shown in Fig.6.3. For an MD SNR of 25 dB, the Fair-SLNR achieves .0034% less network capacity as compared to the Greedy SLNR scheme, which is very marginal. This is because of the assumption of ideal conditions with perfect CSIT and a smaller number of MDs to select from. Also since the cell area is small, the probability of finding large differences in SLNR is also very small.

There is a large difference in network capacity achieved by the Greedy-SLNR
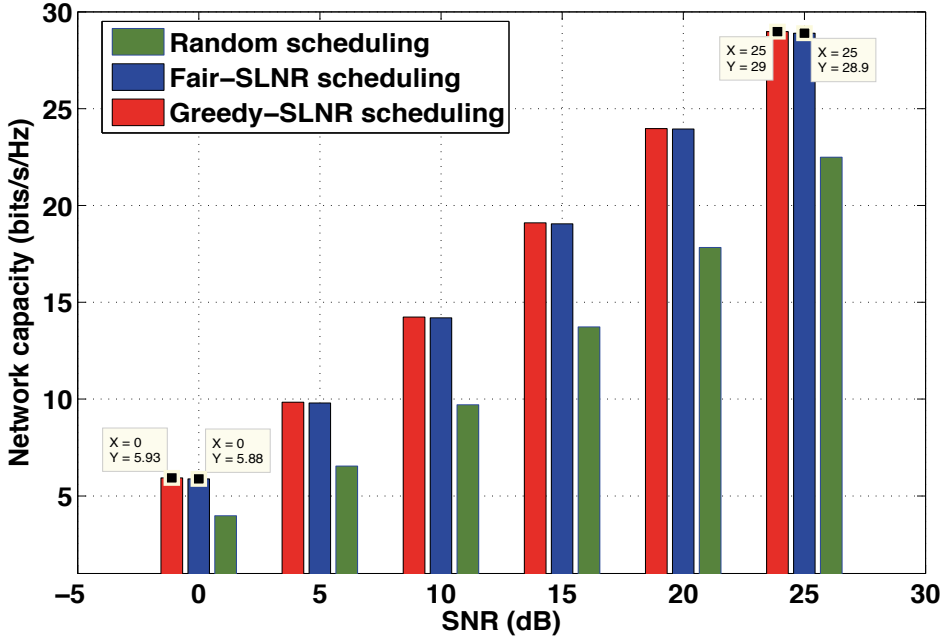
Figure 6.3: *Network capacity vs. SNR*

and Fair-SLNR schemes in comparison with the Random scheduling scheme. For e.g., for MD SNR of 25 dB, the Random scheduling achieves 28.4% and 28.9% less network capacity as compared to the Fair-SLNR and the Greedy-SLNR scheme respectively. This shows that the SLNR scheduling is important, to take into account the channel variations indoor.

Fairness

Now we will quantify the fairness index for the schemes discussed. We utilize the Jain's Fairness Index, which is defined below.

Jain's fairness index (JFI) quantifies the fairness of the achievable MDs throughput values, where there are K MDs and r_i is the average throughput for the i'th MD. JFI can take values ranging from $\frac{1}{K}$ to 1. 1 represents the maximum fairness when all MDs receive the average throughput.

$$JFI = \frac{\left(\sum_{i=1}^{K} r_i \right)^2}{K \sum_{i=1}^{K} r_i^2} \qquad (6.12)$$

In the simulations, we choose that all the MDs have similar throughput requirements (i.e., basically all the MDs are assumed to be accessing the same traffic category). We thus tried to measure the fairness achieved by different
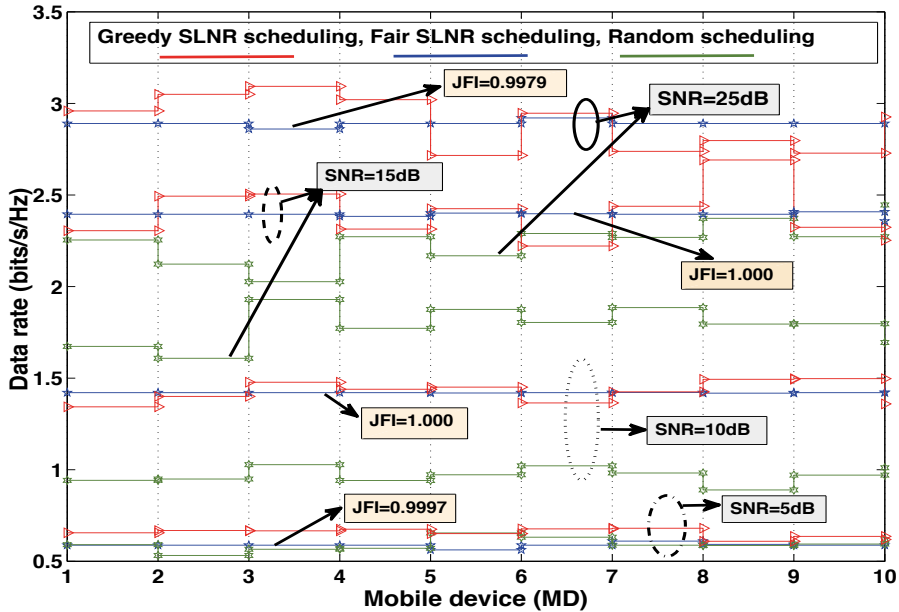
Figure 6.4: *Variation of data rate vs. Mobile device*

schemes. In Fig.6.4, we plot the individual MD data rates achieved by all the MDs
for the different schemes. As can be seen from the plot our throughput Fair-SLNR
scheme achieves a maximal value of fairness in JFI, for all MD SNR levels. We
could also perform the simulations by varying the value of a_k for different MDs
and guarantee QoS across all of the MDs depending on their individual through-
put needs.

6.4 Downlink MU-MIMO: Imperfect CSIT

This section extends our work described in Section 6.3.

The system model for this section is similar to the system model explained
in Section 6.3.1. In Section 6.3, we assumed knowledge of perfect CSIT at the
HCC. But the assumption is not realistic, so we have to relax the perfect CSIT as-
sumption. There are two forms of CSIT errors that can be introduced, as given
below:

- An erroneous estimate of the pilot signals at the MDs, that are used to
  calculate the CSI.

- Errors introduced due to the feedback delay of the CSI from the MDs to the HCC.

Assumption: In this section, we are however neglecting the imperfection in CSIT caused due to feedback delay. This is a valid assumption as we considered that the channels are quasi-static. Thus the feedback delay is much smaller than the coherence time of the channel.
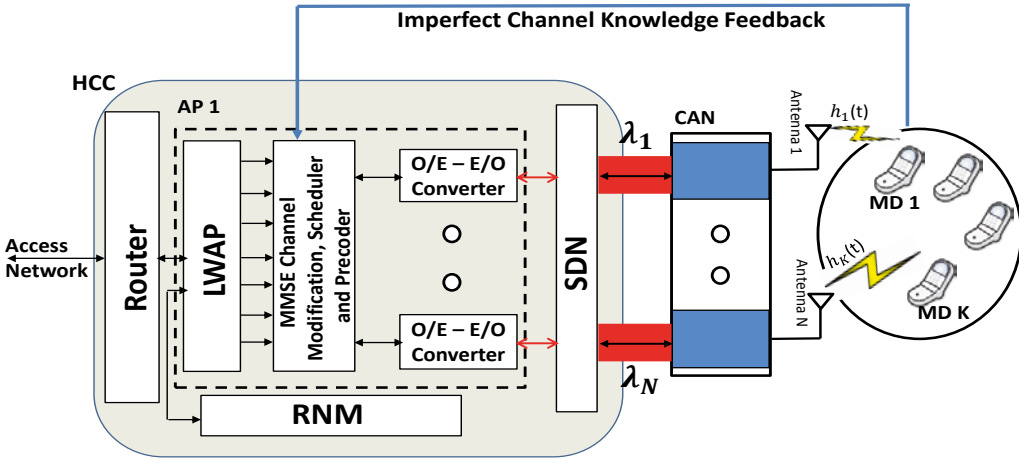
HCC : Home Communication Controller; CAN : Cell Access Node; AP : Access Point;
RNM : Radio Network Manager; SDN : Signal Distribution Network; LWAP : Light-
Weight AP; MD : Mobile Device.

Figure 6.5: *MU-MIMO downlink Fair-SLNR precoding for Fi-Wi indoor with imperfect CSIT*

The SLNR for MD k at time slot t can be given as before (see (6.3)):

$$SLNR_k(t) = \frac{|\mathbf{h}_k(t)\mathbf{b}_k(t)|^2}{\sigma^2 + \sum_{i \neq k} |\mathbf{h}_i(t)\mathbf{b}_k(t)|^2} \qquad (6.13)$$

6.4.1 Error estimation of channel

We assume that the techniques used at the MDs for channel estimation are not perfect, and they introduce errors. Thus the HCC will obtain erroneous CSI values. Let us denote the perfect CSI, for MD k at time t, as $\mathbf{h}_k(t)$. The erroneous estimates are represented as $\hat{\mathbf{h}}_k(t)$ and the difference between them as the error:

$$\mathbf{e}_k(t) = \mathbf{h}_k(t) - \hat{\mathbf{h}}_k(t) \qquad (6.14)$$

The distribution of $\mathbf{e}_k(t)$ is $\mathcal{CN}(0, \sigma_e^2 I)$ [140]. The quality of the channel estimation is indicated by the error variance and is assumed to be known to both the HCC and the MDs. The degradation in the performance of the SLNR-based scheme is significant due to error estimates of the CSI. We can, however, make MMSE based alteration so that we obtain a close approximation of the CSI by reducing the effect of the estimation errors.

Channel modification

This section aims at estimating a modification matrix of size $N \times N$, using the MMSE based approach, to reduce the significant effect of estimation error. For notational simplicity, in this part, we neglect the time index. Let us denote the channel modification matrix as **F** and the full channel estimate matrix as $\hat{\mathbf{H}}$. The entries of $\hat{\mathbf{H}}$ includes the imperfect CSI received from the MDs. The equivalent channel matrix after modification can be expressed as:

$$\check{\mathbf{H}} = \hat{\mathbf{H}}\mathbf{F} \tag{6.15}$$

The modification matrix $\mathbf{F}_{opt}$ can be obtained by minimizing mean squared error, $MSE = E\left[\left\|\mathbf{H} - \check{\mathbf{H}}\right\|^2\right]$, satisfying the power constraint, which can be given as:

$$\mathbf{F}_{opt} = argmin_{Tr(\mathbf{F}^*\mathbf{F})=1} E\left[\left\|\mathbf{H} - \check{\mathbf{H}}\right\|^2\right] \tag{6.16}$$

Here, $Tr(.)$ represents the trace of the matrix. By equating the gradient of the MSE, with respect to **F**, and equating it to zero we obtain [141]:

$$\grave{\mathbf{F}}_{opt} = (K\sigma_e^2 I + \mathbf{H}^*\mathbf{H})^{-1}(\mathbf{H}^*\mathbf{H}) \tag{6.17}$$

where **H** represents the full channel matrix. The obtained $\grave{\mathbf{F}}_{opt}$ is a global minimizer, which can be easily proved by deriving the Hessian matrix and noticing that the Hessian matrix is positive definite. Normalizing $\grave{\mathbf{F}}_{opt}$ to satisfy the power constraint gives:

$$\mathbf{F}_{opt} = \grave{\mathbf{F}}_{opt} / \sqrt{Tr\left(\grave{\mathbf{F}}_{opt}^* \grave{\mathbf{F}}_{opt}\right)} \tag{6.18}$$

The minimum mean squared error variance becomes [141]:

$$\sigma_{mod}^2 = E\left[\left\|\mathbf{H} - \check{\mathbf{H}}\right\|^2\right] = \sigma_e^2 / r \sum_{i=1}^{r} \lambda_i / (\lambda_i + \sigma_e^2) \tag{6.19}$$

where r is the rank and $\lambda_1, \ldots \lambda_r$ are the non-zero eigenvalues of the full transmit channel covariance matrix $\mathbf{H}_{cov}$, which is given by:

$$\mathbf{H}_{cov} = E\left[\mathbf{H}^*\mathbf{H}\right] \tag{6.20}$$

Therefore after modification, to account for the erroneous CSI, the modified SLNR can be given by:

$$SLNR_k^{mod}(t) = \frac{\mathbf{b}_k^*(t)\left(\check{\mathbf{h}}_k^*(t)\check{\mathbf{h}}_k(t) + \sigma_{mod}^2\mathbf{I}\right)\mathbf{b}_k(t)}{\mathbf{b}_k^*(t)\left(\sigma^2\mathbf{I} + \sum_{i\neq k}\sigma_{mod}^2\mathbf{I} + \check{\mathbf{H}}_k^*\check{\mathbf{H}}_k\right)\mathbf{b}_k(t)} \tag{6.21}$$

where $\check{\mathbf{H}}_k$ represents the modified extended channel matrix for MD k obtained after taking into account the imperfection in CSI. Here we also include the time index parameter. The optimal solution for the precoding vector can thus be given by:

$$\mathbf{b}_k^{opt}(t) \propto maxev\left(\check{\mathbf{h}}_k^*(t)\check{\mathbf{h}}_k(t) + \sigma_{mod}^2\mathbf{I},\right.$$

$$\left.\sigma^2\mathbf{I} + \sum_{i\neq k}\sigma_{mod}^2\mathbf{I} + \check{\mathbf{H}}_k^*(t)\check{\mathbf{H}}_k(t)\right) \tag{6.22}$$

The *maxev*(.) is used to represent the maximum eigenvector. After obtaining the modified channel estimates and the optimal precoding vectors, the next step is to precode and schedule the MDs. The main goal of this section is also to maximize the network capacity based on SLNR precoding and scheduling, under imperfect CSIT, taking into account the QoS requirements that each MD demands. The comparative study of the deterioration of the network capacity between perfect and imperfect CSI is presented in a later part of this section.

6.4.2 Fair-SLNR scheduling with imperfect CSIT

Now, we provide the pseudo-code of the algorithm, which is just a mere abstraction of the Fair-SLNR algorithm proposed in Section 6.3.2. However, in this pseudo-code, given in Algorithm 6 the imperfection in CSIT is taken into account and hence modified accordingly.

6.4.3 Bounds on the achievable sum-rate

We provide a bound for the achievable sum-rate of the system per time-slot. If we replace $\mathbf{h}_k$ of (6.1) by $\check{\mathbf{h}}_k$, as we only have knowledge of the modified equivalent

---

Algorithm 6 Fair-SLNR based scheduling

TIME-SLOT (t=1);
$Initialization : S(1) = \{\phi\}; \hat{S}(1) = \{1, 2, ..., K\};$
$s^1(1) = argmax_{k \in \hat{S}(1)} |\check{\mathbf{h}}_k(1)|^2;$
$S(1) = S(1) \bigcup \{s^1(1)\}; \hat{S}(1) = \hat{S}(1) - \{s^1(1)\};$
for j=1:N-1 **do**
  $\check{\tilde{H}}_j(1) = [\check{\mathbf{h}}^T_{s^1(1)}......\check{\mathbf{h}}^T_{s^{|S(1)|}(1)}]^T;$
  while $for\ each\ k \in \hat{S}(1)$ **do**
    $find\ \mathbf{b}^{opt}_k(1)$
    $normalise\ \mathbf{b}^{opt}_k(1)\ to\ unity;$
    $find\ SLNR^{mod}_k(1)$
  end while
  $s^{j+1}(1) = argmax_{k \in \hat{S}(1)} \{SLNR_k(1)\};$
  $S(1) = S(1) \bigcup \{s^{j+1}(1)\}; \hat{S}(1) = \hat{S}(1) - \{s^{j+1}(1)\};$
end for
TIME-SLOT (t=n,$n > 1$**)**;
$Initialization : S(n) = \{\phi\}; \hat{S}(n) = \{1, 2, ..., K\};$
$s^1(n) = argmax_{k \in \hat{S}(n)} \mu_k(n) |\check{\mathbf{h}}_k(n)|^2;$
$S(n) = S(n) \bigcup \{s^1(n)\}; \hat{S}(n) = \hat{S}(n) - \{s^1(n)\};$
for j=1:N-1 **do**
  $\check{\tilde{H}}_j(n) = [\check{\mathbf{h}}^T_{s^1(n)}......\check{\mathbf{h}}^T_{s^{|S(n)|}(n)}]^T;$
  while $for\ each\ k \in \hat{S}(n)$ **do**
    $find\ \mathbf{b}^{opt}_k(n)$
    $normalise\ \mathbf{b}^{opt}_k(n)\ to\ unity;$
    $find\ Fair - SLNR_k(n) = \mu_k(n) * SLNR^{mod}_k(n)$
  end while
  $s^{j+1}(n) = argmax_{k \in \hat{S}(n)} \{Fair - SLNR_k(n)\};$
  $S(n) = S(n) \bigcup \{s^{j+1}(n)\}; \hat{S}(n) = \hat{S}(n) - \{s^{j+1}(n)\};$
end for

---

channel matrices after MMSE estimation, we can write it as follows:

$$
\begin{aligned}
\check{\mathbf{y}}_k(t) &= \check{\mathbf{h}}_k(t)\check{\mathbf{b}}_k(t)x_k(t) + \\
&\quad \check{\mathbf{h}}_k(t)\sum_{i\neq k}\check{\mathbf{b}}_i(t)x_i(t) + w_k(t) \\
&= \check{\mathbf{h}}_k(t)\mathbf{u}_k(t) + \\
&\quad \sum_{i\neq k}\check{\mathbf{h}}_k(t)\mathbf{u}_i(t) + w_k(t)
\end{aligned}
\tag{6.23}
$$

where $\mathbf{u}_k(t)$ represents the precoded signal that is being transmitted. The data rate of MD k, ignoring the time-index, can be given by:

$$
Rate_k = I(\mathbf{u}_k; \check{\mathbf{y}}_k) \tag{6.24}
$$

Now taking $\sum_{i\neq k}\check{\mathbf{h}}_k\mathbf{u}_i + w_k$ as the resultant total noise term owing to the interference and the desired MD's receiver noise and representing it as n_k we have:

$$
\check{\mathbf{y}}_k = \check{\mathbf{h}}_k\mathbf{u}_k + n_k \tag{6.25}
$$

The maximum $Rate_k$ achievable under imperfect CSIT can be given by:

$$
\begin{aligned}
Rate_k &\leq E_{\check{\mathbf{h}}_k}\log\left(1 + \frac{|\check{\mathbf{h}}_k|^2(1/N)}{E[n_k n_k^*|\check{\mathbf{h}}_k]}\right) \\
&\geq E_{\check{\mathbf{h}}_k}\log\left(\frac{|\check{\mathbf{h}}_k|^2(1/N)}{E[n_k n_k^*|\check{\mathbf{h}}_k]}\right)
\end{aligned}
\tag{6.26}
$$

The inequality in equation (6.26) is because we assume a high SNR regime. We replaced $E[|\mathbf{u}_k|^2]$ by $1/N$. Thus:

$$
\begin{aligned}
Rate_k &\geq E_{\check{\mathbf{h}}_k}\log\left(|\check{\mathbf{h}}_k|^2(1/N)\right) - \\
&\quad E_{\check{\mathbf{h}}_k}\log\left(E[n_k n_k^*|\check{\mathbf{h}}_k]\right)
\end{aligned}
\tag{6.27}
$$

The inequality in (6.27) assumes that the resultant noise is Gaussian distributed which is the worst case [142]. So replacing the resultant distribution with any other distribution will perform better. Now applying Jensen's inequality we have:

$$
Rate_k \geq E_{\check{\mathbf{h}}_k}\log\left(|\check{\mathbf{h}}_k|^2(1/N)\right) - \log\left(E[n_k n_k^*]\right) \tag{6.28}
$$

Thus, $Rate_k$ can be expressed as:

$$Rate_k \geq E_{\check{\mathbf{h}}_k} \log\left(|\check{\mathbf{h}}|^2(1/N)\right) - \log\left(\sigma^2 E[|\check{\mathbf{h}}_k|^2]\frac{N-1}{N}\right) \qquad (6.29)$$

Thus the bound for the sum rate, SR, across the selected MDs for a time slot can be given as,

$$\overset{all\ selected\ MDs}{\sum} E_{\check{\mathbf{h}}_k} \log\left(1 + \frac{|\check{\mathbf{h}}_k|^2(1/N)}{E[n_k n_k^*|\check{\mathbf{h}}_k]}\right) \geq SR \geq \overset{all\ selected\ MDs}{\sum} E_{\check{\mathbf{h}}_k} \log\left(|\check{\mathbf{h}}_k|^2(1/N)\right) -$$
$$\log\left(\sigma^2 E[|\check{\mathbf{h}}_k|^2]\frac{N-1}{N}\right) \quad (6.30)$$

6.4.4 Channel adaptive power allocation (CAPA)

In Section 6.3, the SLNR precoding scheme assumed that the transmitter uses equal power for each MD's transmission. But in reality in wireless communication system, the channel state of every MD is usually different. Thus if the transmit power is allocated according to the real CSI, some gains may be achieved due to the improved power efficiency. For MU-MIMO systems, the average BER of all MDs is dominated by the worst one [143]. Therefore considering a channel adaptive scheme based on the SLNR precoding, as proposed in [144], can improve the communication quality of the worst MD by increasing the transmitted power. SLNR is related to the real CSI and thus it is used in distributing the power adaptively according to the CSI. This we refer to as channel adaptive power allocation (CAPA). The detailed power allocation process is described as follows:

The transmitted power is allocated according to each MD's SLNR values. The power distributed to each MD k is inversely proportional to its SLNR value. It can be denoted as:

$$\frac{p_k}{P_{total}} = \frac{1/SLNR_k}{\sum_{k=1}^{N}(1/SLNR_k)} \qquad (6.31)$$

where P_{total} is the total transmit power.

6.4.5 Fair-SLNR scheduling under perfect and imperfect CSIT

This section compares the performance of our proposed downlink MU-MIMO Fair-SLNR scheduling scheme under imperfect and perfect CSIT. It also compares the performance of the scheme under equal power allocation policy and CAPA

Table 6.2: Simulation parameter

Parameter	Value
ξ, a_k	0.1, 1
κ (smoothing factor)	2
SNR-per MD	[0,5,10,15,20,25] dB
N (number of Tx. antenna at CAN)	3
K (number of MDs)	10
Error Variance (σ_e^2)	0.1-0.2

policy. The performance metrics are (a) downlink network capacity, and (b) average network bit error rate.

We perform Monte Carlo simulations in MATLAB to obtain the numerical results. In our figures, we plot the average values of the network capacity and the average network bit error rate obtained over all the simulation runs.The parametric values chosen for the simulation are given in Table 6.2. The choices of parameters for calculating the throughput fairness metric, i.e., the smoothing factor (κ), ξ and a_k, are kept the same as in Section 6.3.3 for the reasons disclosed in that section. We also simulate the wireless channel gains under the same scenario, as described in Section 6.3.3, to maintain consistency in our simulations. The error variance[1] is varied between 0.10 to 0.20.

Network capacity

We again run a Monte-Carlo simulation for each scheme and we compare the network capacity in bits/s/Hz for the schemes w.r.t. the per MD SNR, which is given by $1/\sigma^2$. In Fig. 6.6 the network capacity in bits/s/Hz is compared for different values of transmit SNR for the cases comparing perfect CSIT with imperfect CSIT. We can make the following observations,

- We observe a drop of approximately 20% in network capacity from the perfect CSIT case when comparing against imperfect CSIT, with σ_e^2 equal to 0.10 at 25dB transmit SNR. The decrease in throughput is due to imperfect CSIT which causes the SINR to decrease.

- We observe that at high SNR, of 25dB, the difference in the network capacity achieved for different error variances exhibits a trend of a lesser percent-

---

[1]The simulation range for error variance was chosen arbitrarily. But for our simulations, these choices are sufficient, as we are interested in finding the trend of the variation in our network downlink capacity.
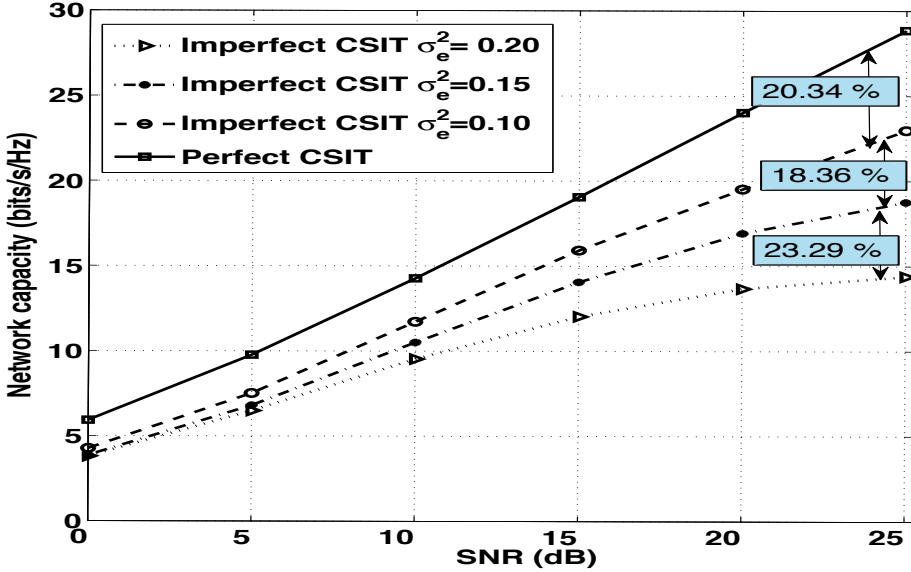
Figure 6.6: *Network capacity vs. SNR*

age of decrease in network capacity for lower error variance as compared to the higher error variance counterpart. For, e.g., the percentage of decrease in network capacity for perfect CSIT (i.e., σ_e^2 is zero) to $\sigma_e^2 = 0.10$, for $\sigma_e^2 = 0.10$ to $\sigma_e^2 = 0.15$ and for $\sigma_e^2 = 0.15$ to $\sigma_e^2 = 0.20$ are 20.34%, 18.36% and 23.29% respectively. This is because at high SNR, the higher signal power compensates for the estimation errors.

- We can also observe that at low SNR, of 0dB, the difference in the network capacity achieved for different error variances exhibits a trend of increasing percentage of decrease in network capacity for lower error variance as compared to the higher error variance counterpart. For, e.g., the percentage of decrease in network capacities for perfect CSIT (i.e., σ_e^2 is zero) to $\sigma_e^2 = 0.10$, for $\sigma_e^2 = 0.10$ to $\sigma_e^2 = 0.15$ and for $\sigma_e^2 = 0.15$ to $\sigma_e^2 = 0.20$ are 27.82%, 9.57% and 1.55% respectively. This shows that at low SNR values, the gap in network capacity widens as the estimation errors are highlighted because of the lower signal power level.

Fig. 6.6 was generated assuming that we have an equal power allocation (EPA) policy. However for the reasons mentioned earlier, in Section 6.4.4, we carried out simulations with CAPA and compared it against the EPA policy for both im-

perfect and perfect CSIT. We noticed the drop in network capacity was large for imperfect CSIT and the gap widens marginally more with CAPA (see Fig. 6.7). For ,e.g., for 25dB SNR the percentage of decrease in network capacity for the EPA and CAPA scheme under $\sigma_e^2 = 0.15$ and $\sigma_e^2 = 0.20$ are 1.81% and 1.45% respectively. It is obvious, as we are trading network capacity for bit error rate (BER) by allocating more power to the worst case MD. Fig. 6.7 shows the variation of the network capacity for the EPA and CAPA policy under both imperfect and perfect CSIT.
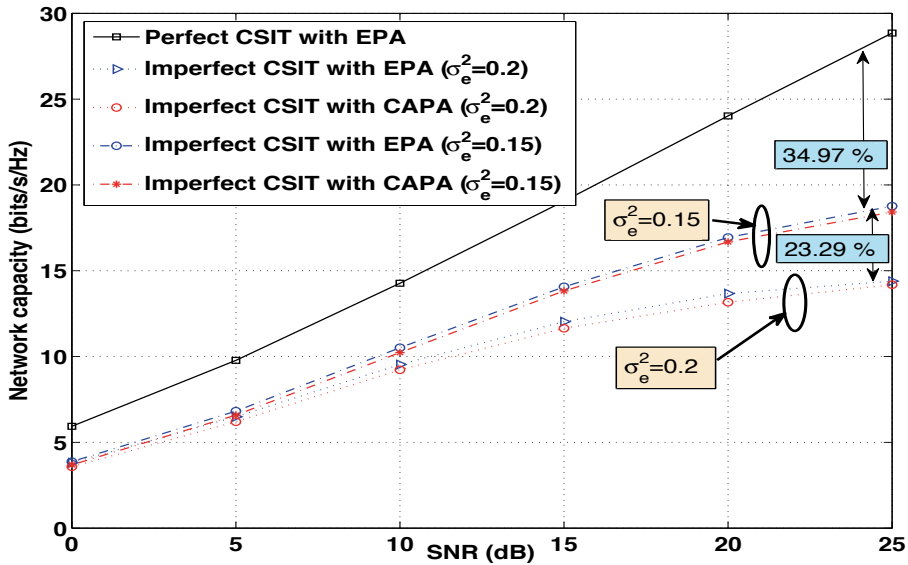
Figure 6.7: *Network capacity vs. SNR for different power allocation policy*

Average network bit error rate

Fig. 6.8 shows how the average network BER varies with the different power allocation policies. We can see that there is a significant improvement of average network BER at high transmit SNR. For BER value of 10^{-7}, the imperfect CSIT with CAPA outperforms EPA by 3dB.

6.5 Conclusion

We proposed a downlink MU-MIMO throughput Fair-SLNR precoding and scheduling algorithm to provide high network downlink capacity, over a Fi-Wi indoor
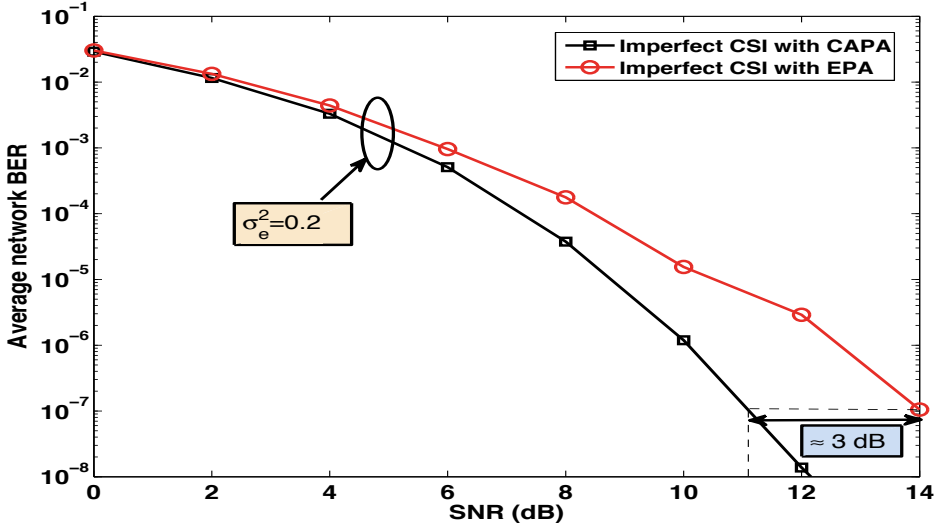
Figure 6.8: *Average network BER Vs. SNR*

cell area, while guarantying QoS for the MDs served. We compared our scheme against a greedy-SLNR and random scheduling scheme, and showed that our Fair-SLNR scheme provides maximum JFI, i.e., 1, while the downlink network capacity is comparable to the greedy-SLNR scheme.

We then compared the performance of our Fair-SLNR scheme under both perfect and imperfect CSIT. We made a close approximation estimate of the perfect CSI from the imperfect channel knowledge by performing MMSE modification. We also provided bounds on the sum rate achievable, per time-slot, for the imperfect CSIT case. From our simulations, we made a few observations. We observe a drop of 20% network capacity, with error variance of 0.10 and at 25 dB transmit SNR. We also observed that, at high SNR, the network capacity exhibits a trend of less percentage of decrease for lower error variance as compared to the high error variance, as the high SNR compensates for the estimation errors. Also, we found out that at low SNR values the gap in network capacity widens, from lower error variance to higher error variance, as the estimation errors are highlighted because of the lower signal power level. Finally, we showed that, in the case of imperfect CSIT, we can opt for CAPA. It performs better in terms of BER, while marginally diminishing the network capacity, in comparison to the EPA scheme with imperfect CSIT.

6.5.1   Limitations and future work

- **Fiber dispersion and propagation delay:** Please refer to Chapter 5 for the explanation.

- **Multiple cells based MU-MIMO Fair-SLNR scheduling:** From the analysis of our single cell based Fair-SLNR scheduling scheme, in downlink MU-MIMO, we observe that it can provide high network capacity as well as QoS, requested by an MD. Therefore, it may be interesting to study our scheme for multiple-cells based MU-MIMO, because then we can take advantage of the distributed antenna system nature of the Fi-Wi architecture to even better coordinate among the MDs, in different cells, and improve the downlink network capacity further.

7

Conclusions & Future Directions

*"An expert is a man who has
made all the mistakes, which can
be made, in a very narrow field."*
- Niels Henrik David Bohr

Conclusions

Indoor networks are a major contributor to the data traffic that is generated in today's world and are growing very rapidly. This dissertation deals with the evolving needs of indoor communication, especially with the shift in paradigm from being just connected to the Internet to a hyper-connected world. The demand generated by indoor MDs has changed vastly owing to the ubiquitous smart phones and the introduction of many new demanding applications and services. The demand for higher capacity with guaranteed QoS, energy-efficiency, reduction of the operational cost, in 5G, has made the engineers reconsider the indoor network architecture. In this dissertation, we adopted the hybrid Fi-Wi architecture described in Chapter 2 because of its centralized management, support of a plurality of wireless standards, scalability, ease of maintenance and other economic aspects that make it future-proof.

Optical fibers provide large bandwidth and future proof backhaul connection. Wireless coverage for the last few meters, on the other hand, provides devices with the much needed freedom of being untethered and mobile. Thus utilizing a Fi-Wi infrastructure we reap the benefits of both worlds. In this dissertation, a centrally managed hybrid Fi-Wi network is discussed. The radio signal generation

and processing of the signals are performed at the centralized HCC. The HCC basically serves as the controller of the indoor network, thus offering the benefits of a centrally managed indoor network. Using RoF technology, the radio signals generated at the HCC are distributed across the CANs inside the building. Thus the CANs along with the HCC form a distributed antenna system. As the RoF technology is agnostic to the radio signals that are transported from the HCC to the CAN, a plethora of wireless standards can be supported via this architecture, thus making the architecture future proof. In this dissertation we consider the most widely accepted indoor communication technology for connection of MDs to the APs. The dissertation proposed techniques for improving network performance and management of WiFi in a hybrid Fi-Wi architecture. In this architecture, APs in spaces in the building were replaced by distributed antennas (namely CANs), and the HCC hosts AP functionality and serves as the network manager. This architecture provides flexibility in connecting different network elements namely CANs and APs. An inherent advantage of this architecture is that we form small femto-cell clusters which are served by individual CANs instead of a single wireless cell. This helps to increase the network capacity and the network reliability and reduces EM radiation by lowering the transmit power levels.

Although the architecture presents lots of advantages, there are several inherent issues that needed to be addressed. The problems were classified into three broad categories:

- **Dynamic radio resource management:** The indoor network should be able to cope with the temporal and spatial variations in MD traffic demand and provide them with the required services. The dynamic connectivity between CANs and APs (colocated at the HCC) allows for re-assigning capacity from APs to cells with different MD traffic demands. In this dissertation, we dealt with techniques for dynamically assigning CAN to APs to deal with the rising MD traffic demand and its variability.

- **Energy-efficiency:** The network should be able to operate energy-efficiently. One of the major issues with the traditional deployment of CE-WLANs is the wastage of energy due to redundant layers of APs which are deployed to provide extra capacity during the most critical traffic demand situations. In a traditional deployment of CE-WLAN, the APs are connected to a central WLAN manger which switches on or off the APs based on the MD traffic. But it costs more energy to operate an AP than a simple CAN. In this dissertation we show that the hybrid Fi-Wi architecture effectively addresses this problem.

- **Improving network capacity:** Finally, the network capacity has to scale to cope with the traffic demand. The hybrid Fi-Wi network utilizes the multiple antennas available at the CANs to implement MU-MIMO techniques. This improves both uplink and downlink capacity per MD and total network capacity while providing fairness and QoS guarantees to MDs. Different uplink and downlink MU-MIMO schemes are thus proposed in this dissertation.

Let us now provide an overview of the conclusions drawn from the previous chapters. We summarize our findings with respect to the aforementioned problems. To achieve dynamic radio resource management in a hybrid Fi-Wi network we proposed the dynamic assignment (DA) scheme in Chapter 3. The DA utilizes the flexible connectivity between CANs and APs (colocated at the HCC) to perform congestion control (uplink delay or downlink delay) in the network. The DA algorithm achieved significantly lower maximum delay values for both cases. For example, we showed that we achieved a 45.7% reduction for 200 MDs distributed non-uniformly, and 66% for 10 video streaming, 51 best effort and 25 constant bit rate MDs distributed non-uniformly, for both maximum AP uplink and downlink delay respectively as compared to the static assignment (SA) scheme. We also proved that the DA algorithm attained an efficient assignment, i.e., an efficient Nash equilibrium solution, using the definitions from coalition game theory. This implies that the DA assignment leads to the maximum total delay (downlink or uplink) reduction for the network.

In Chapter 4 we dealt with the energy-efficiency operation of the indoor Fi-Wi CE-WLAN. We motivated the problem of energy wastage in CE-WLAN by using real life trace-sets from Dartmouth college campus [98]. We provided an architecture for RoF CE-WLAN, where more APs are connected to the SCANs if the traffic demand in the network increases and cannot be satisfied by the connectivity through PCANs. We made use of the dynamic traffic variations over space and time and the flexibility of the AP to CAN connection to make the Fi-Wi network more energy efficient. We discussed the different scenarios of traditional and RoF CE-WLAN deployment, viz., a colocated network entity and a clustered network entity scenario and showed that the clustered network entity scenario can lead to large energy saving for the RoF CE-WLAN architecture, e.g., 25% more energy efficient than traditional CE-WLAN for the academic building in our scenario. We discussed energy saving for both deployments under both scenarios for channel utilization based on the On-Demand strategy and showed large energy savings, energy efficiency and resource utilization for such RoF-based CE-WLAN. Finally, we proposed a power-managed load-balancing (PMLB) scheme

that helped to achieve both energy efficiency and load balancing among the network entities (CANs and APs). It further improved the network performance, e.g., a 52.9% lower energy per bit goodput for the PMLB strategy as compared to the On-Demand strategy for 10 MDs distributed non-uniformly.

Finally, in Chapters 5 and 6, we proposed different physical layer techniques for Fi-Wi uplink and downlink to improve network capacity. Chapter 5, studied the Fi-Wi uplink capacity and the issues that are faced by the WiFi uplink. One of the inherent problems of WiFi implementation in a Fi-Wi architecture is collisions due to hidden node terminals. In Fi-Wi, multiple CANs can connect to the same AP and thus face the hidden node problem. We proposed the use of a multiuser detection technique, successive interference cancellation (SIC), to resolve the problem. We discussed the capacity and probability of outage attainable for the SIC scheme in the Fi-Wi network. We also proposed a transmit power control scheme for SIC, which could be generalized for any number of MDs. Our main contribution is the proposal of a unique opto-spatial multiplexed multiuser-MIMO scheme that results in a higher ergodic capacity with a much lower bit error probability.

The Fi-Wi downlink was discussed in Chapter 6. In this chapter we proposed a downlink MU-MIMO scheduling scheme, Fair-Successive Leakage to Noise Ratio (Fair-SLNR) scheduling, that tries to maximize the overall downlink network capacity over a cell area taking into account the different MD demands of throughput and their respective channel gains. We compared our scheme against the Greedy SLNR scheduling and the Random SLNR scheduling. The Fair-SLNR algorithm tries to ensure the different QoS demanded by the MDs. We studied the Fair-SLNR scheme both under perfect and imperfect CSIT for the equal power allocation (EPA) and the channel adaptive power allocation (CAPA) policy. While the perfect CSIT Fair-SLNR yields the highest network capacity, the drop in capacity for error variance of 0.20 was approximately 50.12% with the EPA scheme (for 25dB SNR). Using the CAPA scheme under the same error variance further reduces the network capacity marginally by 1.45%, but we achieved a lower network bit error rate (BER) for CAPA. For, e.g., a BER value of 10^{-7}, the imperfect CSIT with CAPA outperforms EPA by 3dB.

Table 7.1 provides the summary of our most important findings in the dissertation. Based on the potential and the limitations of our research, we propose, in the section below, an outline of the future course of action that could help to build a better understanding of the Fi-Wi control and network management.

Table 7.1: Conclusions of dissertation results

Chapter	Scheme(s) Proposed	Result
Chapter 3	Dynamic Assignment (DA)	1) Reduction of uplink delay: DA < SA 2) Reduction of downlink delay: DA < SA
Chapter 4	1) On-Demand Strategy 2) PMLB Strategy	1.1) Energy efficiency: RoF CE-WLAN > Traditional CE-WLAN 1.2) Switching changes (APs): Comparable (RoF CE-WLAN $\geq$Traditional CE-WLAN) 1.3) Resource utilization: RoF CE-WLAN > Traditional CE-WLAN 2.1) Power saving: PMLB RoF CE-WLAN = On-Demand RoF CE-WLAN 2.2) Energy per bit Goodput: PMLB RoF CE-WLAN < On-Demand RoF CE-WLAN
Chapter 5	1) SIC WiFi 2) Opto-spatial MU-MIMO WiFi	1) Ergodic Capacity gain: MU-MIMO > SIC > Traditional WiFi 2) Probability of bit error: MU-MIMO < SIC < Traditional WiFi 3) Packet Transmission Time: MIMO < SIC < Traditional WiFi
Chapter 6	Fair-SLNR MU-MIMO scheduling	1) Network capacity: Greedy SLNR < Fair-SLNR < Random SLNR 2) Fairness (JFI): Maximum for Fair-SLNR ($\approx$1) 3) Network capacity: Perfect CSIT > Imperfect CSIT with EPA > Imperfect CSIT with CAPA 4) Average network BER: Imperfect CSIT with EPA > Imperfect CSIT with CAPA

Future directions

Indoor multiple standard radio technology support

We should not limit ourselves to a single radio standard, but rather take advantage of the unique multi-radio support that the Fi-Wi architecture can provide. In this dissertation, we considered only the IEEE 802.11 standard. But different standards should behave as a unique single platform with multiple options, where the MD traffic could be dynamically supported by any of the radio technologies to guarantee QoS across MDs and maximize the overall indoor network performance.

Dynamic resource management via transmit power control, frequency planning and inter-technology handovers

In Chapter 3 we discussed techniques for dynamic resource management using only space, user, time-slots and available network entities (namely, CANs inside rooms and APs collocated at the HCC) as optimizable degrees of freedom. However we did not make use of the transmission power, different wireless standards and the different frequency channels available. These are very important degrees of freedom that should be explored and indeed can help in a better management of radio resources. Use of multiple wireless technologies can help in critical conditions, by allowing vertical handovers between the technologies, when one technology is congested. Differentiation of service level agreement within the set of MDs, that are supported by the Fi-Wi architecture, can also be seen as a different dimension to the dynamic resource management problem.

Energy efficient RoD schemes, using transmit power control, frequency planning, inter-technology operation, and cognitive networking

In Chapter 4 we provided a better understanding of the energy-efficient operation of the indoor CE-WLAN networks using time-slots, space, and user as the optimizable degrees of freedom. However, we neglected the dimension of multiple radio standard support, transmit power and frequency channels available. Thus utilizing the aforementioned neglected degrees of freedom, different resource on demand schemes can be proposed for different scenarios. Many heterogeneous devices have a variety of embedded components like the camera and many sensors which help to build multi-contextual information which can support cognitive functionalities. Artificial intelligence and machine learning techniques provide a variety of autonomous solutions to solve problems even on a wide scale. Thus it

is interesting to know if any approach can be developed to couple the knowledge from those fields to realize the cognitive networking concept for such hybrid Fi-Wi indoor networks.

Massive MU-MIMO for higher capacity

In Chapter 5 and 6 we discussed multi-antenna techniques (MU-MIMO) for improving the uplink and the downlink capacities. A recent development is massive MIMO. Hybrid Fi-Wi networks present an interesting scenario for implementation of massive MIMO systems by utilizing a large number of antennas across the CANs.

A

Coalition Game Theory

Game theory has proven to be useful in modeling interactive decision situations in both wired and wireless communication networks. It provides a useful analytical tool to predict the outcome of complex interactions among rational entities. The concepts of coalition game theory forms an excellent fit to study the problem of optimal CAN-AP association using uplink or downlink delay as the metric denoting the congestion level in the network.

Coalition games for CAN-AP association

$M = \{1, 2, ...m\}$ denotes the set of independent APs and $N = \{1, 2, ...n\}$ denotes the set of CANs as described in Chapter 3. Using the terminology from coalition game theory, we refer to set S_i as a coalition of i. Since there are m APs in the network there are m independent coalitions in the system and each CAN joins any one of those m coalitions.

To propose a coalition game theory framework that models the interaction of the APs, we need the following definitions.

Definition A.1. A coalition $S \subseteq M$ is a set of an AP and the CANs associated with it.

Definition A.2. The set $S = \{S_1, ..., S_m\}$ is a partition of M if $S_i \cap S_l = \phi, \forall i, l \in M$, $i \neq l$ and $\bigcup_{i \in M} S = M$.

Definition A.3. A coalition formation game $< M, U >$ consists of a finite set M and an aggregate utility function $U(.)$ of m coalitions in the system, that associates with every non-empty subset S_i of M, a real number $U(S_i)$ which is the

maximum aggregate payoff[1] available.

We can express the optimization problem w.r.t. total uplink or total downlink delay. Below, we discuss the problem by taking uplink delay, i.e., airtime cost, as the metric.

An AP can serve a CAN only when both are associated with each other. Considering the metric of uplink delay (approximated using airtime cost, as described in Chapter 3), when CAN j is associated with AP k, i.e., in coalition S_k, the airtime cost of CAN j is,

$$\Delta^{\{j\}} = b_{jk} \tag{A.1}$$

The total airtime cost across AP i from CANs associated to it,

$$\Delta^i = \sum_{\forall j \in C^i} \Delta^{\{j\}} \tag{A.2}$$

where, C^i represents the CANs associated with AP i. AP i thus gains a benefit of $U(S_i) = U(\Delta^i)$, where $U(.)$ is taken as a concave function. Then the grand aggregate utility of the *m* coalitions *S* (i.e., $\sum_{i=1}^{m} U(S_i)$) can be given as the sum of the utilities $U(S_i)$ of the coalitions in *S*, i.e., $i \in S$.

Congestion Control Game: Objective Function

The grand aggregate utility function $U(S)$ for a coalition *S* is the maximum aggregate payoff of APs in *S*, and can be denoted by a concave function. The congestion level balancing or maximizing the grand aggregate utility can thus be formulated as a concave optimization problem as given below,

$$max \sum_{i=1}^{m} U(S_i) = max \sum_{i=1}^{m} U(\Delta^i) \tag{A.3}$$

subject to:

$$\Delta^{\{j\}} = b_{jk} \tag{A.4}$$

$$\Delta^i = \sum_{\forall j \in C^i} \Delta^{\{j\}} \tag{A.5}$$

$$b_{jk} \geq 0, \quad j \in N, k \in M \tag{A.6}$$

---

[1]Please note that the maximum aggregate payoff, $U(S_i)$, corresponds to the delay achievable for subset S_i. Thus, $U(S_i)$ utilizes a function, dependent on the delay for S_i, that provides a real value as output of the function. The $U(S_i)$ function ensures that lower the value of delay achievable for subset S_i higher will be the maximum aggregate payoff value.

The aim of the congestion balancing game (assigning CANs to APs) is to find an optimal partition S^* that generates the optimal grand aggregate utility $\sum_{i=1}^{m} U(S_i^*)$.

For comparing two partitions of the same set M which are given as $S = \{S_1, \ldots, S_m\}$ and $F = \{F_1, \ldots, F_m\}$ in a coalition game, a rational operator $\triangleright$ has been defined in [145] .

Definition A.4. A partition S is preferred over partition F i.e. $S \triangleright F$, if and only if $\sum_{i=1}^{m} U(S_i) > \sum_{i=1}^{m} U(F_i)$.

Definition A.5. A partition $S = \{S_1, \ldots, S_m\}$ for the $< M, U >$ coalition formation game is a stable partition [145], if S_m ($\forall m \in M$ and $|S_m| > 0$) does not have an interest in changing the current partition S by moving CAN k ($\forall k \in S_m$) to another coalition S_n ($\forall\, n \in M, n \neq m$ and $|S_n| < N$).

Theorem 3.7.1. *The Dynamic assignment (DA) algorithm produces a stable partition, which achieves minimal total delay for the network.*

Proof. The steps in which we can prove that the dynamic assignment (DA) algorithm terminates in a stable partition, which obtains minimum total delay (i.e., grand optimal aggregate utility) for the indoor network are:

- To prove that the algorithm terminates in a stable partition.

- The stable partition obtains the optimal grand aggregate utility for the network.

Step 1**:** In the algorithm at each round (r) and in every iteration (i) of that round only two coalitions $S_k^r(i)$ and $S_n^r(i)$ may change their aggregate utilities where $r = \{1, 2, \ldots \gamma\}$ and $i = \{1, 2, \ldots |M_c|\}$. The current partition $S^r(i)$ will be updated only if the total utility of the coalitions $S_k^r(i)$ and $S_n^r(i)$ can be increased by moving the CAN t where, $t \in S_k^r(i)$ to $S_n^r(i)$. Since the utilities of other $(m - 2 \times i)$ coalitions remain the same for that iteration i, the grand aggregate utility of the system $\sum_{j=1}^{m} U(S_j^r(i))$ will be non-decreasing. For every round we repeat the process for M_c iterations and thus the grand aggregate utility after every round $\sum_{j=1}^{m} U(S_j^r)$ will be non-decreasing as compared with $\sum_{j=1}^{m} U(S_j^{r-1})$. Thus every round of the DA algorithm produces a sequence of partition $S^1, S^2, \ldots$ with $S^r \triangleright S^{r-1}$ for $r = \{1, 2, \ldots \gamma\}$. Since the number of different partitions for the $< M, U >$ coalition formation game is finite, the sequence of partitions will terminate over time at a partition $S^* = \{S_1^*, \ldots S_m^*\}$, where any non-empty coalition S_k^*, $k \in M$ can never increase the grand aggregate utility of the network by moving the CAN t to S_n^* where $n \in M$ and $n \neq k$. Thus according to **Definition** A.5, $S^* = \{S_1^*, \ldots S_m^*\}$ is a stable partition for the $< M, U >$ coalition formation game.

Step 2**:** Now we have to prove that the optimal aggregate grand utility of the network can be obtained at the stable partition. The grand aggregate utility $\sum_{i=1}^{m} U(S_i)$ is a function of the partition S. Since the number of different partitions for the $< M, U >$ coalition formation game is finite, the number of different grand aggregate utilities of the network is also finite. Using the DA algorithm for CAN partition we have shown that $\sum_{i=1}^{m} U(S_i^r) > \sum_{i=1}^{m} U(S_i^{r-1})$ $\forall r = \{1, 2, ...\gamma\}$. At the stable partition $S^* = \{S_1^*, ..., S_m^*\}$, the grand aggregate utility of the system cannot be increased by updating the partition anymore. Therefore the grand aggregate utility given by stable partition S^* is the optimal aggregate utility. This concludes our proof. □

Bibliography

[1] IMT 2020 5G Promotion Group. IMT Vision towards 2020 and Beyond, 2014.

[2] Ericsson. Ericsson Mobility Report. `www.ericsson.com/res/docs/2014/erricson-mobility-report-june-2014.pdf`, 2014.

[3] Huawei. 5G: A Technology Vision. 2013.

[4] J.G. Andrews, S. Buzzi, Wan Choi, S.V. Hanly, A. Lozano, A.C.K. Soong, and J.C. Zhang. What Will 5G Be? *IEEE Journal on Selected Areas in Communications*, 32(6):1065--1082, June 2014.

[5] E. Dahlman, G. Mildh, S. Parkvall, J. Peisa, J. Sachs, Y. Selén, and J. Sköld. 5G wireless access: requirements and realization. *IEEE Communications Magazine*, 52(12):42--47, December 2014.

[6] Cisco Visual Networking Index: Forecast and Methodology, 2012-2017. In *Cisco White Paper*. May 2013.

[7] Alcatel-Lucent. In-building Wireless Infographic.

[8] B. Bangerter, S. Talwar, R. Arefi, and K. Stewart. Networks and devices for the 5G era. *IEEE Communications Magazine*, 52(2):90--96, February 2014.

[9] Long Zhao, Hui Zhao, Fanglong Hu, Kan Zheng, and Jingxing Zhang. Energy efficient power allocation algorithm for downlink massive MIMO with MRT precoding. In *78th IEEE Vehicular Technology Conference (VTC Fall), 2013*, pages 1--5, September 2013.

[10] F. Rusek, D. Persson, Buon Kiong Lau, E.G. Larsson, T.L. Marzetta, O. Edfors, and F. Tufvesson. Scaling up MIMO: Opportunities and challenges with very large arrays. *IEEE Signal Processing Magazine*, 30(1):40--60, January 2013.

[11] T.S. Rappaport, Shu Sun, R. Mayzus, Hang Zhao, Y. Azar, K. Wang, G.N. Wong, J.K. Schulz, M. Samimi, and F. Gutierrez. Millimeter wave mobile communications for 5G cellular: It will work! *IEEE Access*, 1:335--349, 2013.

[12] V. Chandrasekhar, J.G. Andrews, and Alan Gatherer. Femtocell networks: a survey. *IEEE Communications Magazine*, 46(9):59--67, September 2008.

[13] M. Dohler, R.W. Heath, A. Lozano, C.B. Papadias, and R.A. Valenzuela. Is the PHY layer dead? *IEEE Communications Magazine*, 49(4):159--165, April 2011.

[14] Jeffrey G. Andrews. Towards 5G HetNets. In *IEEE Communication Theory Workshop*, May 2014.

[15] M.G. Larrode. Radio over fiber distributed antenna systems for in-building broadband wireless services. *PhD Dissertation, Eindhoven University of Technology, Eindhoven, The Netherlands*, March 2008.

[16] Bao Linh Dang, M. Garcia Larrode, R. Venkatesha Prasad, Ignas Niemegeers, and A. M. J. Koonen. Radio-over-Fiber based architecture for seamless wireless indoor communication in the 60GHz band. *Comput. Commun.*, 30(18):3598--3613, December 2007.

[17] Dutch IOP GenCom MEANS Project. `www.iop-means.nl`, 2011.

[18] Dutch Ministry of Economic Affairs. `www.goverment.nl/ministries/ ez`.

[19] IOP Generieke Communicatie Program. `www.rvo.nl/ subsidies-regelingen/iop-generieke-communicatie`.

[20] Bao Linh Dang, R.V. Prasad, and I. Niemegeers. On the MAC protocols for Radio over Fiber indoor networks. In *First International Conference on Communications and Electronics, 2006. ICCE '06.*, pages 112--117, October 2006.

[21] Bao Linh Dang, R.V. Prasad, I. Niemegeers, M.G. Larrode, and A.M.J. Koonen. Resource optimization for 60 GHz indoor networks using dynamic extended cell formation. In *Sixth Annual IEEE International Conference on Pervasive Computing and Communications (PerCom)*, pages 354--359, March 2008.

[22] Jing Wang, R. Venkatesha Prasad, and I. G. M. M. Niemegeers. Solving the uncertainty of vertical handovers in multi-radio home networks. *Comput. Commun.*, 33(9):1122--1132, June 2010.

[23] Y. Josse, B. Fracasso, and P. Pajusco. Model for energy efficiency in radio over fiber distributed indoor antenna Wi-Fi network. In *14th International Symposium on Wireless Personal Multimedia Communications (WPMC), 2011*, pages 1--5, October 2011.

[24] S. Chowdhury and M. Maier. Security issues in integrated EPON and next-generation WLAN networks. In *7th IEEE Consumer Communications and Networking Conference (CCNC), 2010*, pages 1--2, January 2010.

[25] Eunsung Oh, B. Krishnamachari, Xin Liu, and Zhisheng Niu. Toward dynamic energy-efficient operation of cellular network infrastructure. *IEEE Communications Magazine*, 49(6):56--61, June 2011.

[26] SCENIHR. Potential health effects of exposure to electromagnetic fields (EMF). [Online; accessed 25-March-2017].

[27] Jerry R. Hampton. *Introduction to MIMO Communications*. Cambridge University Press, 2013. Cambridge Books Online.

[28] David Gesbert, Marios Kountouris, Robert W. Heath, Chan byoung Chae, and Thomas Sälzer. From single user to multiuser communications: Shifting the MIMO paradigm. In *IEEE Sig. Proc. Magazine*, 2007.

[29] AmitP. Jardosh, Konstantina Papagiannaki, ElizabethM. Belding, KevinC. Almeroth, Gianluca Iannaccone, and Bapi Vinnakota. Green WLANs: On-demand WLAN infrastructures. *Mobile Networks and Applications*, 14(6):798--814, 2009.

[30] Z. Uykan and K. Hugl. HSDPA system performance of optical fiber distributed antenna systems in an office environment. In *16th IEEE International Symposium on Personal, Indoor and Mobile Radio Communications (PIMRC), 2005*, volume 4, pages 2376--2380 Vol. 4, September 2005.

[31] B. Glushko, D. Kin, and A. Shar. Gigabit optical wireless communication system for personal area networking. In *8th Conference on Network and Optical Communications (NOC), 2013*, pages 145--148, July 2013.

[32] MICROSENS. Fiber to the office- future-proof networking infrastructure for mordern office environments. `www.microsens.com/fileadmin/user_upload/docs/folder/MICROSENS_FTTO_EN.pdf`, 2012.

[33] Erik Griffith and Oliver Rist. Build a future-proof home network. `www.pcmag.com/article2/0,2817,232617500.asp`, 2008.

[34] Ajung Kim, Young Hun Joo, and Yungsoo Kim. 60 GHz wireless communication systems with radio-over-fiber links for indoor wireless LANs. *IEEE Transactions on Consumer Electronics*, 50(2):517 -- 520, May 2004.

[35] A.J. Seeds and T. Ismail. Broadband access using wireless over multimode fiber systems. *Journal of Lightwave Technology*, 28(16):2430 --2435, August 2010.

[36] M. Crisp, R.V. Penty, I.H. White, and A. Bell. Wideband radio over fiber distributed antenna systems for energy efficient in-building wireless communications. In *IEEE 71st Vehicular Technology Conference (VTC 2010-Spring)*, pages 1 --5, May 2010.

[37] S.K. Dandapat, B. Mitra, R.R. Choudhury, and N. Ganguly. Smart association control in wireless mobile environment using max-flow. *IEEE Transactions on Network and Service Management,*, 9(1):73--86, March 2012.

[38] L. Yang, P. Zerfos, and E. Sadot. Architecture taxonomy for control and provisioning of wireless Access Points CAPWAP, RFC 4118, 2005.

[39] Home gateway technical requirements: Residential profile, version 1.0. *home Gateway Initiative Document HGI-RD001-R2.01.*, 2008.

[40] Sadot E. Yang L., Zerfos P. RFC: Architecture taxonomy for control and provisioning of wireless Access Points. *Network Working group*, 2005.

[41] S. Zou. Optically routed fiber-wireless indoor networks. *PhD Dissertation, Eindhoven University of Technology, Eindhoven, The Netherlands*, April 2015.

[42] Ben Coxworth. Hybrid fiber optic cable carries data and power. `www.gizmag.com/hybrid-data-power-optical-cable/21335/`, 2012.

[43] J. W. H. van Bloem, R. Schiphorst, T. Kluwer, and C. H. Slump. Spectrum utilization and congestion of IEEE 802.11 networks in the 2.4 GHz ISM band. *Journal of Green Engineering*, 2(4):401--430, July 2012.

[44] Anand Balachandran, Geoffrey M. Voelker, Paramvir Bahl, and P. Venkat Rangan. Characterizing user behavior and network performance in a public wireless LAN. In *Proceedings of the 2002 ACM SIGMETRICS International Conference on Measurement and Modeling of Computer Systems*, SIGMETRICS '02, pages 195--205, New York, NY, USA, 2002. ACM.

[45] D. Debbarma, Q. Wang, A. Lo, S.M. Heemstra. de Groot, R.V. Prasad, and V.S. Rao. Multiuser MIMO for capacity gain in Fi-Wi hybrid networks. In *EUROCON, 2013 IEEE*, pages 494--501, July 2013.

[46] Q. Bien, R.V. Prasad, K. Chandra, I. Niemieegers, and H. Nguyen. Resource management in indoor hybrid Fi-Wi network. *Transactions on Emerging Telecommunications Technologies*, 2014.

[47] Anthony J. Nicholson, Yatin Chawathe, Mike Y. Chen, Brian D. Noble, and David Wetherall. Improved Access Point selection. In *Proceedings of the 4th International Conference on Mobile Systems, Applications and Services*, pages 233--245, New York, NY, USA, 2006. ACM.

[48] Zhe Yu, Wei Feng, Wenzhu Zhang, Lin Zhang, and Yong Ren. Virtual sieve: A distributed channel assignment algorithm resolving the hidden node problem. In *Third International Conference on Communications and Mobile Computing (CMC), 2011*, pages 445--448, April 2011.

[49] Ozgur Ekici and Abbas Yongacoglu. A Novel Association algorithm for congestion relief in IEEE 802.11 WLANs. In *Proceedings of the 2006 International Conference on Wireless Communications and Mobile Computing*, IWCMC '06, pages 725--730, New York, NY, USA, 2006. ACM.

[50] Shojiro Takeuchi, Kaoru Sezaki, and Yasuhiko Yasuda. Access point selection strategy in IEEE 802.11 e WLAN networks toward load balancing. *Electronics and Communications in Japan (Part I: Communications)*, 90(4):35--45, 2007.

[51] Eduard Garcia, Josep L. Ferrer, Elena Lopez-Aguilera, Rafael Vidal, and Josep Paradells. Client-driven load balancing through association control in IEEE 802.11 WLANs. *European Transactions on Telecommunications*, 20(5):494--507, 2009.

[52] Murad Abusubaih and Adam Wolisz. An Optimal Station Association policy for multi-rate IEEE 802.11 Wireless Lans. In *Proceedings of the 10th ACM*

Symposium on Modeling, Analysis, and Simulation of Wireless and Mobile Systems, MSWiM '07, pages 117--123, New York, NY, USA, 2007. ACM.

[53] Dhruv Gupta, Prasant Mohapatra, and Chen-Nee Chuah. Seeker: A bandwidth-based association control framework for wireless Mesh networks. *Wireless Networks*, 17(5):1287--1304, 2011.

[54] Jun Zhang and B. Bensaou. Balancing download throughput in densely deployed IEEE 802.11 multi-cell WLANs. In *IEEE International Conference on Communications (ICC), 2013*, pages 6107--6111, June 2013.

[55] G. Athanasiou, T. Korakis, O. Ercetin, and L. Tassiulas. A cross-layer framework for association control in wireless Mesh Networks. *IEEE Transactions on Mobile Computing*, 8(1):65--80, January 2009.

[56] O. Ercetin. Association games in IEEE 802.11 wireless local area networks. *IEEE Transactions on Wireless Communications*, 7(12):5136--5143, December 2008.

[57] M. Cesana, I. Malanchini, and A. Capone. Modelling network selection and resource allocation in wireless access networks with non-cooperative games. In *5th IEEE International Conference on Mobile Ad Hoc and Sensor Systems (MASS) 2008.*, pages 404--409, September 2008.

[58] S. Shakkottai, E. Altman, and A. Kumar. Multihoming of Users to Access Points in WLANs: A population game perspective. *IEEE Journal on Selected Areas in Communications,*, 25(6):1207--1215, August 2007.

[59] Sébastien Deronne, Véronique Moeyaert, and Sébastien Bette. Simulation of 802.11 radio-over-fiber networks using Ns-3. In *Proceedings of the 6th International ICST Conference on Simulation Tools and Techniques*, Simu-Tools '13, pages 190--194, ICST, Brussels, Belgium, 2013. ICST (Institute for Computer Sciences, Social-Informatics and Telecommunications Engineering).

[60] Yuting Fan, Jianqiang Li, Kun Xu, Hao Chen, Xun Lu, Yitang Dai, Feifei Yin, Yuefeng Ji, and Jintong Lin. Performance analysis forIEEE 802.11 distributed coordination function in radio-over-fiber-based distributed antenna systems. *Opt. Express*, 21(18):20529--20543, September 2013.

[61] Li Jianqiang, Fan Yuting, Chen Hao, Lu Xun, and Xu Kun. Performance analysis of WLAN medium access control protocols in simulcast radio-over-fiber-based distributed antenna systems. *Communications, China*, 11(5):37--48, May 2014.

[62] Dimitris Mavrakis. Dow we really need femto cells? `www.visionmobile.com/blog/2007/12/do-we-really-need-femto-cells/`. [Online; accessed 11-May-2016].

[63] Stefan Mangold, Sunghyun Choi, Peter May, Ole Klein, Guido Hiertz, Lothar Stibor, Cf poll Contention, and Free Poll. IEEE 802.11e Wireless LAN for Quality of Service, February 2002.

[64] F. Cacace, G. Iannello, and L. Vollero. *Management, Monitoring and QoS in Multi-Cell Centralized WLANs*. IGI Global, 2010.

[65] Filippo Cacace and Luca Vollero. A delay monitoring method for up-link flows in IEEE 802.11e EDCA networks. In *Proceedings of the 2nd International Conference on Simulation Tools and Techniques*, Simutools '09, pages 87:1--87:8, ICST, Brussels, Belgium, 2009. ICST (Institute for Computer Sciences, Social-Informatics and Telecommunications Engineering).

[66] IEEE 802.11s Draft Standard: Extended Service set Mesh Networking.

[67] I. Dangerfield, D. Malone, and D. J. Leith. Experimental evaluation of 802.11e EDCA for enhanced voice over wlan performance. In *4th International Symposium on Modeling and Optimization in Mobile, Ad Hoc and Wireless Networks*, pages 1--7, April 2006.

[68] F. Cacace, G. Iannello, M. Vellucci, and L. Vollero. A reactive approach to QoS provisioning in IEEE 802.11e WLANs. In *Next Generation Internet Networks, 2008. NGI 2008*, pages 253--260, April 2008.

[69] H. Win and A. Pathan. On the issues and chalenges of Fiber-Wireless (Fi-Wi) networks. *Journal of Engineering*, (Article ID 645745), 2013.

[70] J. Sangiamwong and T. Sugiyama. Hidden node problem aware routing metric for wireless LAN Mesh Networks. In *IEEE 18th International Symposium on Personal, Indoor and Mobile Radio Communications (PIMRC), 2007*, pages 1--5, September 2007.

[71] Feng Li, Mingzhe Li, Rui Lu, Huahui Wu, M. Claypool, and R. Kinicki. Measuring queue capacities of IEEE 802.11 wireless access points. In *Broadband Communications, Networks and Systems, Fourth International Conference on BROADNETS 2007*, pages 846--853, September 2007.

[72] Llya Grigorik. Uplink latency of WiFi and 4G networks. `www.igvita.com/2014/04/21/uplink-scheduling-in-4G-networks/`. [Online; accessed 11-May-2016].

[73] Attahiru Sule Alfa. *Queueing Theory for Telecommunications - Discrete Time Modelling of a Single Node System*. Springer, 2010.

[74] U. Narayan Bhat. *An Introduction to Queueing Theory: Modeling and Analysis in Applications*. Birkh, 2nd edition, 2015.

[75] B. Canberk, I.F. Akyildiz, and S. Oktug. A QoS-aware framework for available spectrum characterization and decision in Cognitive Radio networks. In *IEEE 21st International Symposium on Personal Indoor and Mobile Radio Communications (PIMRC), 2010*, pages 1533--1538, September 2010.

[76] R. Balakrishnan and B. Canberk. Traffic-aware QoS provisioning and admission control in OFDMA hybrid small cells. *IEEE Transactions on Vehicular Technology,*, 63(2):802--810, February 2014.

[77] Sunghyun Choi, J. del Prado, N. Sai Shankar, and S. Mangold. IEEE 802.11 e contention-based channel access (EDCF) performance evaluation. In *IEEE International Conference on Communications, 2003. ICC '03.*, volume 2, pages 1151--1156 vol.2, May 2003.

[78] C.H. Foh and J.W. Tantra. Comments on the paper 'analysis of collision probabilities for saturated IEEE 802.11 MAC protocol'. *Electronics Letters*, 43(10):596--596, May 2007.

[79] A. Balachandran, S. Nandy, V. P. Rangan, and G. M. Voelker. Online load balancing and first-hop bandwidth allocation in public-area wireless networks. *Technical Report CS2003-0748, University of California, San Diego*, June 2003.

[80] Mirco Musolesi and Cecilia Mascolo. Mobility Models for Systems Evaluation. A Survey. In *Middleware for Network Eccentric and Mobile Applications*, pages 43--62. Springer, February 2009.

[81] Christian Bettstetter. Mobility modeling in wireless networks: Categoriza-tion, smooth movement, and border effects. *SIGMOBILE Mob. Comput. Commun. Rev.*, 5(3):55--66, July 2001.

[82] Dieter Mitsche, Giovanni Resta, and Paolo Santi. The random waypoint mobility model with uniform node spatial distribution. *Wireless Networks*, 20(5):1053--1066, 2014.

[83] A. Duda. Understanding the performance of 802.11 networks. In *IEEE 19th International Symposium on Personal, Indoor and Mobile Radio Communi-cations*, pages 1--6, September 2008.

[84] Anand Balachandran, Paramvir Bahl, and Geoffrey M. Voelker. Hot-spot congestion relief in public-area wireless network. In *WMCSA*, pages 70--. IEEE Computer Society, 2002.

[85] IEEE standard for information technology-- local and metropolitan area networks-- specific requirements-- part 11: Wireless LAN Medium Access Control (MAC) and Physical Layer (PHY) specifications amendment 2: Fast basic service set (BSS) transition. *IEEE Std 802.11r-2008 (Amendment to IEEE Std 802.11-2007 as amended by IEEE Std 802.11k-2008)*, pages 1--126, July 2008.

[86] Jerome Henry. 802.11r. `www.wirelessccie.nl/2016/01/802.11r.html`. [Online; accessed 11-May-2016].

[87] Aerohive Networks. `http://www.aerohive.com/resources/oxford-brookes-university/`, 2014.

[88] Andrew Burger. Report: Wi-Fi households to approach 800 million by 2016. `www.telecompetitor.com/report-wi-fi-households-to-approach-800-million-by-2016/`. [Online; accessed 11-May-2016].

[89] Takefumi Hiraguri, Masakatsu Ogawa, Makoto Umeuchi, and Tetsu Sakata. Study of power saving scheme suitable for Wireless LAN in multimedia communication. In *Proceedings of the 2009 IEEE Conference on Wireless Communications & Networking Conference*, WCNC'09, pages 1403--1408, Piscataway, NJ, USA, 2009. IEEE Press.

[90] Tsern-Huei Lee and Jing-Rong Hsieh. An efficient scheduling algorithm for scheduled automatic power save delivery for Wireless LANs. In *IEEE 71st*

Vehicular Technology Conference (VTC 2010-Spring), 2010, pages 1--5, May 2010.

[91] The Power Consumption Database. `www.tpcdb.com/list.php?type=11`, 2016.

[92] D. Qiao, Sunghyun Choi, Amit Jain, and K.G. Shin. Adaptive transmit power control in IEEE 802.11a wireless LANs. In *The 57th IEEE Semiannual Vehicular Technology Conference, 2003. VTC 2003-Spring.*, volume 1, pages 433--437, April 2003.

[93] Nilesh Mishra, Kameswari Chebrolu, Bhaskaran Raman, and Abhinav Pathak. Wake-on-WLAN. In *Proceedings of the 15th International Conference on World Wide Web*, WWW '06, pages 761--769, New York, NY, USA, 2006. ACM.

[94] R. Nagareda, A. Hasegawa, T. Shibata, and S. Obana. A proposal of power saving scheme for wireless access networks with Access Point sharing. In *International Conference on Computing, Networking and Communications (ICNC), 2012*, pages 1128--1132, January 2012.

[95] Marco Ajmone Marsan, Luca Chiaraviglio, Delia Ciullo, and Michela Meo. A simple analytical model for the energy-efficient activation of Access Points in dense WLANs. In *Proceedings of the 1st International Conference on Energy-Efficient Computing and Networking*.

[96] A.S. Gowda, A.R. Dhaini, L.G. Kazovsky, Hejie Yang, S.T. Abraha, and A. Ngoma. Towards Green Optical/Wireless in-building networks: Radio-Over-Fiber. *Journal of Lightwave Technology,*, 32(20):3545--3556, October 2014.

[97] Y. Josse, B. Fracasso, G. Castignani, and N. Montavont. Energy-efficient deployment of distributed antenna systems with Radio-over-Fiber links. In *IEEE Online Conference on Green Communications (GreenCom), 2012*, pages 7--13, September 2012.

[98] David Kotz, Tristan Henderson, Ilya Abyzov, and Jihwang Yeo. CRAW-DAD data set Dartmouth/campus (v. 2007-02-08). Downloaded from http://crawdad.org/dartmouth/campus/, February 2007.

[99] Wikipedia. Wavelength-division multiplexing --- wikipedia, the free encyclopedia, 2015. [Online; accessed 9-August-2015].

[100] D. Wake, A. Nkansah, N.J. Gomes, C. Lethien, C. Sion, and J.P. Vilcot. Optically powered remote units for Radio-over-Fiber systems. *Journal of Lightwave Technology*, 26(15):2484--2491, August 2008.

[101] R. Karp. Reducibility among combinatorial problems. In R. Miller and J. Thatcher, editors, *Complexity of Computer Computations*, pages 85--103. Plenum Press, 1972.

[102] Diptanil DebBarma. Energy efficient RoF based centralized enterprise WLAN (CE-WLAN). In *Proc. of IEEE EUROCON*, 2015.

[103] ITU-R. Recommendation ITU-R P.1238-8: Propagation data and predicting methods for the planning of indoor radiocommunication systemsand radio local area networks in the frequency range 300 MHz to 100 GHz. Technical report, 2015.

[104] Roberto Battiti Marco, Marco Conti, Enrico Gregori, Mikalai Sabel, and Consiglio Nazionale Delle Ricerche. Price-based congestion-control in Wi-Fi hot spots. In *Proc. WiOpt'03, INRIA Sophia-Antipolis*, pages 3--5, 2003.

[105] Aruba Networks. Configuring WLAN settings for an SSID profile. `www.arubanetworks.com/techdocs/instantHTML/Content/Chapter8%20Network%20ConfigurationWLANpro.htm`. [Online; accessed 20-June-2016].

[106] Jean pierre Ebert, Brian Burns, and Adam Wolisz. A trace-based approach for determining the energy consumption of a WLAN network interface, 2002.

[107] About Technology. `http://compnetworking.about.com/b/2009/06/11/how-much-power-does-a-network-router-consume.htm/`, 2009.

[108] Aruba Networks. `http://arubanetworks.com/company/press/`, 2009.

[109] Daquan Feng, Chenzi Jiang, Gubong Lim, Jr. Cimini, L.J., Gang Feng, and G.Y. Li. A survey of energy-efficient wireless communications. *IEEE Communications Surveys Tutorials,*, 15(1):167--178, January 2013.

[110] A.Y. Wang and C.G. Sodini. On the energy efficiency of wireless transceivers. In *IEEE International Conference on Communications, 2006. (ICC '06)*, volume 8, pages 3783--3788, June 2006.

[111] Jinkyu Lee and Ikjun Yeom. Avoiding collision with hidden nodes in IEEE 802.11 wireless networks. *IEEE Communications Letters*, 13(10):743 --745, october 2009.

[112] Li Bin Jiang and Soung Chang Liew. Improving throughput and fairness by reducing exposed and hidden nodes in 802.11 networks. *IEEE Transactions on Mobile Computing*, 7(1):34 --49, January 2008.

[113] Ting Chao Hou, Ling Fan Tsao, and Hsin Chiao Liu. Analyzing the throughput of IEEE 802.11 DCF scheme with hidden nodes. In *IEEE 58th Vehicular Technology Conference, 2003. VTC 2003-Fall. 2003*, volume 5, pages 2870 -- 2874 Vol.5, October 2003.

[114] Li Bin Jiang and Soung Chang Liew. Removing hidden nodes in IEEE 802.11 wireless networks. In *IEEE 62nd Vehicular Technology Conference, 2005. VTC-2005-Fall. 2005*, volume 2, pages 1127--1131, September 2005.

[115] Shiann-Tsong Sheu, T. Chen, Jenhui Chen, and Fun Ye. The impact of RTS threshold on IEEE 802.11 MAC protocol. In *Proceedings of Ninth International Conference on Parallel and Distributed Systems*, pages 267 --272, December 2002.

[116] J. Kazemitabar and H. Jafarkhani. Multiuser interference cancellation and detection for users with more than two transmit antennas. *IEEE Transactions on Communications*, 56(4):574 --583, April 2008.

[117] Hu Jin, Bang Chul Jung, Ho Young Hwang, and Dan Keun Sung. A MIMO-based collision mitigation scheme in uplink WLANs. *IEEE Communications Letters*, 12(6):417 --419, June 2008.

[118] Hu Jin, Bang Chul Jung, and Dan Keun Sung. A tradeoff between single-user and multi-user MIMO schemes in multi-rate uplink WLANs. *IEEE Transactions on Wireless Communications*, 10(10):3332 --3342, October 2011.

[119] Hu Jin, Jiyoung Cha, and Dan Keun Sung. A downlink and uplink collision mitigation scheme for multi-user MIMO-based WLANs through relaying. In *6th International ICST Conference on Communications and Networking in China (CHINACOM), 2011*, pages 516 --520, August 2011.

[120] Daniel Halperin, Thomas Anderson, and David Wetherall. Taking the sting out of carrier sense: Interference cancellation for Wireless LANs. In *In Proceedings of the 14th ACM international conference on Mobile computing and networking*, 2008.

[121] Souvik Sen, Naveen Santhapuri, Romit Roy Choudhury, and Srihari Nelaku-diti. Successive interference cancellation: A back-of-the-envelope perspective. In *Proceedings of the 9th ACM SIGCOMM Workshop on Hot Topics in Networks*, Hotnets-IX, pages 17:1--17:6, New York, NY, USA, 2010. ACM.

[122] WLAN by German Engineering. WLAN maximum transmission power (ETSI), 2014.

[123] Yogita Chapre, Prasant Mohapatra, Sanjay Jha, and Aruna Seneviratne. Received signal strength indicator and its analysis in a typical WLAN system (short paper). *2013 IEEE 38th Conference on Local Computer Networks (LCN 2013)*, pages 304--307, 2014.

[124] David Tse and Pramod Viswanath. Fundamentals of wireless communications, 2004.

[125] P. Mahasukhon, M. Hempel, H. Sharif, Ting Zhou, Song Ci, and Hsiao-Hwa Chen. BER analysis of 802.11b networks under mobility. In *IEEE International Conference on Communications. ICC '07*, pages 4722 --4727, June 2007.

[126] Kang-Won Lee, M. Cheng, and Li Fung Chang. Wireless QoS analysis for a Rayleigh fading channel. In *IEEE International Conference on Communications. ICC 98. 1998.*, volume 2, pages 1089 --1093 vol.2, June 1998.

[127] CISCO. Enterprise best practices for iOS devices on Cisco Wireless LAN. `www.cisco.com/c/dam/en/us/td/docs/wireless/controller/technotes/8-3/Enterprise_Best_Practices_for_Apple_Devices_on_Cisco_Wireless_LAN.pdf`, 2016. [Online; accessed 2-Feb-2017].

[128] Commotion. Learn wireless basics. [Online; accessed 2-Feb-2017].

[129] Hai L. Vu and Taka Sakurai. Collision probability in saturated IEEE 802.11 networks. In *In Australian Telecommunication Networks and Applications Conference*, 2006.

[130] S. H. Lee, John Thompson, and J. U. Kim. QoS-guaranteed multiuser scheduling in MIMO broadcast channels. *ETRI Contribution to a Journal*, 31/5:481--488, 2009.

[131] M. Sharif and B. Hassibi. A comparison of time-sharing, DPC, and beam-forming for MIMO broadcast channels with many users. *IEEE Transactions on Communications*, 55(1):11--15, January 2007.

[132] M. Kobayashi, N. Jindal, and G. Caire. Training and feedback optimization for multiuser MIMO downlink. *IEEE Transactions on Communications*, 59(8):2228--2240, August 2011.

[133] M. H M Costa. Writing on dirty paper (corresp.). *IEEE Transactions on Information Theory*, 29(3):439--441, 1983.

[134] M. Sadek, A. Tarighat, and A.H. Sayed. A leakage-based precoding scheme for downlink multi-user MIMO channels. *IEEE Transactions on Wireless Communications,*, 6(5):1711--1721, 2007.

[135] Xin Xia, Gang Wu, Shu Fang, and Shaoqian Li. SINR or SLNR: In successive user scheduling in MU-MIMO broadcast channel with finite rate feedback. In *International Conference on Communications and Mobile Computing (CMC), 2010*, volume 2, pages 383--387, 2010.

[136] P. Patcharamaneepakorn, A. Doufexi, and S. Armour. Reduced complexity joint user and receive antenna selection algorithms for SLNR-based precoding in MU-MIMO systems. In *IEEE 75th Vehicular Technology Conference (VTC Spring), 2012*, pages 1--5, 2012.

[137] Hoon Kim, Keunyoung Kim, Youngnam Han, and Jiwoong Lee. An efficient scheduling algorithm for QoS in wireless packet data transmission. In *The 13th IEEE International Symposium on Personal, Indoor and Mobile Radio Communications, 2002*, volume 5, pages 2244--2248, 2002.

[138] H. MacLeod, C. Loadman, and Z. Chen. Experimental studies of the 2.4-GHz ISM wireless indoor channel. In *Proceedings of the 3rd Annual Communication Networks and Services Research Conference, 2005.*, pages 63--68, 2005.

[139] M. Sadek, A. Tarighat, and A.H. Sayed. Active antenna selection in multiuserMIMO communications. *IEEE Transactions on Signal Processing*, 55(4):1498--1510, 2007.

[140] Taesang Yoo and A. Goldsmith. Capacity and power allocation for fading MIMO channels with channel estimation error. *IEEE Transactions on Information Theory*, 52(5):2203--2214, 2006.

[141] Peng Cao, Guixia Kang, Ningbo Zhang, and Ping Zhang. A modified precoding scheme for MIMO downlink channel with imperfect CSIT. In *11th IEEE Singapore International Conference on Communication Systems, 2008. ICCS 2008.*, pages 841--845, 2008.

[142] I. Shomorony and A. S. Avestimehr. Is Gaussian noise the worst-case additive noise in wireless networks? In *2012 IEEE International Symposium on Information Theory Proceedings (ISIT)*, pages 214--218, July 2012.

[143] Y. Xiao and S. Zhou. Downlink Linear Max-MSE transceiver design for multiuser MIMO systems via dual decomposition. In *VTC Spring 2008 - IEEE Vehicular Technology Conference*, pages 847--851, May 2008.

[144] Jie Wang, Xiaotian Wang, Yongliang Guo, and Xiaohu You. A channel adaptive power allocation scheme based on SLNR precoding for multiuser MIMO systems. In *IEEE 72nd Vehicular Technology Conference Fall (VTC 2010-Fall), 2010*, pages 1--4, 2010.

[145] Krzysztof R. Apt and Andreas Witzel. A Generic Approach to Coalition Formation. In *COMSOC*, pages 347--367, December 2006.

[146] J. Wang. Networking technologies for future home networks using 60 GHz radio. *PhD Dissertation, Delft University of Technology, Delft, The Netherlands*, May 2010.

Notations & Symbols

Notation

a	Scalar
b	Vector
H	Matrix
I	Identity Matrix
$a \bigcup b$	Union of a and b
$\mathbf{H}^T$	Transpose of Matrix **H**
$\mathbf{H}^H$	Hermitian of Matrix **H**
$\|\mathbf{H}\|$	Frobenius norm of Matrix **H**
$\tilde{\mathbf{H}}$	Extended Matrix **H**
$Tr\left(\mathbf{H}\right)$	Trace of Matrix **H**
$E\left[.\right]$	Expectation
$max\left\{a,b\right\}$	Maximum of a and b
$\left\vert.\right\vert$	Absolute value
$\left\Vert.\right\Vert$ or $\det\left(.\right)$	Determinant
$\log_x\left(.\right)$	Logarithm of $(.)$ to base x
$\exp\left(.\right)$	Exponential of $(.)$
$N\left(a,b\right)$	Gaussian Distribution with mean a and variance b

$maxev\left(\mathbf{H}\right)$	Maximum eigenvalue of Matrix **H**
$I\left(a,b\right)$	Mutual Information a and b
$P\left(a\right)$	Probability Distribution Function of a
$P\left[a\leq b\right]$	Cumulative Distribution Function

Symbol

y	Received Signal
x	Transmitted Signal
h	Channel gain
$\mathbf{H}$	Channel Gain Matrix
α	Amplification Factor
P	Power
n	Noise
B	Bandwidth
X	Received Signal Strength
r	Rate
τ	Probability of Collision
L	Packet Length
C	Capacity
γ	Signal to Noise Ratio
E_b	Bit Energy
T	Message Transmission Time
$\mathbf{b}$	Precoding vector
κ	Smoothing factor
$\hat{\mathbf{h}}$	Erroneous Channel Estimate vector

e	Error vector
θ	Channel Utilization Threshold
D	Average Queue Waiting Time
d	Distance
O_{ca}	Channel Access Overhead
O_p	Protocol Overhead
B_t	Number of bits in test packet
$R_a^b(i)$	Transmission rate between AP b and MD i under CAN a
e_{pt}	Packet error rate for the test packet
TX_j	Packet transmission time ratio for MD j
B_t	Number of bits in test packet
T_t	Total time interval of the test data frame
$\Delta^{b\{a\}}(i)$	Airtime cost of MD i across CAN a connected to AP b
Δ^b	Total airtime cost across AP b
A_a^b	Total number of MDs across CAN a connected to AP b
C^b	Set of CANs operating under AP b
η	Packet Collision Ratio
$F_i(t)$	Number of packet arrivals across MD i's queue until time t
$\mathbf{q}(t)$	Queue length Vector until time t
ν	Mean arrival rate vector
R_{mi}^{nD}	Down-link rate achieved by MD i connected to AP m using CAN n
T_s	Duration of slot time
$\bar{q}_i(t)$	MD i's average queue length
$D_{i_{CBR}}$	Average waiting time for constant bit rate MD i

$\sigma^2_{\overline{T_{iCBR}}}$	Variance of service time for constant bit rate MD i
$D_{i_{VS}}$	Average waiting time for video streaming MD i
$\sigma^2_{\overline{T_{iVS}}}$	Variance of service time for video streaming MD i
s	Shape parameter
$D_{i_{BE}}$	Average waiting time for best effort MD i
$\sigma^2_{\overline{T_{iBE}}}$	Variance of service time for best effort MD i
σ^2_t	Variance of the inter-arrival time
b^{nD}_{mi}	Down-link throughput for MD i connected to AP m using CAN n
p^D_{mi}	Probability of successful transmission between AP m and MD i
P_m	Transmission time of the payload
H_m	Transmission time of the header packet and the data packet
T_{SIFS}	Transmission time consumed by short interframe space
T_{DIFS}	Transmission time consumed by distributed interframe space
T_{ACK}	Transmission time due to acknowledgment
CW_{avg}	Average contention window length
$p^{collision}_{mi}$	Collision probability of AP m's transmission to MD i
W^{nD}_{mi}	Down-link packet transmission time from AP m to MD i using CAN n
L_i	Average packet length for MD i
V^{nD}_{mi}	Down-link delay for MD i connected to AP m using CAN n
V^D_m	Down-link delay across AP m
ψ	MAC Control Packet
ϑ	Probability of a MD transmitting in an arbitrary slot
$U(.)$	Utility Function

Acronyms

4G	Fourth Generation
5G	Fifth Generation
ABS	Association Based Strategy
ACK	Acknowledgment
AGC	Automatic Gain Controller
AP	Access Point
ATT	Attenuator
BE	Best Effort
BER	Bit Error Rate
CAPWAP	Control And Provisioning of Wireless Access Point
CA	Centralized Assignment
CAN	Cell Access Node
CAPA	Channel Adaptive Power Allocation
CBR	Constant Bit Rate
CCDF	Complementary Cumulative Distribution Function
CCI	Co-Channel Interference
CDF	Cumulative Distribution Function
CE-WLAN	Centralized Enterprise-WLAN

CSI	Channel State Information
CSIT	Channel State Information at Transmitter
CSIR	Channel State Information at Receiver
CSMA/CA	Carrier Sensed Multiple Access/Collision Avoidance
CTS	Clear To Send
DAS	Distributed Antenna System
DPC	Dirty Paper Coding
DIFS	Distributed Interframe Space
DSSS-DBPSK	Direct Sequence Spread Spectrum- Differential Binary Phase Shift Keying
EBG	Energy per Bit Goodput
EDCF	Enhanced Distributed Coordinated Function
EPA	Equal Power Allocation
ev	eigen-vector
Fi-Wi	Fiber-Wireless
HCC	Home Communication Controller
HetNet	Heterogeneous Networking
HGI	Home Gateway Initiative
Hz	Hertz
ICT	Information and Communications Technology
ILP	Integer Linear Programming
ISM	Industrial, Scientific and Medical
JFI	Jain's Fairness Index
LD	Laser Diode

LTE	Long Term Evolution
LWAP	Light-weight Access Point
MAC	Medium Access Control
MEANS	Management and Control of Energy-efficient Ad-hoc Networks and Services
MEMS	Micro-Electro-Mechanical Systems
MIMO	Multiple-Input and Multiple-Output
MMSE	Minimum Mean Squared Error
MD	Mobile Device
MU-MIMO	Multiuser-Multiple Input and Multiple Output
MUX	Multiplexer
OFM	Optical Frequency Multiplication
PCAN	Primary Cell Access Node
PA	Power Amplifier
PD	Photo-Diode
PF	Proportional Fairness
PHY	Physical
PMLB	Power Managed Load Balanced
QoS	Quality of Service
RNM	Radio Network Manager
RoD	Resource on Demand
RoF	Radio-over-Fiber
RR	Round Robin
RSS	Received Signal Strength

RSSI	Received Signal Strength Indicator
RTS	Request To Send
Rx/TRx	Transceiver
SA	Static Assignment
SCAN	Secondary Cell Access Node
SCM	Sub-Carrier Multiplexing
SDN	Signal Distribution Network
SIC	Successive Interference Cancellation
SIFS	Short Interframe Space
SINR	Signal-to-interference-and-noise Ratio
SLNR	Signal-to-leakage-and-noise ratio
SNMP	Simple Network Management Protocol
SNR	Signal to Noise Ratio
SU-MIMO	Single User-MIMO
TIA	Trans-impedance Amplifier
UMTS	Universal Mobile Telecommunications System
VoIP	Voice over Internet Protocol
VS	Video Streaming
W	Watt
WDM	Wavelength Division Multiplexing
WiFi	Wireless Fidelity
WLAN	Wireless Local Area Network
xDSL	the Digital Subscriber Line
ZF	Zero-Forcing

List of Publications

Journal Proceedings

1. **[*J* 1*:*]** <u>D. DebBarma</u>,"Reduction of Downlink Delay time for heterogeneous users in Fi-Wi Indoor networks" Transactions on Emerging Telecommunications Technologies, 2015.

2. Qing Wang, <u>D. DebBarma</u>; A. Lo; Z. Cao; I. Niemegeers; S. M. Heemstra de Groot, "Distributed Antenna System for Mitigating Shadowing Effect in 60 GHz WLAN", Wireless Personal Communications, Springer, 2015.

3. Qing Wang; <u>D. DebBarma</u>; A. Lo; Ignas Niemegeers; Sonia M. Heemstra de Groot,"Sum-rate Performance of Large Centralized and Distributed MU-MIMO Systems in Indoor WLAN," Infocommunications Journal, vol. 7, no. 3, 2015.

Conference, Symposium and Workshop Proceedings

4. **[*C* 1*:*]** <u>D. DebBarma</u>, Qing Wang; Chetan B. M.; Ignas Niemegeers; Sonia M. Heemstra de Groot,"Channel Utilization Based Energy Efficient RoF Centralized Enterprise WLAN," Proceedings of IEEE 22nd Symposium on Communications and Vehicular Technology in the Benelux (SCVT), 2015, Luxembourg City.

5. **[*C* 2*:*]** <u>D. DebBarma</u>, Qing Wang; Chetan B. M.; Ignas Niemegeers; Sonia M. Heemstra de Groot,"Energy Efficient Fi-Wi LAN with Performance optimization," Proceedings of IEEE 22nd Symposium on Communications and Vehicular Technology in the Benelux (SCVT), 2015, Luxembourg City.

6. Qing Wang; <u>D. DebBarma</u>; A. Lo; Ignas Niemegeers; Sonia M. Heemstra de Groot,"Sum-rates of Radio-over-Fiber Small Cell Networks and Massive MIMO for Indoor Communication," Proceedings of IEEE 22nd Symposium on Communications and Vehicular Technology in the Benelux (SCVT), 2015, Luxembourg City.

7. Qing Wang; <u>D. DebBarma</u>; A. Lo; Ignas Niemegeers; Sonia M. Heemstra de Groot,"Feedback Bits Allocation for Large Distributed Antenna Systems in Indoor WLAN," Proceedings of IEEE 22nd Symposium on Communications and Vehicular Technology in the Benelux (SCVT), 2015, Luxembourg City.

8. [*C*3*:*] <u>D. DebBarma</u>," Energy efficient RoF based Centralized Enterprise WLAN (CE-WLAN)" Proceedings of IEEE EUROCON-2015, Spain.

9. Q. Wang; <u>D. DebBarma</u>; Z. Cao; A. Lo; I. G. M. M. Niemegeers; S. M. Heemstra de Groot," Performance Analysis of Large Centralized and Distributed MU-MIMO Systems in Indoor WLAN" Proceedings of IEEE Europen Wireless-2015, Budapest.

10. [*C* 4*:*] <u>D. DebBarma</u>; Q. Wang; I. G. M. M. Niemegeers; S. M. Heemstra de Groot; A. Lo, "Coalition game-theory-based congestion control in Hybrid Fi-Wi indoor network," Proceedings of Third International Conference on Future Generation Communication Technology (FGCT), 2014, pp.25-32, 13-15 Aug. 2014.

11. [*C* 5*:*] <u>D. DebBarma</u>; Q. Wang; I. Niemegeers; S. M. Heemstra de Groot, "Downlink throughput characterization of RoF based hybrid 802.11 Fi-Wi," Proceedings of IEEE 21st Symposium on Communications and Vehicular Technology in the Benelux (SCVT), 2014, pp.63-68, 10-10 Nov. 2014.

12. [*C* 6*:*] <u>D. DebBarma</u>; S. Zou; Q. Wang; A. Lo; I. Niemegeers; S. M. Heemstra de Groot, "Green hybrid Fi-Wi LAN," Proceedings of IEEE 21st Symposium on Communications and Vehicular Technology in the Benelux (SCVT), 2014, pp.41-46, 10-10 Nov. 2014.

13. Q. Wang; Z. Cao; <u>D. DebBarma</u>; I. Niemegeers; S. M. Heemstra de Groot; A. Lo, "Measurements and performance of large MIMO systems at 2.4 GHz for indoor WLAN," Proceedings of IEEE 21st Symposium on Communications and Vehicular Technology in the Benelux (SCVT), 2014, pp.35,40, 10-10 Nov. 2014.

14. **[*C*7*:*]** <u>D. DebBarma</u>; Q. Wang; A. Lo; S. M. Heemstra de Groot; R. V. Prasad; V. S. Rao, "Multiuser — MIMO for capacity gain in Fi-Wi hybrid networks," Proceedings of IEEE EUROCON, 2013, pp.494,501, 1-4 July 2013.

15. **[*C*8*:*]** <u>D. DebBarma</u>; Q. Wang; S. M. Heemstra de Groot; A. Lo, "A through-put fair SLNR scheduling algorithm for hybrid Fi-Wi indoor downlink MU-MIMO," Proceedings of IEEE 24th International Symposium on Personal Indoor and Mobile Radio Communications (PIMRC), 2013, pp.902,906, 8-11 Sept. 2013.

16. **[*C*9*:*]** <u>D. DebBarma</u>; Q. Wang; S. M. Heemstra de Groot; A. Lo, "Effects of imperfect CSIT on downlink MU-MIMO fair SLNR scheduling algorithm," Proceedings of IEEE 20th Symposium on Communications and Vehicular Technology in the Benelux (SCVT), 2013, pp.1,6, 21-21 Nov. 2013. **(Best Paper award Finalist)**

17. Q. Wang; <u>D. DebBarma</u>; A. Lo; S. M. Heemstra de Groot; I. Niemegeers, "Successive interference cancellation in the uplink of Radio-over-Fiber systems," Proceedings of IEEE EUROCON, 2013, pp.521,528, 1-4 July 2013.

18. Q. Wang; <u>D. DebBarma</u>; S. M. Heemstra de Groot; I. Niemegeers; A. Lo, "Cell switching mechanisms for access point sharing in WLAN over radio-over-fiber systems," Proceedings of IEEE 20th Symposium on Communications and Vehicular Technology in the Benelux (SCVT), 2013, pp.1,6, 21-21 Nov. 2013. **(Best Paper award Finalist)**

Other

19. K. Dong; <u>D. DebBarma</u>; R. V. Prasad; C. Guo,"Poster: performance study of clustering of Zigbee devices in OPNET" SIGMETRICS Performance Evaluation Review 39, 2 (September 2011), 71-71.

20. **[*O*1*:*]** <u>D. DebBarma</u>; Q. Wang; A. Lo; I. G. M. M. Niemegeers; S. M. Heemstra de Groot, "MEANS: radio-over-fiber architecture for enhancing indoor wireless communication," Poster: ICT OPEN and CWTe Research Retreat-2013, Eindhoven, The Netherlands.

21. Q. Wang; <u>D. DebBarma</u>; A. Lo; I. G. M. M. Niemegeers; S. M. Heemstra de Groot, "Techniques for efficient resource sharing in radio-over-fiber indoor

networks," Poster: ICT OPEN and CWTe Research Retreat-2013, Eindhoven, The Netherlands.

22. **[O 2:]** <u>D. DebBarma</u>; Q. Wang; A. Lo; I. G. M. M. Niemegeers; S. M. Heemstra de Groot, "Indoor Fiber-Wireless LAN for Dynamic Resource Management and Energy Efficient Communication," Poster: CWTe Research Retreat-2014, Eindhoven, The Netherlands.

23. **[O 3:]** <u>D. DebBarma</u>; Q. Wang; A.Lo; I. G. M. M. Niemegeers; S. M. Heemstra de Groot, "Energy Efficient Radio-over-Fiber based Hybrid Fiber-Wireless Centralized Enterprise WLAN (CE-WLAN)," Poster: An Innovative Truth VIII and CWTe Research Retreat-2015, Eindhoven, The Netherlands.

Publication and chapter relation: ●(Strong relation), ○(Weak relation)

	Chapter 3	Chapter 4	Chapter 5	Chapter 6
[J 1:]	●			
[C 1:]		●		
[C 2:]		●		
[C 3:]		●		
[C 4:]	●			
[C 5:]	○			○
[C 6:]		●		
[C 7:]			●	
[C 8:]				●
[C 9:]				●
[O 1:]	●	●	●	●
[O 2:]	●	●		
[O 3:]		●		

Acknowledgements

Curriculum Vitae

Diptanil DebBarma was born in Agartala, India, on June 28, 1986. He received his B.Eng. degree on Electronics and Telecommunication engineering from Sathyabama University, Chennai, India on 2008. During his B.Eng. period he was the recipient of North East Regional scholarship. He graduated as one of the University rank holder. Through GATE exam he was selected among the top 0.1% candidates to pursue his M.Eng. degree on Telecommunications from the most prestigious Indian Institute of Science (IISc), Bangalore, India. He graduated with M.Eng. on 2010. During his whole M.Eng. tenure at IISc he was recipient of the Ministry of Human Resource and Development (MHRD) scholarship. His research at IISc was focused on designing improved network coded half-duplexed amplify and forward transmission protocols for wireless medium access control.

On March 2011, he started working towards his PhD degree under the supervision of Prof. Ignas Niemegeers in the Wireless and Mobile Communication (WMC) group at Delft University of Technology (TU Delft). On January 2013 he joined the Electro-Optical Communications group (ECO) of COBRA research institute at Eindhoven University of Technology (TU/e) under the supervision of Prof. Sonia M. Heemstra de Groot to continue his PhD work. His research work was funded generously under the Dutch national IOP GenCom project MEANS. In the project, he was responsible for designing schemes for efficient network

and control management of the hybrid fiber-wireless indoor networks. His research interest includes many topics, including wireless communication, wireless network, stochastic network control, network coding implementation in wireless medium access control, information theory, MU-MIMO, cooperative and distributed MIMO techniques but are not limited to the aforementioned topics. He served as a reviewer for many premier wireless communication conferences and journals namely, ICC, WCNC, VTC, PIMRC, TVT, JNCA, and IEEE Access.